2013

MINIMIZATION OF ELECTRICAL LOSSES IN A VECTOR CONTROLLED INDUCTION MACHINE DRIVE

Debarshi Biswas
Universty of Windsor

MINIMIZATION OF ELECTRICAL LOSSES IN A VECTOR CONTROLLED INDUCTION MACHINE DRIVE

By

DEBARSHI BISWAS

A Thesis

Submitted to the Faculty of Graduate Studies

through the Department of Electrical and Computer Engineering

in Partial Fulfillment of the Requirements for

the Degree of Master of Applied Science at the

University of Windsor

Windsor, Ontario, Canada

2013

Minimization of Electrical losses In a Vector Controlled Induction Machine Drive

By

Debarshi Biswas

APPROVED BY:

Dr. S. Das, Outside Reader
Department of Civil and Environmental Engineering

Dr. K. Tepe, Departmental Reader
Department of Electrical and Computer Engineering

Dr. N. C. Kar, Advisor
Department of Electrical and Computer Engineering

September 17, 2013

AUTHOR'S DECLARATION OF ORIGINALITY

I hereby certify that I am the sole author of this thesis and that no part of this thesis has been published or submitted for publication.

I certify that, to the best of my knowledge, my thesis does not infringe upon anyone's copyright nor violate any proprietary rights and that any ideas, techniques, quotations, or any other material from the work of other people included in my thesis, published or otherwise, are fully acknowledged in accordance with the standard referencing practices. Furthermore, to the extent that I have included copyrighted material that surpasses the bounds of fair dealing within the meaning of the Canada Copyright Act, I certify that I have obtained a written permission from the copyright owner(s) to include such material(s) in my thesis and have included copies of such copyright clearances to my appendix.

I declare that this is a true copy of my thesis, including any final revisions, as approved by my thesis committee and the Graduate Studies office, and that this thesis has not been submitted for a higher degree to any other University or Institution.

ABSTRACT

Induction motors have found application in household goods as well as in industries. These machines are rugged and very easy to maintain, making them a favorite with the consumers. With the introduction of vector control induction motor drives have gained a lot of popularity. Induction motors, however, prove to be inefficient at low speeds when compared to other AC machines. Hence there is a need to improve the efficiency of induction machines over their entire speed range. Thus it is desirable to design a loss minimization controller which can improve the efficiency. This thesis therefore documents the following:

- Modeling of an induction motor with core loss included.
- Realization of vector control for an induction motor drive with loss element included.
- Derivation of the loss minimization condition.
- Procedure to successfully calculate the gains of a PI controller.

To

My mother and father: Alpana Biswas, Debasish Biswas

My sister: Priyanka Biswas

My brother-in-law: Kiran Surendra

ACKNOWLEDGEMENTS

I would like to express my appreciation and sincere gratitude towards my supervisor, Dr. Narayan Kar for his invaluable support and guidance throughout the course of this program. His encouragement helped me achieve what was simply an idea at the beginning of my tenure as a research assistant. He has truly been as inspiration. Words cannot express the respect I have for him.

I would also like to thank Dr. Kaushik Mukherjee, a visiting professor to CHARGE labs at the University of Windsor, for his unconditional support during his tenure here in Windsor. His constant nurturing helped me understand the minute intricacies that were related to this research. I am indebted to him for sharing his knowledge with me.

I would like to extend my gratefulness to my committee members, Dr. Kemal Tepe and Dr. Sreekanta Das, for providing their valuable suggestions and presenting their insight on my topic of research. Their critiques were indeed helpful in adding value to my research.

Last but not the least, I would like thank my mother, father, sister and brother-in-law who stood by me from the moment I started my research. My father has been my biggest strength as he instilled the confidence in me that I could finish what I started. I owe him due credit for any success that I gain out this exercise.

TABLE OF CONTENTS

LIST OF TABLES

LIST OF FIGURES

NOMENCLATURE

v_{qs} : Q-axis stator voltage

v_{ds} : D-axis stator voltage

v_{qs_comp} : Q-axis compensation voltage

v_{ds_comp} : D-axis compensation voltage

i_{qs} : Q-axis stator current

i_{ds} : D-axis stator current

i_{qr} : Q-axis rotor current

i_{dr} : D-axis rotor current

i_{qm} : Q-axis magnetizing current

i_{dm} : D-axis magnetizing current

i_{qc} : Q-axis current in the core loss branch

i_{dc} : D-axis current in the core loss branch

λ_{qs} : Q-axis stator flux

λ_{ds} : D-axis stator flux

λ_{qr} : Q-axis rotor flux

λ_{dr} : D-axis rotor flux

λ_{r} : Rated flux

R_s : Stator resistance

R_r : Rotor resistance

R_c : Core loss resistance

L_{ls} : Stator leakage inductance

L_{lr} : Rotor leakage inductance

L_m : Magnetizing inductance

T_e : Electromagnetic torque

T_l : Load torque

ω : Speed of arbitrarily rotating dq-frame rad/sec

ω_r : Rotor speed in rad/sec

ω_{sl} : Slip speed in rad/sec

θ : Angle of transformation from three phase to two phase

J : Moment of inertia

P : Number of poles

p : Differentiation operator

iK_p : Inner loop proportional gain

oK_p : Outer loop proportional gain

iK_i : Inner loop integral gain

ζ_i, ζ_o : Damping factor for inner and outer loop respectively

ω_{ni}, ω_{no} : Natural frequency for inner and outer loop respectively

P_{total} : Total loss

P_{SCL} : Stator copper loss

P_{Core} : Core loss

P_{RCL} : Rotor copper loss

i_{dm_opt} : Optimal d-axis magnetizing current

f_a, f_b, f_c : Component of any variable in phase A, B or C respectively

f_q, f_d : Component of any variable in q or d-axis respectively

f_0 : Zero sequence component of any variable

1. INTRODUCTION

1.1. INTRODUCTION TO INDUCTION MOTOR

With the inception of AC distribution systems, application of AC motors has widened to a large extent. This has prompted motor manufacturers to build AC motors that will cater to the various types of applications. All electric motors transform electric power into mechanical power. In DC motors, there is a physical connection between the stator and the rotor. This allows the transfer of power. However, in AC motors there is no such physical connection between the stationary and the rotating part. The conversion of electrical to mechanical energy occurs through induction and hence the name induction motors. Induction motors are found in many applications today, whether it be in small scale or large scale. Because induction motors are constant speed motors, they are found in many household appliances such as pumps and fans. In industries they are used for heavy duty applications. Induction motors are the largest consumer of electrical power [1]. The reasons for this popularity are rugged construction, low maintenance cost, reliable and inexpensive compared to other motors. But possibly the biggest advantage is that it does not need any starter motor and it can be directly connected to a power source. It does however have disadvantages. An induction motor works best when it is running at or near its rated loading capacity. The motor can still be used at lower loading conditions but at the cost of efficiency. Energy consumption has become an issue over the past few years. It is of utmost importance that attention is paid to make machines run more efficiently. Speed control can bring about significant energy savings but vector controlled induction motor drives focus mainly on delivering high dynamic performance. Thus, it is necessary to focus our attention on designing drives that deliver performance without

compensating for efficiency. Advancements in the design process and improvements in materials used to construct induction motors have helped improve the efficiency of induction motors. However, there is no substitute for a controller dedicated to optimize the efficiency. Loss minimization can be achieved in many different ways. The ideal loss minimization controller should not only reduce the heat signature of the motor but also account for losses in the converter in conjunction with delivering the required load torque. Designing a loss minimization controller will definitely help overcome the primary disadvantage of induction motors.

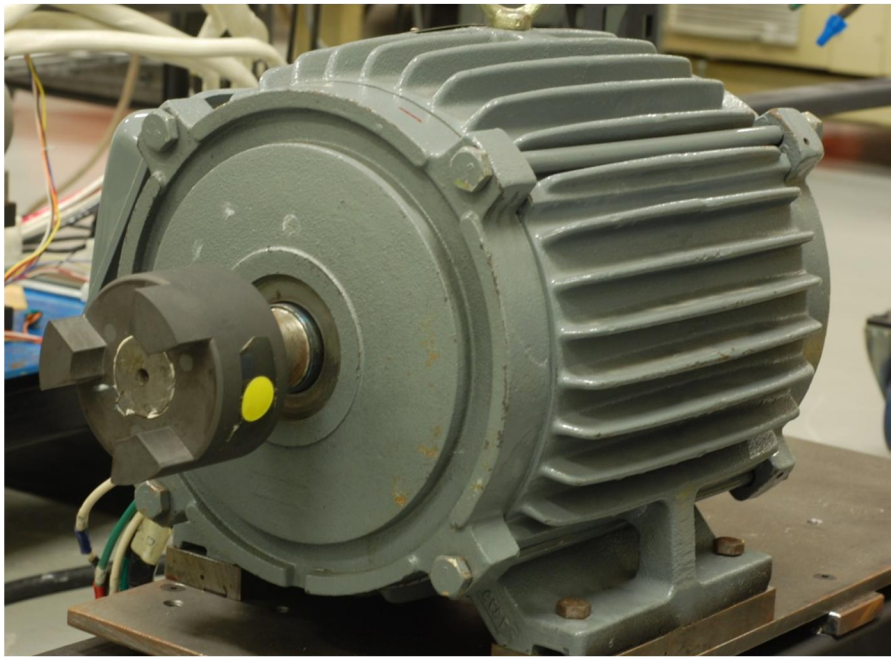

Fig. 1.1: Typical induction motor with cooling fins on the stator and coupler on the rotor shaft.

1.2. Construction and Operation of an Induction Motor

An induction motor is made up of two major components. The outer stationary casing is called the stator. The stator is made up laminated stamping slotted to hold the windings. A three phase supply feeds the stator. The windings are wound to create a

specific number of poles. There are two kinds of rotors for the induction motors. They are the squirrel cage rotor and the wound rotor. The squirrel cage rotor essentially has metal bars shorted at the ends by metal rings called the end rings. This construction makes the rotor look like a squirrel cage and hence the name. Because this kind of a construction lacks any physical wiring, there is no access to the rotor. This feature makes squirrel cage motors very rugged and usable in almost any condition. The wound rotor, as the name suggests, has windings in the rotor which are a mirror image of the windings in the stator. These motors are used in specific applications due to the access to the windings. However, wound rotor machines have reliability issues when compared to squirrel cage machines and are more expensive. In this thesis only the squirrel cage induction motor will be considered.

An induction motor is essentially a transformer with a rotating secondary. Exciting the stator windings creates a rotating flux. The speed at which the rotating flux rotates is called the synchronous speed. The rotating flux cuts across the rotor bars and an e.m.f. is induced in the stationary rotor as per Faraday's law. The magnitude of this induced e.m.f. is proportional to the relative velocity between the rotating flux and the rotor bars. Because the rotor bars are short circuited, a current is produced due to this induced e.m.f. The direction of this current, as per Lenz's law, is such that it opposes the cause that produces it. The cause in this case is the relative velocity between rotating flux and the rotor bars. In order to oppose this cause the rotor begins to rotate in the in same direction as the rotating flux. It should be noted that the rotor can never catch up to the rotating flux. If this happened there would be no relative motion between the flux and the rotor conductors and the rotor would simply stop spinning. Thus the shaft speed of an

induction motor is always less than the synchronous speed. The difference in of these two speeds is known as the slip speed which is generally expressed as a percentage of the synchronous speed [2].

1.3. EVOLUTION OF INDUCTION MOTOR DRIVES

Before vector control was developed for induction motors, scalar control was widely used in speed control of these machines. Perhaps the most popular strategy is the volts/hertz method. Although scalar control is simple it has a few drawbacks. The biggest disadvantage of this method is that it has slow transient response time. This means that it is slow to transition from one operating point to another. In case of any disturbance it is slow to recover to its original operating point as well. The second flaw of this strategy is that the slightest of change in supply can upset the air gap flux of the machine which will in turn affect the speed of the motor. Overall, it can be concluded that scalar control is not very precise. Some industrial applications may not need such precise speed of operation but there are many applications that need higher performance drives. F. Blaschke proposed a revolutionary idea which changed the way induction motors were controlled [3]. Separately excited DC motors have naturally decoupled armature and field flux. As a result DC motors have very quick transient response. With the advent of vector control, AC machines, like the induction motor, could also be made to behave like a separately excited DC motors. An analogy between the two has been drawn in the subsequent chapters. Vector control or field oriented control (FOC) was an immense step forward in terms of performance. Realization of FOC in real-time also became a possibility with the availability of processors with high computational power.

1.4. LITERATURE REVIEW

Strategies to control loss minimization can be broadly classified into two categories: loss minimization controller and search control. Loss minimization controller utilizes the machine parameters to estimate the loss model. The controller thus designed using this procedure is then responsible for selecting an appropriate flux level which facilitates the minimization of losses. Much research has been conducted in this field using this strategy [4-13]. Earlier, scalar control was the most widely used technique to control the speed of induction motors. Scalar control essentially employs choosing a specific stator voltage and a frequency to facilitate speed control in the induction machine. For a given operating point for an induction motor there are combinations of stator voltages and frequencies that exist which promote loss minimization. This has been very aptly described in [4, 5]. Another method to achieve optimum efficiency has been presented by H. G. Kim et al. in [6] by using a current source inverter. It was suggested that the optimum efficiency could be achieved for a specific combination of torque and speed by reducing the air gap flux. As a current source inverter is being used the air gap flux can be expressed as functions of stator currents and rotor slip. In addition to reducing the losses, this method also improved the power factor at light loads. The relationship between the stator current and the slip frequency, the condition for loss minimization, was obtained numerically. The control loop was then designed based on these calculations to accommodate for variable flux. Kioseridis et al. [7] presented a loss minimization scheme using the loss model of an induction motor. The scheme is simple and employs optimal air gap flux to achieve loss minimization in scalar controlled induction motor drives. The simplistic approach helps keep the cost and the complexity

of the drive at a bare minimum. P. Famouri and J. J. Cathey [8] proposed a closed loop control technique using per unit values. The modeling of the losses was done using the copper losses, core loss, losses crossing the air gap and the rotational losses. These were then used to calculate the per unit efficiency as a function of slip and frequency. Implementation of the closed speed loop was a significant improvement over the previous open loop volt/hertz technique. Lorenz and Yang [9] proposed a dynamic programming method which would enhance the efficiency in a field oriented induction motor drive being operated in a closed cycle. Losses taken into account were the copper and core losses. The copper loss was expressed as a function of the square of the currents. The core loss on the other hand was modeled as a function of frequency, exhibiting the hysteresis and eddy current losses distinctively. The loss of the drive was also considered and defined as an objective function. The constraints of the objective function were the limits on motor flux, speed, voltage and current. The optimal trajectory for the flux and flux producing current were computed by solving the problem. The entire control strategy was then implemented using a microcontroller. Garcia et al. [10] proposed a novel method to minimize copper losses and iron losses in variable speed variable torque induction motor drive while maintaining a good dynamic response. It has been very clearly stated that a good control over the magnetic flux would result in obtaining a balance between the copper and iron losses. This balance between the copper loss and core loss would essentially assist in achieving optimum efficiency. The induction motor model been expressed in dq-coordinate system. However, for simplicity, the leakage inductance was deleted from the motor model. Resistances were used to represent the loss elements as a function of stator currents. Based on the loss model they derived the

condition for minimum loss where the d-axis current was made the control variable as this component of stator current would eventually influence the flux level in the induction motor. Chakraborty and Hori [11] approached the problem of loss minimization from different perspective altogether. They proposed a hybrid scheme to address this issue which consisted of combining loss model approach and search control approach in a vector controlled induction motor. The loss model approach calculated the optimum flux level numerically. The search control algorithm on the other hand estimated the optimum flux level based on the measurement of the input the power through an iterative process. Combining both the loss minimization techniques gave rise to the development of a very capable controller. The hybridization of the two loss minimization methods ensured that the controller had a fast response by virtue of the loss model approach. Also, the search algorithm provided sufficient immunity to variation in motor parameters. Although the performance of the controller is greatly increased, the approach adopted by the authors in [11] adds to the complicacy of the overall system. The authors used the same approach to model the losses as used in [10]. However, a simple and approximate model of the induction motor to achieve their objective. In [12], the authors, Bernal et al., proposed a generalized loss model using the dq-theory. This loss model would cater to machines such as permanent magnet synchronous motors, induction motors, and dc motors which could be used to the fulfill the needs required in the design procedure of controllers facilitating to loss minimization. Effects due to core saturation have also been accounted for by the authors. Interestingly, the loss model proposed in [10] has again been used to the model the induction motor losses. S. Lim et al. [13] proposed a model which included the leakage inductance in the induction motor model. In addition to this, the authors also

connected a dependent voltage source with the core loss resistor as a part of the equivalent circuit for the induction motor. Based on their modeling, it was reported that the findings were aligned to the complete induction motor model when compared to the data presented by previous researchers.

Search controller works on the principle of minimum input power measurement in order to choose the optimum flux level [14-19]. Moreira et al. [14] introduced a new method to implement search control algorithm for induction motors. He proposed that the third harmonic of the air gap flux could be used to determine the currents responsible for producing the flux and torque in the machine which could be utilized to maximize the efficiency of the induction motor. He also used this technique to estimate the speed of the rotor. Necessary adjustments could be made to the flux producing component of the stator current to ensure production of minimum input power. Sul and Park [15] proposed an idea where an induction motor could be more efficient if the value of slip was appropriately chosen. Their idea discarded the need for sensors required to measure speed. Instead, the stator voltage and the stator current were used to estimate all the necessary values, slip speed being one of them. All these values were then stored in a microprocessor which would essentially serve as a look up table. The control system would then refer to the look up table and choose the optimum slip by trial and error at first. The control system would then ensure the induction motor is then operated by tracking the optimal slip. Kirschen et al. [16] maximized the efficiency of the induction motor drive by making flux the control variable. The flux command was gradually decreased in very small steps to get to the point where minimum power was required to run the motor. The solution, although easy to implement, takes a long time to converge to

a solution. This is because the step size by which the flux command is reduced is very small. Again, there is no option but to choose small step size for flux reduction because sudden variations in flux levels in the motor can cause unwanted pulsations in the torque profile. In spite of choosing a small enough torque pulsations could not be done away with as evident from the results published. Sousa et al. [17] extended the work already presented in [16]. A fuzzy logic based controller was used to achieve maximum efficiency in an indirect vector controlled induction motor. The fuzzy controller ensured there was an adaptive decrement in the d-axis current, which would eventually reduce the flux in the machine. This approach was chosen to speed up convergence as search controllers in general are slow to converge to a solution. In [16] a fixed step size was chosen for the reduction of the flux command. However, Sousa et al. manipulated the step size with the help of fuzzy logic controller. Thus, based on the input power measurement, the controller would initially choose a suitable step size to reduce the current signal by. But as the d-axis current approached the optimum value the step size itself would automatically be reduced by virtue of adaptive control. Also, a feed forward compensation technique was used to reduce the pulsations in the torque profile. Kim et al. [18] proposed a strategy to control induction motors which would deliver "maximum power efficiency" augmented with unexceptional dynamic performance. Their strategy was to adjust the squared rotor flux as per the requirement dictated by the minimum power algorithm till the input power was at its minimum. Unwanted torque ripple was mitigated by decoupling the speed of the motor and the rotor flux. This decoupling action was achieved with the help of a nonlinear controller. The design process of the controller was dependent on a very accurate measurement of the rotor resistance. The measurement

of the rotor resistance needed to be very accurate because it would eventually affect the estimation of the rotor flux. Unfortunately, the resistance of the rotor would change with changes in the temperature inside the induction motor. This could adversely affect the estimated value of the flux. As a result, the authors devised an online method to measure the rotor resistance so that any slight change in its value could be quickly tracked and accounted for by the controller. Undoubtedly, the adoption of this method was a clear improvement over the previous methods. However, inclusion of these features in the algorithm added to the complexity of the overall system. Ta and Hori [19] devised a novel technique to improve the convergence of search controllers. They developed an algorithm which would provide the optimum value of the current needed for minimum loss by employing the "golden section technique". Their proposed strategy provided a fast convergence without the need for measuring speed or torque. In addition to this, the controller was immune to variation in parameters. There was however issues related to the selection of the upper and lower limits of the current responsible for setting up the flux.

1.5. PROBLEM STATEMENT

From the previous sections it is clear that loss minimization controller has its own advantages. Firstly, the controller offers fast response. Secondly, opting for this methodology to implement loss minimization overcomes the issue of torque ripple completely which is a common problem with search controllers.

Even though there are advantages, loss minimization controller does have flaws. The very first flaw is in the designing of the controller itself. Design of the controller revolves around how accurately the modeling of the motor has been done. Accuracy of

the mathematical model dictates the accuracy of the controller. Any approximations made in the mathematical model of the motor will affect the performance of the controller. However, it is not always possible to include all the facets of modeling simply because it adds to complexity of the overall system. An example of approximations made in motor modeling can be found in [10]. The authors presented an equivalent circuit of the induction motor where the leakage inductance was ignored. This approximation was made in order to avoid making the overall system more complex. The same approach was chosen by the authors in [11, 12].Thus, the design process of the loss minimization controller always includes a tradeoff between the complexity and accuracy of the system.

Another factor that affects the loss modeling approach is variation in parameters. As the motor runs the temperature inside it rises. It is a well-known fact that resistance is a function of temperature. Thus, any fluctuation in temperature will cause the resistance of any element to change. Due to this phenomenon, factors affecting parameter variation should be accounted for in the modeling else no matter how accurate the mathematical model is, in reality the performance of the controller will be affected. In previous works, such as [13], the parameters of the induction motor have been considered to be constant. Even though the system may behave perfectly theoretically, practically variation in parameters due to temperature change will undoubtedly affect the performance of the system. Online estimation of parameters is a solution to mitigate this issue but the complexity of the system increases exponentially. However, as mentioned earlier, incorporating all the minute intricacies to develop a perfect controller would give rise to a very complex system.

Search controllers on the other hand do not need prior knowledge of the machine parameters. The issue with search controllers is that they are slow to converge and produce ripples in the torque profile of the machine. The search controller works on the principle of detecting the minimum input power. This process is an iterative process which eventually is the primary reason for slow convergence. Again, because the flux level gets adjusted in every iteration, the torque also gets affected as a result. Also, while implementing search control algorithm, adjustment of the flux should be done in sufficiently small steps. Sudden and large changes in flux can adversely affect the torque produced by the machine [16].

1.6. OBJECTIVE OF THIS RESEARCH

Substantial research has been conducted in the field of loss minimization. Different avenues have also been explored to achieve this [4-19]. In this thesis, the strategy of loss minimization controller has been adopted.

Various mathematical models of the induction motor have been proposed by various researchers. Out of these different models the two axis model proposed by P. C. Krausse is widely accepted. The model he proposed can be very easily derived from the three phase steady state circuit of an induction motor. There are two primary reasons for choosing a two axis model. Firstly, with the help of two axis equivalent circuit there are only two components of the motor variables that need to be taken into consideration, viz. q-axis and d-axis components. Secondly, for analytical purposes, a suitable frame of reference can be chosen based upon the type application the induction motor is being used for. In this thesis all analysis will be done based on the assumption that the

induction motor is operating in the synchronously rotating frame. This reference frame would be ideal because all sinusoidal variables will appear as DC values. Also, unlike in [10], his model includes the leakage inductance. The biggest flaw of using such an equivalent circuit is that it lacks the core loss resistor. In order to formulate the loss model it is most desirable that core loss is also included as a part of the equivalent circuit. Importance is given to the inclusion of core loss because the primary losses experienced by the induction motor are copper loss (stator and rotor) and core loss. The other losses such friction and windage loss are comparatively much lesser than copper and core loss as a result of which they are neglected.

Once the equivalent circuit of the induction motor has been well established focus will be shifted to modeling the losses. The copper losses will be modeled as functions of the square of the current. The core loss on the other hand can be modeled in two ways. The first method would be to express the iron loss as a function of square of the current. The other method is to express it as a summation of hysteresis loss and eddy current loss. In this thesis all the losses will be modeled as functions of square of the current. The total loss expression will be finally expressed as a function of the magnetizing current. It will be shown in the later chapters that choosing the magnetizing current as the control variable will be most convenient in order to implement the control strategy. The next step would be to derive the condition for minimum loss which is the primary objective of this thesis.

The second objective of this thesis is to design a proportional and integral (PI) controller for the system. The PI controller is one of the very basic controllers in existence. Many modern control methods have been developed since but if designed

properly a PI controller is capable of delivering commendable performance when compared to the new age controllers. There are two principle methods by which the gains of a PI controller can be determined. The first method involves solving a set of equations to determine the controller gains and the second method is to determine those values by trial and error. Much research has been done where the gains of a PI controller has been determined by trial and error method. The issue with this method is that it could be time consuming to come across a value of the gain that serves the purpose. Again, even if the gains are determined, it cannot be pointed out for sure that the values chosen are the most apt for the given system. In this thesis the proportional gain and the integral gain have been calculated mathematically. Another advantage of the mathematical calculation is that the method introduces two new variables which dictate the values of the proportional and integral gain. These two variables are more significant when compared to proportional and integral gain because it is these performance parameters that dictate how the system will behave when subjected to a specific input.

1.7. ORGANIZATION OF THE THESIS

The following chapters of this thesis are organized as follows. Chapter 2 introduces the dq-model of the induction machine. The beginning of the chapter gives a brief history as to how the transition from three phase to two axis theory came about. It also helps in learning the method necessary to transform from three phase to two phase. The chapter ends by introducing all mathematical equations that describes the induction motor in dq-reference frame. Chapter 3 dives into the details of vector using the machine equations described in chapter 2. An analogy is drawn between the working principle of a shunt DC machine and general vector control theory for induction motors. The analogy

gives a clearer picture as to why the theory for vector control was developed. The conditions that govern vector control are stated. The equations necessary to implement indirect field oriented (IFOC) vector control are then derived followed by the requirements of the PI controller. Chapter 4 speaks more about the induction motor model. However, it provides vivid details of the changes needed to incorporate core loss into the already established dq-model of the induction machine. The equations required to implement IFOC are derived again to account for the changes brought about by the inclusion of core loss. The focus then shifts to the design methodology adopted in this thesis to calculate the gains for the PI controller. Chapter 5 gives extensive details on how the losses are modeled. With the assistance of this loss model the condition for minimizing the losses in an induction motor is then derived. The results obtained from simulations are documented in chapter 6. Finally, chapter 7 presents the conclusion and future scopes of this research followed by the references.

2. INDUCTION MOTOR MODELING

2.1. TWO AXIS THEORY OF MOTOR MODEL

R. H. Park introduced a method in the late 1920s which enabled the elimination of time varying inductance from stator equations. This method was however applied to synchronous machines. Essentially he referred the stator variables to a frame of reference fixed in the rotor. This method today is popularly known as Park's transformation. In the 1930s however, H. C. Stanley proposed a method which would enable the change of variables for induction machines. Unlike R. H. Park's transformation, Stanley's method referred the rotor variables to a fixed stationary frame in the stator. G. Kron suggested another method whereby time varying mutual inductances of a symmetrical induction motor were eliminated by referring the motor variables to a reference frame rotating in synchronism with the rotating magnetic field. This reference frame is called the synchronously rotating frame. D. S. Berenton employed the change of variables for symmetrical induction machines from a reference frame fixed in the rotor. In essence this was the transformation done using Park's transformation but applied to induction motors.

These techniques were developed in order to cater to a particular application. However, in the1950s it became clear that any real transformation that is used to analyze induction machines could be generalized. This general solution would help in eliminating the time varying inductances by referring them to a rotating reference rotating at any arbitrary angular velocity. It should be noted that when using stator reference frame for analysis the angular velocity of the reference frame would be zero [20].

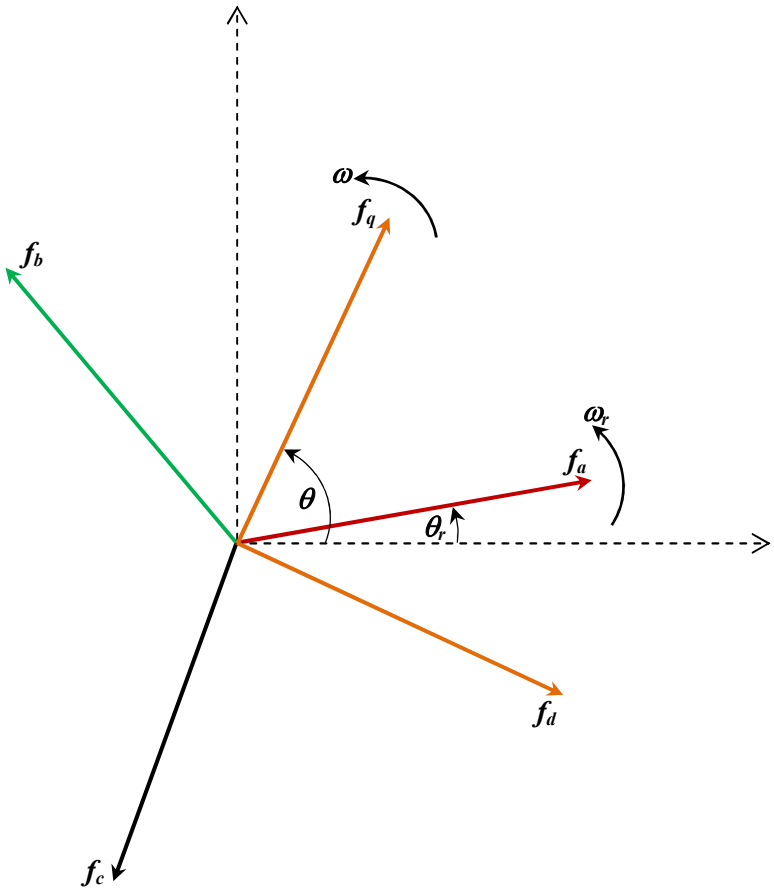

Fig 2.1: Phasor diagram depicting the positions of three phase values (marked in red, green and black) and the corresponding dq values (marked in orange).

The following equation shows how the three-phase variables can be expressed in an arbitrary reference frame.

$$\begin{bmatrix} f_q \\ f_d \\ f_0 \end{bmatrix} = \frac{2}{3} \begin{bmatrix} \cos\theta & \cos\left(\theta - \frac{2\pi}{3}\right) & \cos\left(\theta + \frac{2\pi}{3}\right) \\ \sin\theta & \sin\left(\theta - \frac{2\pi}{3}\right) & \sin\left(\theta + \frac{2\pi}{3}\right) \\ \frac{1}{2} & \frac{1}{2} & \frac{1}{2} \end{bmatrix} \begin{bmatrix} f_a \\ f_b \\ f_c \end{bmatrix} \tag{2.1}$$

It can also be shown that the three phase variables can again be obtained from the following relationship

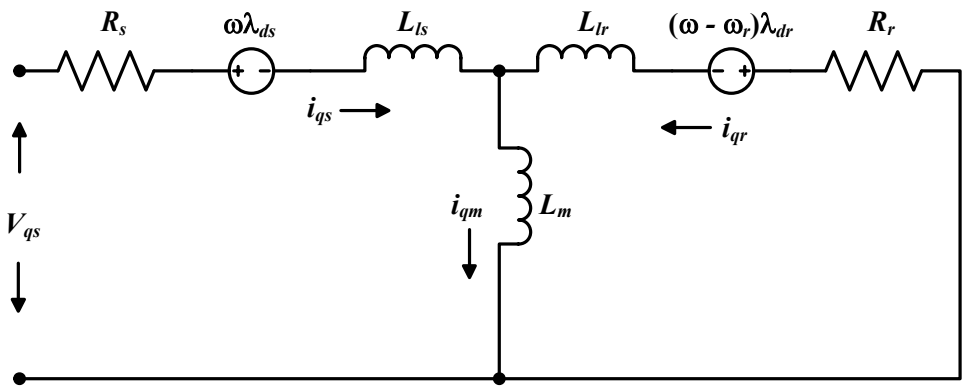

(a)

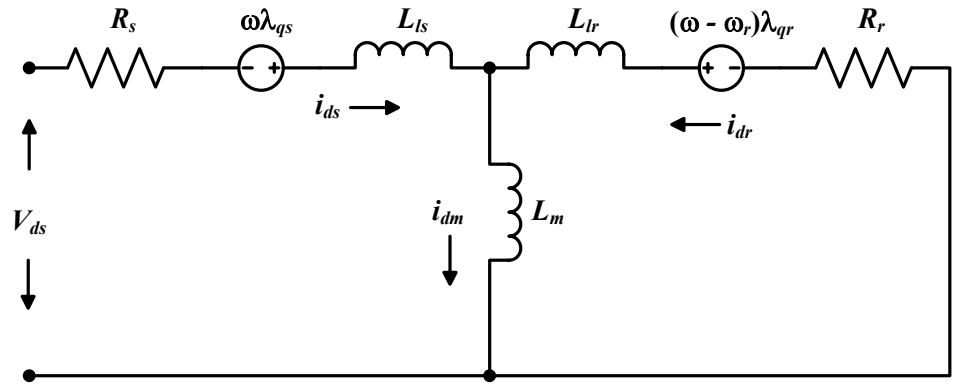

(b)

Fig 2.2: Equivalent circuit of an induction motor. A) q-axis. B) d-axis.

$$\begin{bmatrix} f_a \\ f_b \\ f_c \end{bmatrix} = \begin{bmatrix} \cos\theta & \sin\theta & 1 \\ \cos\left(\theta - \frac{2\pi}{3}\right) & \sin\left(\theta - \frac{2\pi}{3}\right) & 1 \\ \cos\left(\theta + \frac{2\pi}{3}\right) & \sin\left(\theta + \frac{2\pi}{3}\right) & 1 \end{bmatrix} \begin{bmatrix} f_q \\ f_d \\ f_0 \end{bmatrix} \tag{2.2}$$

In equations (2.1) and (2.2) the variable *f* could be interpreted as voltage, current or flux linkage. The 0 in the subscript represents the zero sequence of the respective variable.

The angular velocity ω and the angular displacement θ are related as per the following expression

$$\theta = \int \omega dt \tag{2.3}$$

2.2. MODELING OF AN INDUCTION MOTOR

Any induction motor is governed by the following equations [20].

Voltage equations:

$$v_{qs} = R_s i_{qs} + p\lambda_{qs} + \omega\lambda_{ds} \tag{2.4}$$

$$v_{ds} = R_s i_{ds} + p\lambda_{ds} - \omega\lambda_{qs} \tag{2.5}$$

$$v_{qr} = 0 = R_r i_{qr} + (\omega - \omega_r)\lambda_{dr} + p\lambda_{qr} \tag{2.6}$$

$$v_{dr} = 0 = R_r i_{dr} - (\omega - \omega_r)\lambda_{qr} + p\lambda_{dr} \tag{2.7}$$

The rotor voltages, as depicted by equations (2.6) and (2.7), have been equated to zero because the windings in the rotor of an induction motor are intentionally short circuited.

Flux equations:

$$\lambda_{qs} = L_{ls} i_{qs} + L_m (i_{qs} + i_{qr}) \tag{2.8}$$

$$\lambda_{ds} = L_{ls} i_{ds} + L_m (i_{ds} + i_{dr}) \tag{2.9}$$

$$\lambda_{qr} = L_{lr} i_{qr} + L_m (i_{qs} + i_{qr}) \tag{2.10}$$

$$\lambda_{dr} = L_{lr} i_{dr} + L_m (i_{ds} + i_{dr}) \tag{2.11}$$

Mechanical equations

$$T_e = \frac{3P}{4}\frac{L_m}{\left(L_{lr} + L_m\right)}\left(\lambda_{qr} i_{dr} - \lambda_{dr} i_{qr}\right) \tag{2.12}$$

$$T_e - T_l = \frac{2J}{P} p\omega_r \tag{2.13}$$

3. VECTOR CONTROL OF INDUCTION MOTOR

3.1. THEORY OF VECTOR CONTROL

Speed control in induction motors, using scalar control techniques, have been observed since the earliest of days. The preferred control method was volts per hertz method, alternately known as scalar control of induction motors. However, scalar control did not have fast response, as sometimes demanded by the user. DC machines, on the other hand, could provide very fast transient response. Thus, vector control was formulated in order to make the AC machine behave like a DC machine. The analogy between the speed control of DC machine and vector control is explained in the next section.

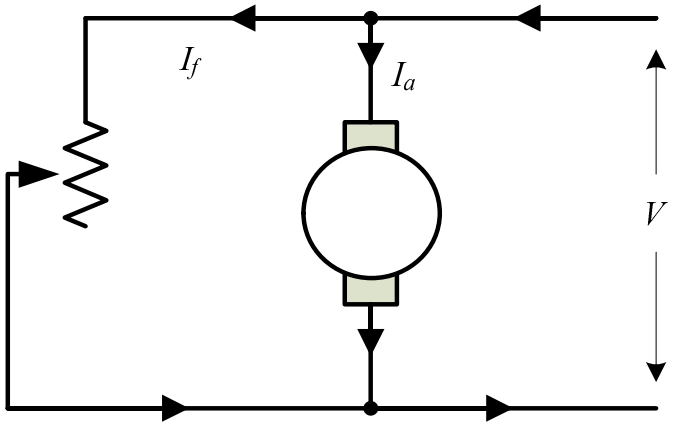

Fig. 3.1: DC shunt motor.

3.3.1. ANALOGY BETWEEN VECTOR CONTROLLED INDUCTION MOTOR AND SPEED CONTROL OF A SHUNT DC MOTOR

Before diving into the theory of vector control of an induction motor, the working principle of a separately excited DC motor should be understood. This is necessary because vector control forces the induction motor to behave like a DC shunt motor. There

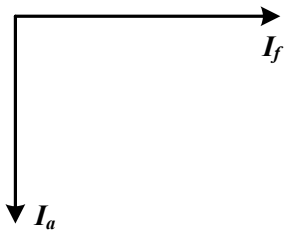

Fig 3.2: Orthogonal orientation of armature current and field current in a separately excited DC machine.

are two separate currents at work inside a DC motor. One is called the armature current and the other is known as the field current. The construction of a DC motor, as depicted in figure 3.1, is such that both the currents are orthogonal to each other. Because the currents are responsible for producing the armature and field fluxes, it can inferred that these fluxes will also be orthogonal. This means that if we depict both the armature and field currents along with the fluxes through a phasor diagram they would be perpendicular to each other as shown in figure 3.2. From the phasor diagram it can be concluded that changing any one of the current values will not affect the other. In other words, it can be said that changes in armature current will not affect the field current or the field. Again, the armature current, which directly affects the developed torque of a DC motor, remains unaffected if any change is observed in the field current. This is the very reason as to why a DC motor has very fast torque response.

The same idea is extended to induction motors. Through vector control, the d and q-axis currents are decoupled and made orthogonal. In order to make the sinusoidal variables such as voltages, currents and fluxes appear as DC quantities the induction motor is considered to be in a synchronously rotating frame. For an induction motor the q-axis current is analogous to the armature current and the d-axis current is analogous to the field current. Thus, the torque can be made to change simply by controlling the q-axis

current while the d-axis current remains unaffected. Again, the rotor flux, which is a function of the d-axis current, can be easily controlled by varying the d-axis current itself while the torque and q-axis current remain unchanged.

3.3.2. FIELD ORIENTED CONTROL

Vector control, alternately known as field oriented control, is one of the modern control techniques used to control AC machines. This thesis only looks at the methodology that can be applied to induction motors only. The name, vector control, has emerged from the fact that the control is achieved in field coordinates. The parameters that are controlled with the help of this technique are as follows:

- Stator flux
- Air-gap flux
- Rotor flux

Essentially, the voltages, currents and flux linkages are represented in the form of vectors. With the help of the controller the specific orientation is achieved. Normally, while trying to implement vector control rotor flux orientation is best choice as it provides natural decoupling when compared to stator flux orientation or air-gap flux orientation.

3.3.3. INDIRECT FIELD ORIENTED VECTOR CONTROL

Indirect field oriented control (IFOC) eliminates the use of sensors which are used to measure terminal voltages and currents to determine the unit vector components $\cos\theta$ and $\sin\theta$. In this method the unit vector signals are generated in feed forward manner

[21]. This method is cost effective but any changes in the parameters of the motor while in operation makes the controller vulnerable to degradation in performance [22].

At the very outset the conditions that govern vector control must be to understood. There are three main criteria that need to be satisfied:

- $\lambda_{dr} = \lambda_r$, a constant at steady state (3.1)
- $\lambda_{qr} = 0, \frac{d\lambda_{qr}}{dt} = 0$ (3.2)
- $\frac{d\lambda_{dr}}{dt} = 0$, when in steady state (3.3)

With the above conditions in mind the equations for vector control can now be derived.

Substituting $\lambda_{dr}=\lambda_r$, equation (2.8) can be written as

$$\lambda_r = L_{lr} i_{dr} + L_m (i_{ds} + i_{dr}) \tag{3.4}$$

Simplifying equation (3.4) further yields

$$i_{dr} = \frac{\lambda_r}{L_r} - \frac{L_m i_{ds}}{L_r} \tag{3.5}$$

Where $L_r=L_{lr}+L_m$

Substituting $\lambda_{qr}=0$ in equation (2.7) and simplifying the same yields

$$i_{qr} = \frac{-L_m i_{qs}}{L_r} \tag{3.6}$$

Plugging in equation (3.5) in equation (2.4)

$$R_r\left(\frac{\lambda_r}{L_r}-\frac{L_m i_{ds}}{L_r}\right)-(\omega-\omega_r)\lambda_{qr}+p\lambda_{dr}=0 \tag{3.7}$$

Introducing the conditions (3.2) and (3.3) in equation (3.7) reduces it to

$$\lambda_r = L_m i_{ds} \tag{3.8}$$

Again, substituting (3.6) in (2.3) yields

$$R_r\left(\frac{-L_m i_{qs}}{L_r}\right)+\omega_{sl}\lambda_r+p\lambda_{qr}=0 \tag{3.9}$$

Where $\omega-\omega_r=\omega_{sl}$ and introducing the conditions (3.1) and (3.2) in (3.9) gives

$$\omega_{sl}=\frac{R_r L_m i_{qs}}{\lambda_r L_{lr}} \tag{3.10}$$

Substituting (3.1), (3.2),(3.5) and (3.6) in the torque equation numbered (2.9) yields

$$T_e=\frac{3P}{4}\frac{L_m^2}{L_r}i_{ds}i_{qs} \tag{3.11}$$

The above equations clearly portray the fact that the conditions assumed for vector control, equations (3.1) through (3.3), indeed decouple the q and d-axis currents. It can easily be concluded that i_{ds} is the flux producing component while i_{qs} is solely responsible for changes in the electromagnetic torque.

3.4. REQUIREMENTS OF THE PI CONTROLLER

It is clear from the equations presented in section 3.3.3 that the control variables for successfully implementing vector control are the q and d-axis stator currents.

Changing the values of these currents will enable the user to very quickly change the torque at a particular set speed. From figure 3.3 it is clear that the voltage equations need to be expressed as a function of the stator currents. In order to achieve this it is first necessary to express the stator fluxes in terms of stator currents only. The procedure is as follows.

First equation (2.5) is considered. It is a function of i_{qs} and i_{qr}. As mentioned earlier, the control variables are the q and d-axis stator currents. Thus, i_{qr} needs to be eliminated from the flux equation.

Substituting equation (3.6) in (2.5) eliminates i_{qr}. The flux equation can be rewritten as

$$\lambda_{qs} = \sigma L_s i_{qs} \tag{3.12}$$

Where

$$\sigma = 1 - \frac{L_m^2}{L_s L_r}$$
$$L_s = L_{ls} + L_m$$
$$L_r = L_{lr} + L_m$$

Similarly, equation (2.6) is a function of ids and i_{dr}. Thus, substituting equation (3.5) in (2.6) yields

$$\lambda_{ds} = \sigma L_s i_{ds} + \frac{L_m \lambda_r}{L_r} \tag{3.13}$$

The stator voltages can now be expressed in terms of stator currents. Thus, substituting equations (3.12) and (3.13) in (2.1) and simplifying the same, we get:

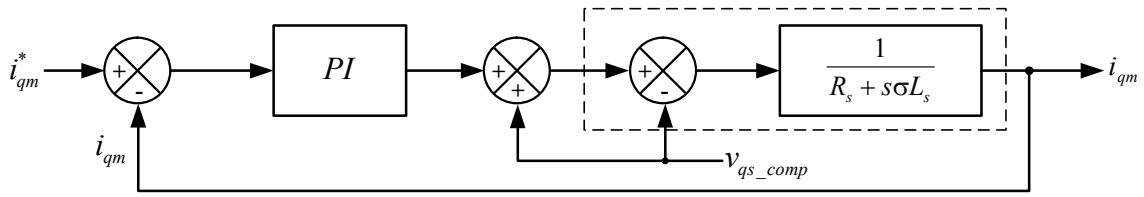

(a)

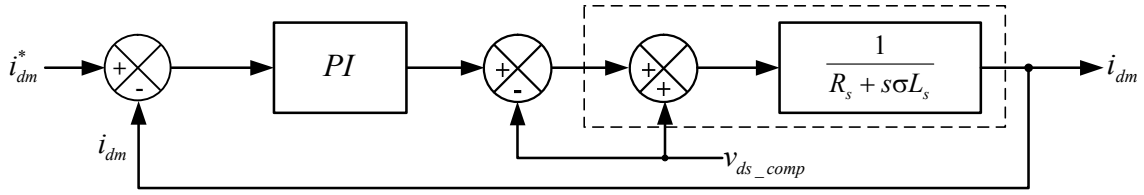

(b)

Fig. 3.3: Current control loop. (a) Q-axis. (b) D-axis.

$$v_{qs} = R_s i_{qs} + \sigma L_s p i_{qs} + \omega\sigma L_s i_{ds} + \frac{\omega L_m \lambda_r}{L_r} \tag{3.14}$$

$$v_{ds} = R_s i_{ds} + \sigma L_s p i_{ds} - \omega\sigma L_s i_{qs} \tag{3.15}$$

A close look at equations (3.14) and (3.15) reveals that both the q-axis and d-axis voltages have dependency on i_{qs} and i_{ds}. In other words, the voltage equations are not decoupled. Considering in vector control, the control variable of choice are the q and d-axis stator currents, any change in one variable will automatically affect the other. Thus, the cross coupled terms need to be compensated for. Figure 3.3 shows the procedure by which the effect of the cross coupled terms can be negated. In equation (3.14) any term which is a function of i_{ds} is treated as a disturbance. Since the magnitude of this disturbance can be estimated, introducing a signal opposite in polarity but bearing the same magnitude into the system will negate the effect this disturbance. Similarly, in

equation (3.15), any term which is function of i_{qs} is treated as a disturbance and its effect it negated in the same manner as explained above.

4. VECTOR CONTROL OF INDUCTION MOTOR MODEL WITH CORE LOSS INCLUDED

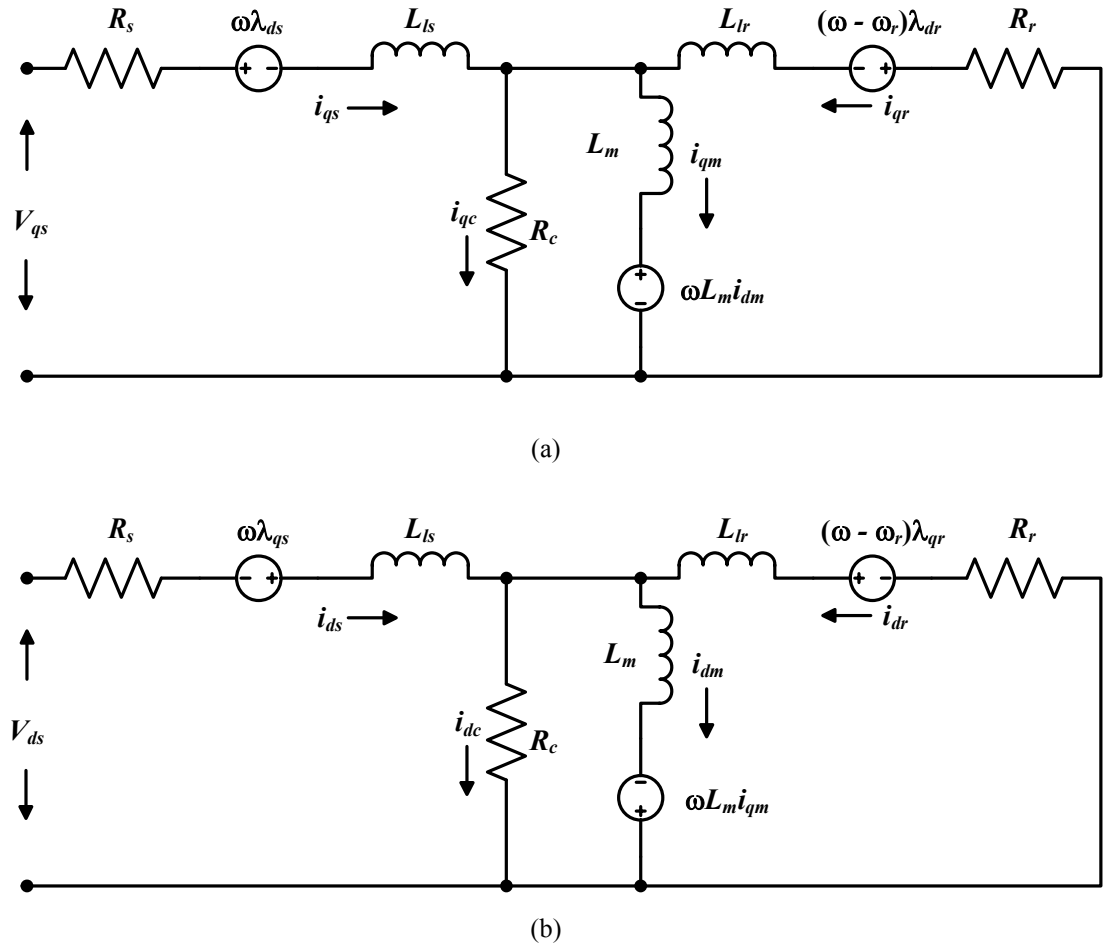

Fig: 4.1: Dynamic model of an induction motor including core loss. (a) q-axis. (b) d-axis.

4.1. MOTOR MODEL INCLUDING CORE LOSS

The three phase steady state induction motor model including core loss is well established [2] and so is the dynamic motor model [20] neglecting core loss. However, not much attention has been paid to the dynamic model as far as the inclusion of core is concerned. Considering this thesis deals with minimization of the losses it is of utmost importance that a dynamic model with core loss included is developed. An extension of

the model presented in [20] was proposed by [23]. The equations depicting the induction motor including core loss are depicted by the following equations:

Voltage equations:

$$v_{qs} = R_s i_{qs} + p\lambda_{qs} + \omega\lambda_{ds} \tag{4.1}$$

$$v_{ds} = R_s i_{ds} + p\lambda_{ds} - \omega\lambda_{qs} \tag{4.2}$$

$$v_{qr} = 0 = R_r i_{qr} + (\omega - \omega_r)\lambda_{dr} + p\lambda_{qr} \tag{4.3}$$

$$v_{dr} = 0 = R_r i_{dr} - (\omega - \omega_r)\lambda_{qr} + p\lambda_{dr} \tag{4.4}$$

It should be noted that the voltage has been equated to zero in equation (4.3) and (4.4) because in a squirrel cage induction motor the rotor bars are shorted with end rings.

Current equations:

$$R_c i_{qc} = L_m p i_{qm} + \omega L_m i_{dm} \tag{4.5}$$

$$R_c i_{dc} = L_m p i_{dm} - \omega L_m i_{qm} \tag{4.6}$$

$$i_{qs} + i_{qr} = i_{qm} + i_{qc} \tag{4.7}$$

$$i_{ds} + i_{dr} = i_{dm} + i_{dc} \tag{4.8}$$

Flux equations:

$$\lambda_{qs} = L_{ls} i_{qs} + L_m i_{qm} \tag{4.9}$$

$$\lambda_{ds} = L_{ls} i_{ds} + L_m i_{dm} \tag{4.10}$$

$$\lambda_{qr} = L_{lr} i_{qr} + L_m i_{qm} \tag{4.11}$$

$$\lambda_{dr} = L_{lr} i_{dr} + L_m i_{dm} \tag{4.12}$$

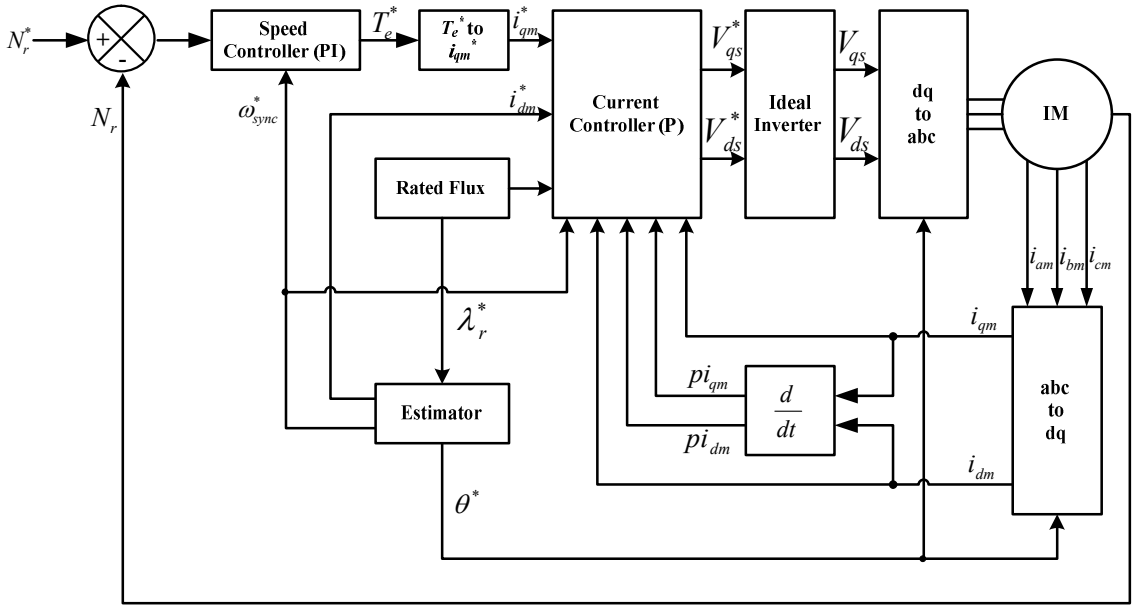

Fig. 4.2: Block diagram implementing vector control with core loss included in the modeling.

Mechanical equations

$$T_e = \frac{3P}{4}\frac{L_m}{\left(L_{lr}+L_m\right)}\left\{\lambda_{dr}\left(i_{qs}-i_{qc}\right)-\lambda_{qr}\left(i_{ds}-i_{dc}\right)\right\} \tag{4.13}$$

$$T_e - T_l = \frac{2J}{P}p\omega_r \tag{4.14}$$

It should be noted here that addition of core loss in the model of an induction motor increases the order of the system by two.

4.2. INDIRECT FIELD ORIENTED VECTOR CONTROL

In chapter 3 all the necessary expressions for vector control were derived. The theory essentially remains the same apart from the changes observed in the equations which will be elaborated in this section. Including the core loss element increases the order induction motor equations by two. Along with that, the control variable can no

longer be chosen as the stator currents. Magnetizing currents are chosen as the control variables to implement vector control when core loss is included in the modeling of an induction motor. The block diagram for explaining this method is shown in figure 4.2.

The three main criteria for vector control are reiterated again. They are as follows:

- $\lambda_{dr} = \lambda_r$, a constant at steady state (4.15)
- $\lambda_{qr} = 0, \frac{d\lambda_{qr}}{dt} = 0$ (4.16)
- $\frac{d\lambda_{dr}}{dt} = 0$, when in steady state (4.17)

With the above conditions in mind the equations for vector control can now be derived.

Thus, after substituting $\lambda_{dr} = \lambda_r$, equation (4.12) can be written as

$$\lambda_r = L_{lr} i_{dr} + L_m i_{dm} \tag{4.18}$$

From (4.18),

$$i_{dr} = \frac{\lambda_r - L_m i_{dm}}{L_{lr}} \tag{4.19}$$

Substituting (4.19) in (4.4) yields

$$R_r \left(\frac{\lambda_r - L_m i_{dm}}{L_{lr}} \right) - (\omega - \omega_r)\lambda_{qr} + p\lambda_{dr} = 0 \tag{4.20}$$

Introducing the conditions (4.15) and (4.17) in (4.20) reduces it to

$$\lambda_r = L_m i_{dm} \tag{4.21}$$

Substituting (4.16) in (4.11) yields

$$i_{qr} = \frac{-L_m i_{qm}}{L_{lr}} \tag{4.22}$$

Again, substituting (4.22) in (4.3) yields

$$R_r\left(\frac{-L_m i_{qm}}{L_{lr}}\right) + (\omega - \omega_r)\lambda_{dr} + p\lambda_{qr} = 0 \tag{4.23}$$

Writing $\omega - \omega_r = \omega_{sl}$ and introducing the conditions (4.15) and (4.16) in (2.23) gives

$$\omega_{sl} = \frac{R_r L_m i_{qm}}{\lambda_r L_{lr}} \tag{4.24}$$

Substituting (4.15), (4.16) and (4.22) in the torque equation numbered (4.13) yields

$$T_e = \frac{3P}{4}\frac{L_m}{(L_{lr} + L_m)}\left\{\lambda_r i_{qm}\left(1 + \frac{L_m}{L_{lr}}\right)\right\} \tag{4.25}$$

From the above equations it is evident that the d and q-axis currents have been decoupled and are completely independent of each other.

4.3. DESIGNING THE CONTROLLER

Now that the equations for vector control have been derived, focus should now be shifted to the requirements of the PI controller. There will be three controllers in used in the entire system. One PI controller will be for the outer loop or the speed control loop. The inner loop or the current control loop will be controlled using a proportional or P

controller. First, the transfer function of the inner loop needs to be calculated and then the same can be calculated for the outer loop.

4.3.1. REQUIREMENTS OF THE CURRENT LOOP CONTROLLER

Unlike classical vector control, where the core loss element is neglected, the control variable for vector control with loss included will be i_{qm} and i_{dm}, the q and d-axis magnetizing currents respectively.

From (4.5)

$$i_{qc} = \frac{L_m}{R_c} p i_{qm} + \frac{\omega L_m}{R_c} i_{dm} \tag{4.26}$$

Similarly from (4.6)

$$i_{dc} = \frac{L_m}{R_c} p i_{dm} - \frac{\omega L_m}{R_c} i_{qm} \tag{4.27}$$

Substituting (4.22) and (4.26) in (4.7)

$$i_{qs} = i_{qm}\left(1 + \frac{L_m}{L_{lr}}\right) + \frac{L_m}{R_c} p i_{qm} + \frac{\omega L_m}{R_c} i_{dm} \tag{4.28}$$

Similarly substituting (4.19) and (4.27) in (4.8)

$$i_{ds} = i_{dm}\left(1 + \frac{L_m}{L_{lr}}\right) + \frac{L_m}{R_c} p i_{dm} - \frac{\omega L_m}{R_c} i_{qm} - \frac{\lambda_r}{L_{lr}} \tag{4.29}$$

Having expressed the stator currents in terms of magnetizing currents, the stator fluxes now need to be expressed in terms of the magnetizing currents

Substituting (4.28) in (4.9)

$$\lambda_{qs} = i_{qm}\left[L_{ls}\left\{1+\frac{L_m}{L_{lr}}\right\} + L_m \right] + \frac{L_{ls}L_m}{R_c}\, pi_{qm} + \frac{\omega L_{ls}L_m}{R_c}\, i_{dm} \tag{4.30}$$

Similarly, substituting (4.29) in (4.10)

$$\lambda_{ds} = i_{dm}\left[L_{ls}\left\{1+\frac{L_m}{L_{lr}}\right\} + L_m \right] + \frac{L_{ls}L_m}{R_c}\, pi_{dm} - \frac{\omega L_{ls}L_m}{R_c}\, i_{qm} - \frac{L_{ls}\lambda_r}{L_{lr}} \tag{4.31}$$

Equations (4.30) and (4.31) appear visually cumbersome. In order to keep maintain the aesthetics of the above mentioned equations a substitution is made where

$$\sigma = L_{ls}\left\{1+\frac{L_m}{L_{lr}}\right\} + L_m \tag{4.32}$$

Substituting (4.32) in (4.30) and (4.31) yields

$$\lambda_{qs} = \sigma i_{qm} + \frac{L_{ls}L_m}{R_c}\, pi_{qm} + \frac{\omega L_{ls}L_m}{R_c}\, i_{dm} \tag{4.33}$$

$$\lambda_{ds} = \sigma i_{dm} + \frac{L_{ls}L_m}{R_c}\, pi_{dm} - \frac{\omega L_{ls}L_m}{R_c}\, i_{qm} - \frac{L_{ls}\lambda_r}{L_{lr}} \tag{4.34}$$

Equations (4.1) and (4.2) will be considered. Investigation reveals that both these q and d-axis voltages are in terms of stator currents and stator fluxes. Considering the control variable is the magnetizing current, the final step would be to express the stator voltages in terms of magnetizing currents. It should be noted that making the necessary substitutions will yield an extremely complex expression. Hence each voltage equation,

v_{qs} and v_{ds}, will be expressed as a sum of two terms. These terms will be examined separately for ease of analysis.

Let us assume

$$v_{qs} = v_{qs}^{'} + v_{qs\_comp} \tag{4.35}$$

$$v_{ds} = v_{ds}^{'} + v_{ds\_comp} \tag{4.36}$$

Where

$$v_{qs}^{'} = i_{qm}\left[R_s\left(1+\frac{L_m}{L_{lr}}\right)-\frac{\omega^2 L_{ls}L_m}{R_c}i_{qm}\right]+pi_{qm}\left[\frac{R_sL_m}{R_c}+\sigma\right]+\frac{L_{ls}L_m}{R_c}p^2 i_{qm} \tag{4.37}$$

$$v_{qs\_comp} = i_{dm}\left[\frac{\omega R_s L_m}{R_c}+\omega\sigma\right]+\frac{2\omega L_{ls}L_m}{R_c}pi_{dm}-\frac{\omega L_{ls}\lambda_r}{L_{lr}} \tag{4.38}$$

$$v_{ds}^{'} = i_{dm}\left[R_s\left(1+\frac{L_m}{L_{lr}}\right)-\frac{\omega^2 L_{ls}L_m}{R_c}i_{qm}\right]+pi_{dm}\left[\frac{R_sL_m}{R_c}+\sigma\right]+\frac{L_{ls}L_m}{R_c}p^2 i_{dm} \tag{4.39}$$

$$v_{ds\_comp} = -\left[i_{qm}\left\{\frac{\omega R_s L_m}{R_c}+\omega\sigma\right\}+\frac{2\omega L_{ls}L_m}{R_c}pi_{qm}+\frac{R_s\lambda_r}{L_{lr}}\right] \tag{4.40}$$

Upon closer inspection of equations (4.35) and (4.36), it can be concluded that both v_{qs} and v_{ds} are functions of i_{qm} and i_{dm} .This means there is coupling between the q and d-axis terms. Due to this coupling, any change in one variable will influence the other variable, which is unwanted as the basic idea of vector control is to make the AC machine behave like a shunt DC motor. To overcome this problem a method is adopted, generally known

as compensation. In essence, the controller generates two signals which negates the effect of the cross coupling terms v_{qs_comp} and v_{ds_comp}. The signal that assists in decoupling is generally added to the output of the current regulator [21] as shown in the figure 4.4.

Applying Laplace transform to (4.35) yields,

$$V_{qs}(s) = I_{qm}(s)\left[\left\{R_s\left(1+\frac{L_m}{L_{lr}}\right)-\frac{\omega^2 L_{ls}L_m}{R_c}\right\}+s\left\{\frac{R_s L_m}{R_c}+\sigma\right\}+s^2\frac{L_{ls}L_m}{R_c}\right]+V_{qs\_comp}(s) \quad (4.41)$$

Solving for $I_{qm}(s)$, we get

$$I_{qm}(s) = \frac{V_{qs}(s)-V_{qs\_comp}(s)}{\left\{R_s\left(1+\frac{L_m}{L_{lr}}\right)-\frac{\omega^2 L_{ls}L_m}{R_c}\right\}+s\left\{\frac{R_s L_m}{R_c}+\sigma\right\}+s^2\frac{L_{ls}L_m}{R_c}} \quad (4.42)$$

Similarly, applying Laplace transform to (4.36) yields,

$$V_{ds}(s) = I_{dm}(s)\left[\left\{R_s\left(1+\frac{L_m}{L_{lr}}\right)-\frac{\omega^2 L_{ls}L_m}{R_c}\right\}+s\left\{\frac{R_s L_m}{R_c}+\sigma\right\}+s^2\frac{L_{ls}L_m}{R_c}\right]-V_{ds\_comp}(s) \quad (4.43)$$

Again, solving for $I_{dm}(s)$, we get

$$I_{dm}(s) = \frac{V_{ds}(s)+V_{ds\_comp}(s)}{\left\{R_s\left(1+\frac{L_m}{L_{lr}}\right)-\frac{\omega^2 L_{ls}L_m}{R_c}\right\}+s\left\{\frac{R_s L_m}{R_c}+\sigma\right\}+s^2\frac{L_{ls}L_m}{R_c}} \quad (4.44)$$

4.3.2. CALCULATING THE PROPORTIONAL GAIN OF THE CURRENT LOOP CONTROLLER

A simple proportional (P) control will be used to regulate the inner or current loop. Such a controller was chosen to avoid increasing the order of the transfer function as will be in the calculations to follow.

I. Transfer Function of a Closed Loop

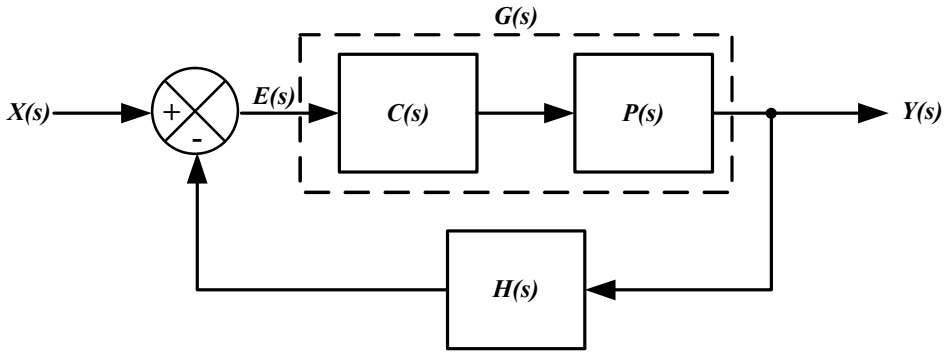

Fig. 4.3: Representation of a simple feedback loop.

Mathematically, transfer function is defined as the ratio of Laplace transform of the output of the system to the Laplace transform of the input, given that all initial conditions are zero [24]. Figure 4.2shows a simple feedback loop. It consists of an error calculator which generates a signal $E(s)$, a controller $C(s)$, a plant $P(s)$ and a feedback loop with delay of $H(s)$.The input and output to the system are denoted by $X(s)$ and $Y(s)$ respectively.

$$TF = \frac{Y(s)}{X(s)} \tag{4.45}$$

$$Y(s) = E(s).C(s).P(s) \tag{4.46}$$

$$E(s) = X(s) - Y(s).H(s) \tag{4.47}$$

Substituting (4.47) in (4.46)

$$Y(s) = \left[X(s) - Y(s).H(s)\right]G(s) \tag{4.48}$$

Where $G(s) = C(s).P(s)$

Simplifying (4.48) will yield the transfer function as stated below

$$\frac{Y(s)}{X(s)} = \frac{G(s)}{1 + G(s).H(s)} \tag{4.49}$$

II. Design Methodology to Determine Proportional Gain

It can be seen that equations (4.42) and (4.44) have the same denominator. Again, from figure 4.4, it can be easily concluded that both q and d-axis loops have the same parameters. Thus, any one closed loop system can be considered to calculate the expression for proportional gain.

The denominator of equation (4.42) is considered.

Let

$$C_1 = \frac{L_{ls} L_m}{R_c}$$

$$C_2 = \frac{R_s L_m}{R_c} + \sigma$$

$$C_3 = R_s \left(1 + \frac{L_m}{L_{lr}}\right) - \frac{\omega^2 L_{ls} L_m}{R_c}$$

The plant in *s* domain can be written as

$$P(s) = \frac{1}{s^2 C_1 + s C_2 + C_3} \tag{4.50}$$

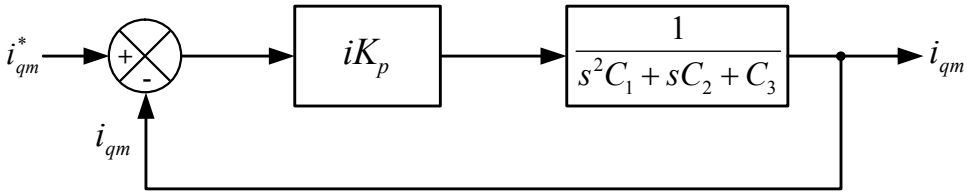

(a)

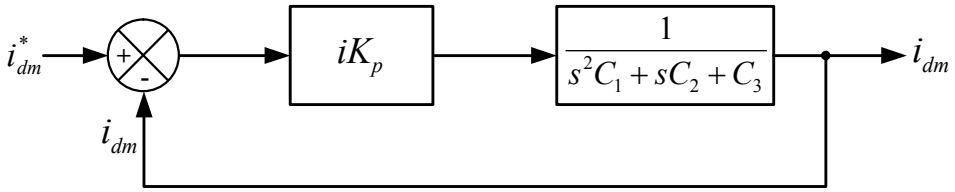

(b)

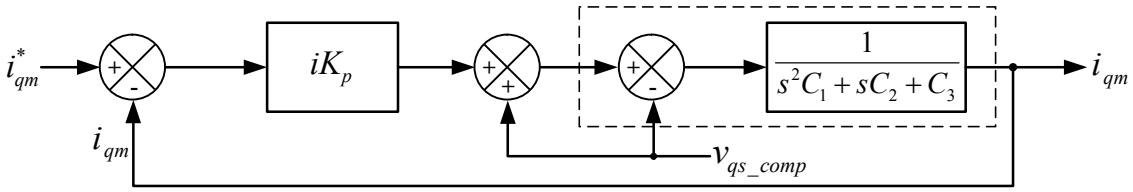

(c)

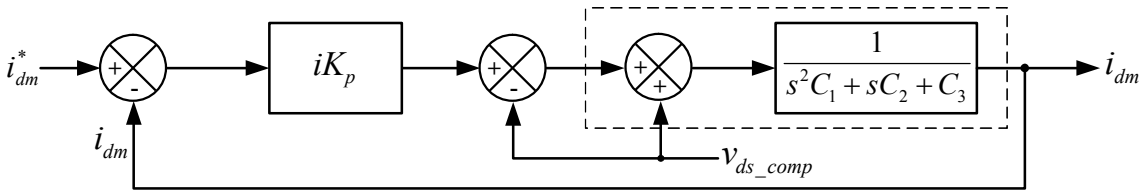

(d)

Fig. 4.4: Dynamics of the current control loop. (a) Q-axis. (b) D-axis. (c) Q-axis with compensation mechanism. (d) D-axis with compensation mechanism.

The controller equation in s domain is given by

$$C(s) = iK_p \tag{4.51}$$

$$\begin{aligned} \therefore G(s) &= C(s).P(s) \\ &= \frac{iK_p}{s^2C_1 + sC_2 + C_3} \end{aligned} \tag{4.52}$$

$$H(s) = 1 \tag{4.53}$$

$$\begin{aligned} 1 + G(s).H(s) &= 1 + \frac{iK_p}{s^2C_1 + sC_2 + C_3} \\ &= \frac{s^2C_1 + sC_2 + C_3 + K_p}{s^2C_1 + sC_2 + C_3} \end{aligned} \tag{4.54}$$

Substituting equations (4.52), (4.53) and (4.54) in (4.49) will provide us with the transfer function. After simplification, the transfer function for the inner loop is as follows.

$$TF_{in} = \frac{iK_p / C_1}{s^2 + sC_2 / C_1 + \left(C_3 + iK_p\right) / C_1} \tag{4.55}$$

The denominator of the transfer function thus obtained is called the characteristic function. This is of interest as the calculation of the controller parameters will be done using the characteristic equation. This denominator will now be compared to the standard characteristic equation for a second order transfer function which is given by

$$s^2 + 2\zeta_i\omega_{ni}s + \omega_{ni}^2 \tag{4.56}$$

Here *i* in the subscript denotes that these parameters represent the inner loop.

Comparison of the coefficients of the denominator of equation (4.55) and (4.56) yields

$$\frac{C_2}{C_1} = 2\zeta_i \omega_{ni} \tag{4.57}$$

$$\frac{C_3 + iK_p}{C_1} = \omega_{ni}^2 \tag{4.58}$$

From (4.57)

$$\omega_{ni} = \frac{C_2}{C_1 2\zeta_i} \tag{4.59}$$

Substituting (4.59) in (4.58) and simplifying the same yields

$$iK_p = \frac{C_2^2 +}{4\zeta_i^2 C_1} C_3 \tag{4.60}$$

This design method is called pole placement as the user is essentially choosing the poles of the system. By choosing ω_{ni} and ζ_i the user can choose the type of response that he wants as different values of these parameters will yield different responses. These parameters are commonly known as the performance parameter because they affect the behavior of the closed loop system. The parameter ω_{ni} determines the speed of the response and ζ_i determines the shape [25].

4.3.3. DESIGN METHODOLOGY OF THE OUTER SPEED LOOP CONTROLLER

The outer speed loop including the PI controller is shown in figure 4.5. The input to the outer loop is given by the user, which is the reference speed at which the user wants the motor to run. The actual speed is measured which is fed the error generator.

The error signal is then fed to the PI controller. The output of the PI controller is treated as the reference torque level. This reference torque is then used to generate the reference current level which is used as an input to the inner current control loop.

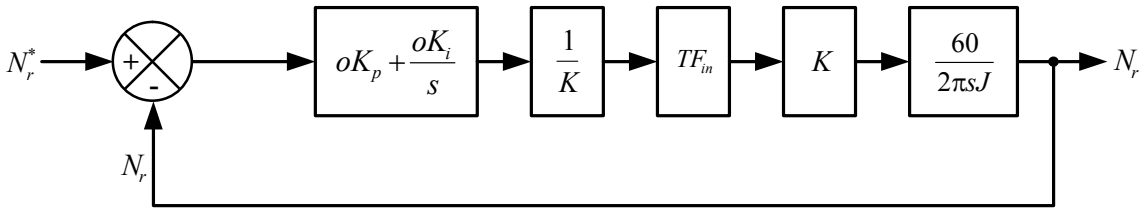

Fig. 4.5: Outer speed control loop

In order to calculate the transfer function of the outer loop we consider equation (4.25) and express current as function of torque. Applying Laplace transform to the same yields

$$I_{qm}(s) = \frac{T_e(s)}{K} \tag{4.61}$$

Where

$$K = \frac{3P}{4}\frac{L_m}{(L_{lr} + L_m)}\left(1 + \frac{L_m}{L_{lr}}\right)\lambda_r$$

For a PI controller the transfer function is given as

$$C(s) = oK_p + \frac{oK_i}{s} \tag{4.62}$$

From figure 4.4

$$G(s) = \left(oK_p + \frac{oK_i}{s} \right) \frac{1}{K} \left(\frac{iK_p}{s^2 C_1 + sC_2 + C_3 + iK_p} \right) \frac{60K}{s2\pi J} \tag{4.63}$$

Simplifying equation (4.63) eventually yields

$$G(s) = \frac{60iK_p \left(soK_p + oK_i \right)}{2\pi J \left[s^4 C_1 + s^3 C_2 + s^2 \left(C_3 + iK_p \right) \right]} \tag{4.64}$$

$$1 + G(s)H(s) = \frac{2\pi J \left[s^4 C_1 + s^3 C_2 + s^2 \left(C_3 + iK_p \right) \right] + 60iK_p \left(soK_p + oK_i \right)}{2\pi J \left[s^4 C_1 + s^3 C_2 + s^2 \left(C_3 + iK_p \right) \right]} \tag{4.65}$$

Using equations (4.64) and (4.65), the transfer function of the outer loop can be very easily calculated with the help of equation (4.49). After performing the necessary simplifications the denominator of the transfer function will be the same as the numerator of the equation (4.65), which, after simplification will yield

$$s^4 2\pi JC_1 + s^3 2\pi JC_2 + s^2 2\pi J \left(C_3 + iK_p \right) + s60iK_p oK_p + 60iK_p oK_i \tag{4.66}$$

From equation (4.66) it can be concluded that the transfer function is a fourth order transfer function. Calculating the gains of the PI controller using this characteristic equation is tedious. Thus, powers of s greater than three are neglected from the characteristic equation because neglecting the higher powers does not exhibit any visual change in the response of the system. Eventually, the numerator and the denominator of the transfer function are divided by $2\pi JC_2$. The characteristic equation, (4.66), thus reduces to

$$s^3 + \frac{s^2 \left(C_3 + iK_p \right)}{C_2} + \frac{s60iK_p oK_p}{2\pi JC_2} + \frac{60iK_p oK_i}{2\pi JC_2} \tag{4.67}$$

Equation (4.67) will now be compared with the standard characteristic equation of a third order system given by

$$s^3 + s^2\omega_{no}\left(2\zeta_o + \alpha\right) + s\omega_{no}^2\left(1 + 2\zeta_o\alpha\right) + \alpha\omega_{no}^3 \tag{4.68}$$

The subscript *o* in the equation above denotes that the parameters belong to the outer speed loop. Comparing the coefficients of (4.67) and (4.68) yields

$$\frac{C_3 + iK_p}{C_2} = \omega_{no}\left(2\zeta_o + \alpha\right) \tag{4.69}$$

$$\frac{60iK_poK_p}{2\pi JC_2} = \omega_{no}^2\left(1 + 2\zeta_o\alpha\right) \tag{4.70}$$

$$\frac{60iK_poK_i}{2\pi JC_2} = \alpha\omega_{no}^3 \tag{4.71}$$

From (4.69)

$$\alpha\omega_{no} = \frac{C_3 + iK_p}{C_2} - 2\zeta_o\omega_{no} \tag{4.72}$$

Substituting (4.72) in (4.71) and solving for oK_i

$$oK_i = \frac{2\pi JC_2\omega_{no}^2}{60iK_p}\left(\frac{C_3 + iK_p}{C_2} - 2\zeta_o\omega_{no}\right) \tag{4.73}$$

Again, substituting equation (4.72) in equation (4.71) and solving for oK_p

$$oK_p = \frac{2\pi JC_2\omega_{no}}{60iK_p}\left[\omega_{no} + 2\zeta_o\left(\frac{C_3 + iK_p}{C_2} - 2\zeta_o\omega_{no}\right)\right] \tag{4.74}$$

The values of ζ_o and ω_{no} need to be chosen appropriately so that the desired response can be obtained from the system.

5. LOSS MINIMIZATION CONTROLLER

5.1. LOSS REDUCTION TECHNIQUES

The operating point of an induction motor where it is driving full load is when it is most efficient. The issue, however, is that there are many applications where the motor needs to be driven at different loads. For vector controlled drives the motor is always fed with the rated flux. This condition, augmented with light loads, is highly undesirable because it is at these operating points that the inefficiency of induction motors begin to surface.

Only considering the losses in the induction motor is not enough. Most applications today use motor drives. Driving an induction motor through a drive also adds to the losses experienced by the total system. The components that add to the overall losses in the system are the converters. There are also some losses incurred due to the fact that the input voltages and currents are not perfect sinusoids.

It is therefore important to know which aspects of a motor drive contribute to losses. A typical IM drive is shown in figure5.1. From the diagram a rough idea of the losses can be derived. They are as follows:

- Losses contributed by the harmonics present in the input current that is drawn from the grid.
- Both the rectifier and the inverter contribute to losses due to switching and conduction. Also, current ripples are introduced by the pulse width modulation (PWM) converter which adds to the loss.

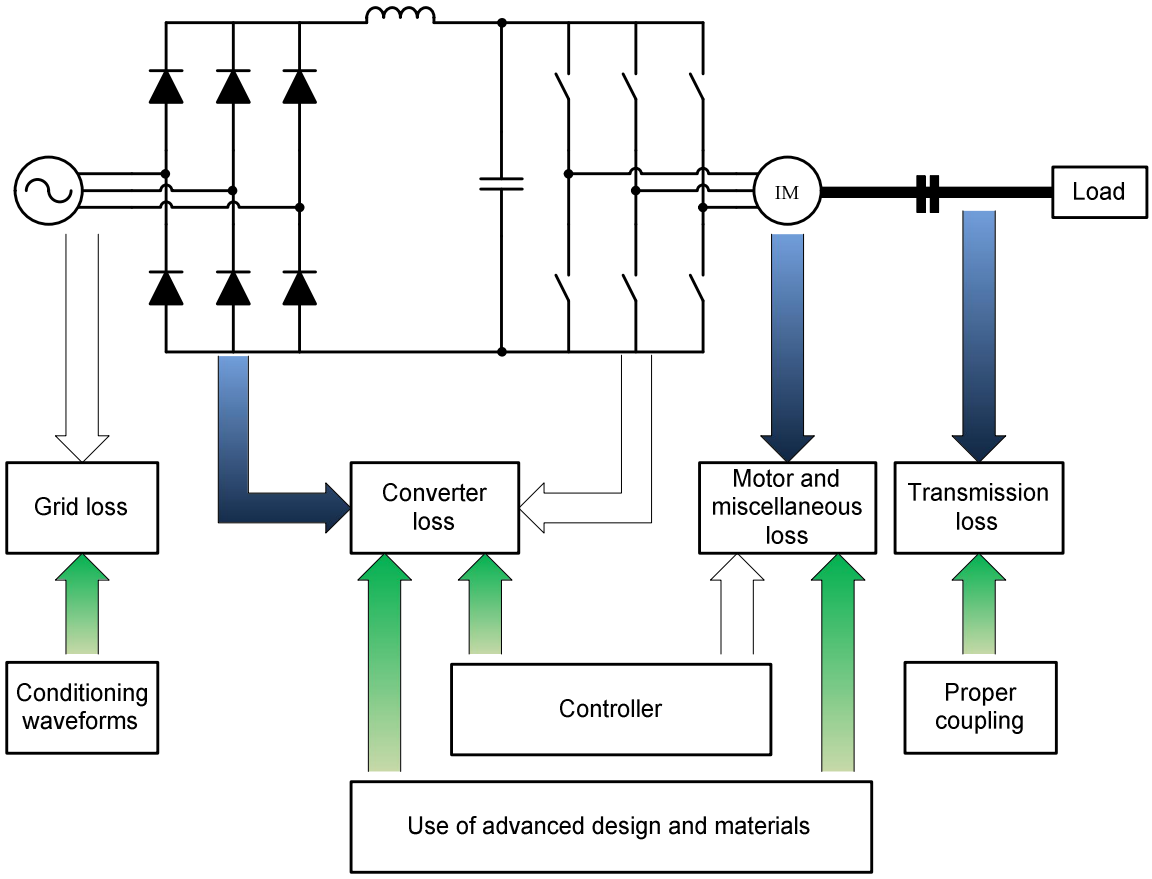

Fig. 5.1: Typical induction motor drive showing the losses incurred by each component (blue arrows) and the methodology used to improve the efficiency (green arrows).

- The currents being injected into the machine are responsible for causing losses in the motor, namely stator copper loss, core or iron loss and rotor copper loss.
- Miscellaneous losses such friction and windage losses also plague the induction motor although for practical purposes these losses can be neglected when compared to the previously mentioned losses.
- The method of coupling the load with the shaft of the motor also affects the efficiency. Belt and pulley system will generally be less efficient than direct coupling.

Here in this thesis, only stator, core and rotor losses are taken into consideration while deriving the condition to minimize the losses.

There are many avenues which can be chosen to facilitate reduction in losses. One method would be to choose different materials in the construction of the motor. Normally, aluminum was the metal of choice to fabricate the rotors for induction motors. The rotors would be fabricated by pressure die casting. Unfortunately, aluminum rotor induction motors could not exhibit the expected efficiency. Recently, copper has been chosen as an alternate to aluminum so far as the construction of the rotors are concerned. Recent studies have shown that using a copper rotor induction motor has increased the efficiency by 2.1% [26]. Use of copper and low hysteresis laminated steel in the construction of induction motors have proven to be useful in making the motors less prone to copper and iron losses [27, 28]. Proper conditioning of the input waveforms will reduce the harmonic losses [29, 30]. Developing a control technique which will solely be responsible for reducing the losses will further enhance the efficiency.

5.2. CONTROL STRATEGIES USED FOR LOSS MINIMIZATION

5.2.1. SEARCH CONTROL (SC)

The search controller is preferred by many researchers because the controller action works on the principle of input power measurement and does not depend on the machine parameters. The input power is measured and the appropriate value of the control variable is iteratively searched until the minimum input power is detected necessary to observe the same output power. It should be noted however that the rotor speed and torque expected at the shaft is assumed to be constant until the minimum input power is detected. An advantage of using this kind of a controller is that if the input power is measured, the losses that appear due to the rectifier can also be accounted for. Unfortunately, more sensors are needed to carry out this measurement and hence this

process can prove to be expensive. To overcome this shortcoming, the DC link power is measured which involves the use of an extra current sensor [31]. The biggest issue with this approach is that the input power must be accurately measured. If not measured properly the controller can exhibit oscillatory response [32]. Also, this kind of a controller is plagued by torque ripples [14 - 19].

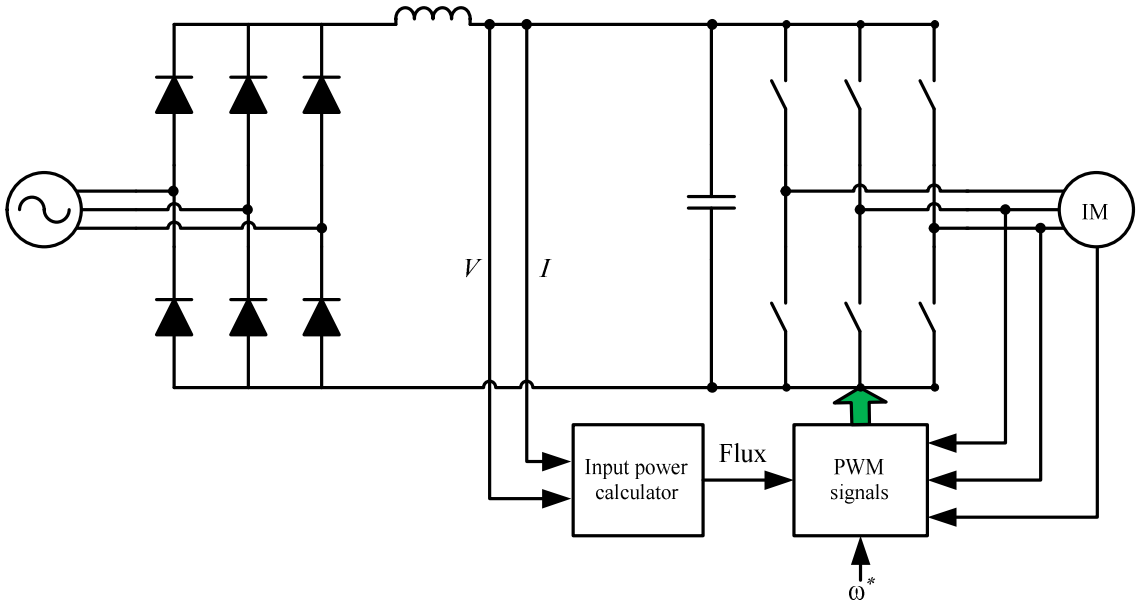

Fig. 5.2: Basic block diagram of a search controller.

5.2.2. LOSS MODEL BASED CONTROLLER (LMC)

LMC, unlike SC, uses the loss model to compute the loss minimization criteria. In this thesis the control variable is chosen to be the d-axis magnetizing current. Normally in vector control all the variables are expressed in d-q coordinates. The biggest advantage of using this approach is that it does not exhibit torque and has converges to a solution faster when compared to SC. However, considering that LMC utilizes the loss model, the performance of the controller is dictated by the accuracy of the model. Also, any

variation in parameters due to temperature changes and other factors will affect the controller performance unless these factors were taken into account during modeling.

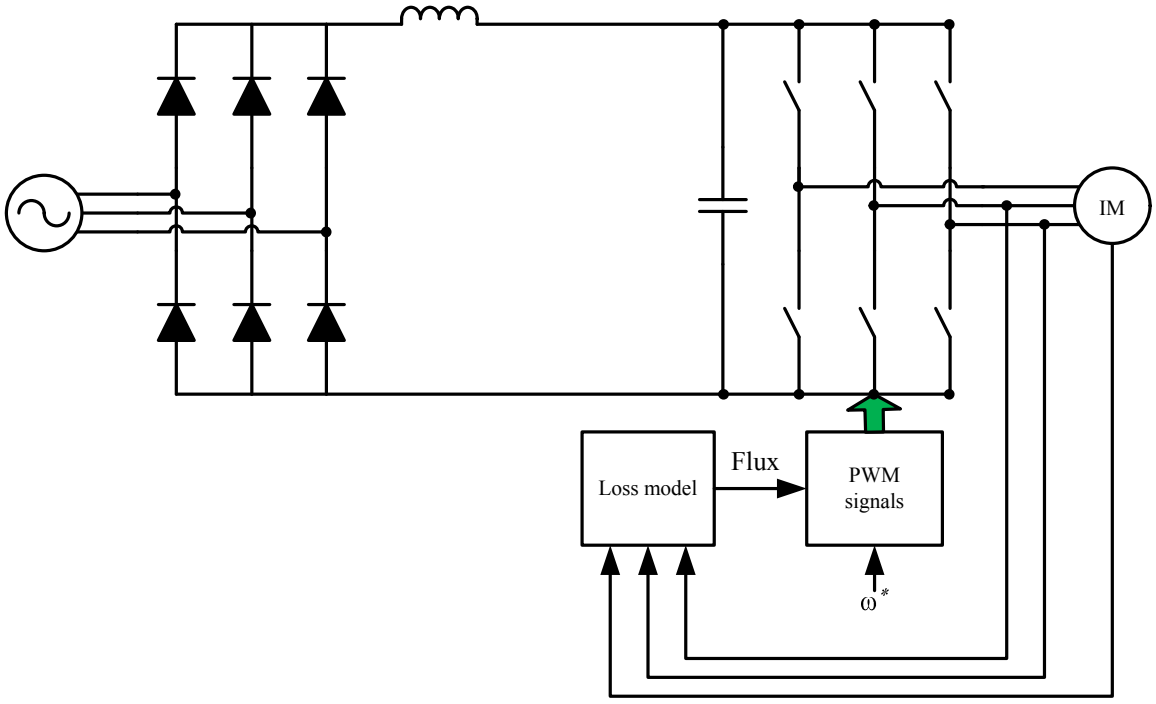

Fig. 5.3: Basic block diagram for loss minimization controller.

5.3. THEORY FOR MINIMIZING LOSSES

5.3.1. MODELING THE LOSSES

The three kinds of losses that have been included in this thesis are the stator copper loss, core loss and core loss or iron loss. The expressions for the different types of losses are being derived from the induction motor model as described in chapter 4. From the induction motor model the total loss is defined as:

$$\begin{aligned} P_{total} &= P_{SCL} + P_{Core} + P_{RCL} \\ &= R_s\left(i_{qs}^2 + i_{ds}^2\right) + R_c\left(i_{qc}^2 + i_{dc}^2\right) + R_r\left(i_{qr}^2 + i_{dr}^2\right) \end{aligned} \tag{5.1}$$

The losses have been modeled based on the classical definition which states that the total loss across any resistance is the product of the value of the resistance and the square of the current flowing through it. In this case there are two components of the current, one corresponds to the q-axis and the other denotes the d-axis component.

As already stated in chapter 4, the control variable chosen to implement this control strategy are the magnetizing currents. Thus, all the losses stated in equation (5.1) must be expressed in terms of magnetizing currents. Rewriting the losses with the correct substitutions yields

$$P_{SCL} = R_s \left[i_{qm}^2 \left\{ \left(1 + \frac{L_m}{L_{lr}} \right)^2 + \frac{\omega^2 L_m^2}{R_c^2} \right\} + i_{dm}^2 \left(1 + \frac{\omega^2 L_m^2}{R_c^2} \right) + 2 i_{qm} i_{dm} \frac{\omega L_m^2}{R_c L_{lr}} \right] \tag{5.2}$$

$$P_{Core} = \frac{\omega^2 L_m^2}{R_c} \left(i_{qm}^2 + i_{dm}^2 \right) \tag{5.3}$$

$$P_{RCL} = i_{qm}^2 \frac{R_r L_m^2}{L_{lr}^2} \tag{5.4}$$

5.3.2. CRITERIA FOR LOSS MINIMIZATION

In the previous section, the losses have been modeled in terms of the magnetizing current. The magnetizing current consists of two components, the q and d-axis components. In other words, the total loss is a function of two variables. It would be convenient, however, to express the total loss in terms of a single variable so that it is easier to calculate condition for loss minimization. Close inspection of equation (4.25) reveals that the electromagnetic torque T_e and q-axis magnetizing branch current i_{qm} are

correlated. Thus, expressing i_{qm} as a function of T_e will eliminate one variable from the total loss expression.

From (4.25)

$$i_{qm} = \frac{4T_e L_{lr}}{3PL_m \lambda_r} \tag{5.5}$$

The reason behind expressing i_{qm} as a function of electromagnetic torque is that for a particular operating point the torque is a constant. However, before equation (5.5) is plugged into the loss expressions it should be noted the rated flux λ_r can be expressed in terms of i_{dm}. Making this substitution in equation (5.5) yields

$$i_{qm} = \frac{4T_e L_{lr}}{3PL_m^2 i_{dm}} \tag{5.6}$$

Equation (5.6) successfully establishes a relationship between i_{qm} and i_{dm}. This means that all the losses, copper as well as core loss, can now be expressed in terms of a single variable i_{dm}, the d-axis magnetizing current.

Using equations (5.2), (5.3) and (5.4), the total loss expression can be written as

$$P_{total} = i_{qm}^2 K_1 + i_{dm}^2 K_2 + i_{qm} i_{dm} K_3 \tag{5.7}$$

Where

$$K_1 = R_s \left\{ \left(1 + \frac{L_m}{L_{lr}} \right)^2 + \frac{\omega^2 L_m^2}{R_c^2} \right\} + \frac{\omega^2 L_m^2}{R_c} + \frac{R_r L_m^2}{L_{lr}^2}$$

$$K_2 = R_s\left(1+\frac{\omega^2 L_m^2}{R_c^2}\right)+\frac{\omega^2 L_m^2}{R_c}$$

$$K_3 = \frac{2\omega L_m^2 R_s}{R_c L_{lr}}$$

Plugging in the equation (5.6) in (5.7) gives the total loss expression as a function of i_{dm} as shown below

$$P_{total} = \frac{1}{i_{dm}^2}\left(\frac{4T_e L_{lr}}{3PL_m^2}\right)^2 K_1 + i_{dm}^2 K_2 + \frac{4T_e L_{lr} K_3}{3PL_m^2} \tag{5.8}$$

At this point it should be noted that even though K_1, K_2 and K_3 are dependent on ω, like torque, the speed is also constant at a given operating point.

Differentiating equation (5.8) with respect to i_{dm} yields

$$\frac{dP_{total}}{di_{dm}} = -\frac{2}{i_{dm}^3}\left(\frac{4T_e L_{lr}}{3PL_m^2}\right)^2 K_1 + 2i_{dm}K_2 \tag{5.9}$$

For minimum loss equation (5.9) must be equated to zero. This results in

$$i_{dm\_opt} = \sqrt{\frac{4T_e L_{lr}}{3PL_m^2}} \times \sqrt[4]{\frac{K_1}{K_2}} \tag{5.10}$$

Equation (5.10) represents the reference d-axis magnetizing current that the controller should generate. This reference value of magnetizing current is responsible for changing the flux level of the machine. Changing the flux level is discouraged for fast torque response but this is essential in order to facilitate loss minimization.

5.4. BLOCK DIAGRAM OF THE PROPOSED SCHEME

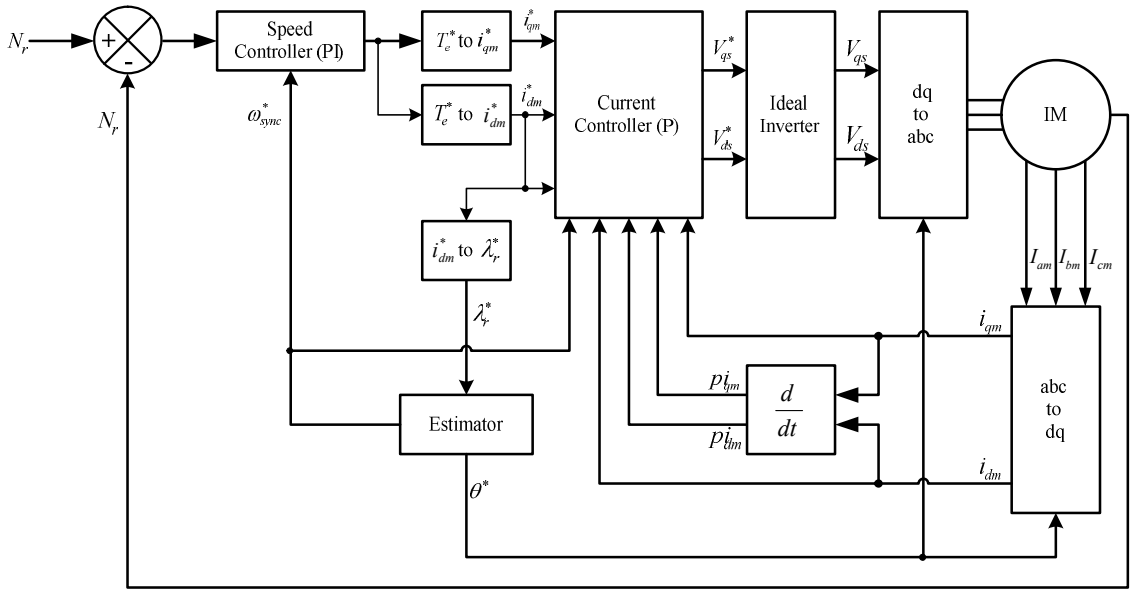

Fig. 5.4: Block diagram of proposed loss minimization controlled induction motor drive.

The block diagram of the proposed loss minimization scheme is shown in figure 5.4. The reference signal is an input from the user which dictates at what speed the user wants the machine to spin. This reference signal is fed to the error generator. The other input that is fed to the error generator is the actual speed of the rotor. The actual speed is measured value obtained with the help of a speed encoder. The error generator calculates the difference between the reference speed and the actual speed and yields an error signal which is then fed to the speed controller. The speed controller is responsible for generating a reference torque level. The reference torque level has an extremely important part to play because both the reference levels for magnetizing currents will be derived from this single torque reference. The first current reference to be calculated will be the q-axis magnetizing current. This will be generated using the equation (4.25). The d-axis magnetizing current will then be calculated using equation (5.10) required to

implement minimum loss condition. The reference rotor flux level can now be generated very easily which will then be fed to the estimator. The estimator will have two output signals. They are the reference synchronous speed and the angle of transformation. The reference synchronous speed is fed to the speed controller and the current controller because the gains of both the controllers are dependent on the synchronous speed. The other inputs to the current controller include the reference magnetizing current signals and the measured magnetizing currents. The current controller finally generates an output signal synonymous with the voltage needed to run the induction motor. In this diagram an ideal inverter is considered for simplicity.

6. SIMULATION RESULTS

In this chapter all the results obtained through this research will be presented. There will be three sections to this chapter. The first section of this chapter will showcase the characteristics of an induction motor under direct online (DOL) starting conditions. The second section will provide details on the vector control of the same induction motor followed by section three which will demonstrate the operation and the performance of the loss minimization controller. MATLAB/Simulink was used to program the necessary equations to successfully develop the computer model. The parameters of the 7.5 hp induction motor used to obtain all the results are listed in the appendix.

6.1. DOL STARTING OF INDUCTION MOTOR

It has been proved time and again as to how effective and capable the dynamic model of the induction motor is. However, potency of the induction motor model with core loss included needs to be established because of its limited use in the field of study. In this section the behavior of the induction motor will be demonstrated when it undergoes DOL starting. In DOL starting the motor is directly connected to the grid. There are no drives involved in this starting procedure.

The induction under consideration is supplied with the rated voltage. Unlike in real scenarios the voltage is considered to be a perfect sinusoid and free from any harmonics. This is depicted in figure 6.1. As mentioned in chapter 3, there are three reference frames for orientation of the induction motor. In this thesis only the synchronously rotating reference frame is considered. The primary reason for this is that any sinusoid in three phase is transformed to DC values when viewed from this reference

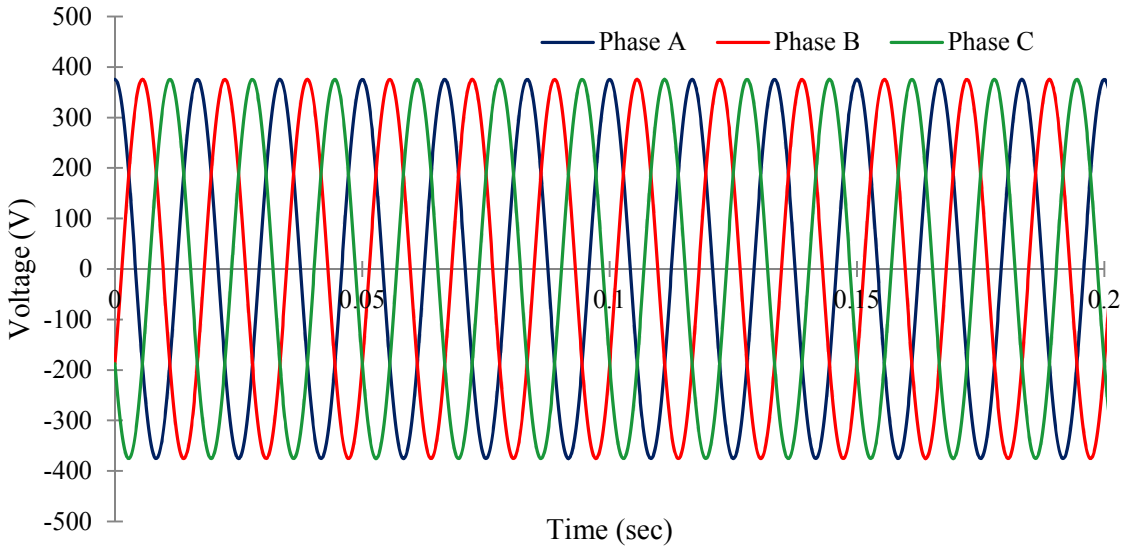

Fig. 6.1: Three phase voltage supplied to the induction motor from the grid.

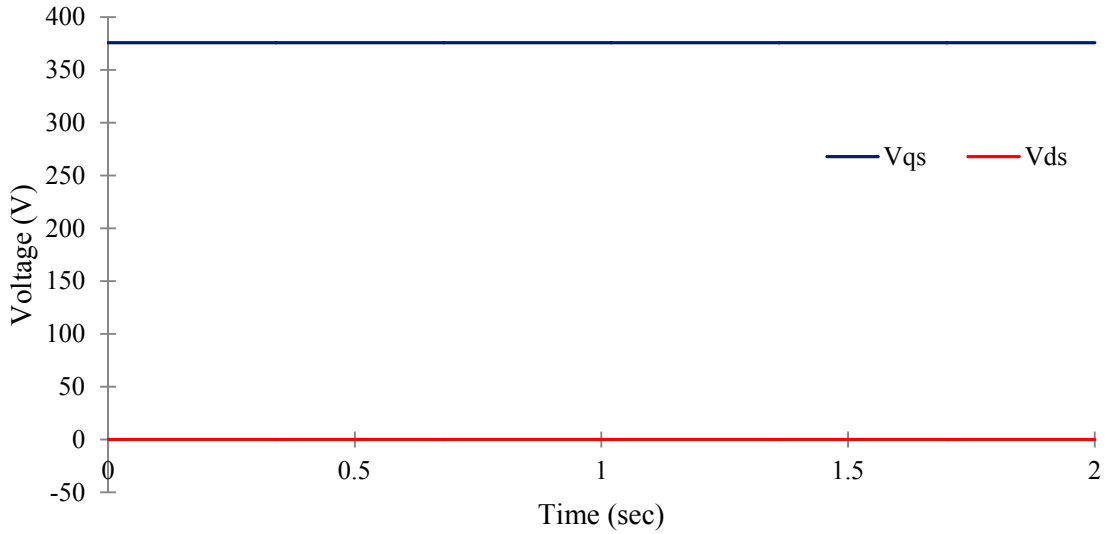

Fig 6.2: Two axis representation of three phase voltage in synchrounously rotatin reference frame.

frame. This is especially helpful when designing a controller as DC values are easier to analyze. Figure 6.2 depicts the same waveform as presented in figure 6.1 but in synchronously rotating reference frame.

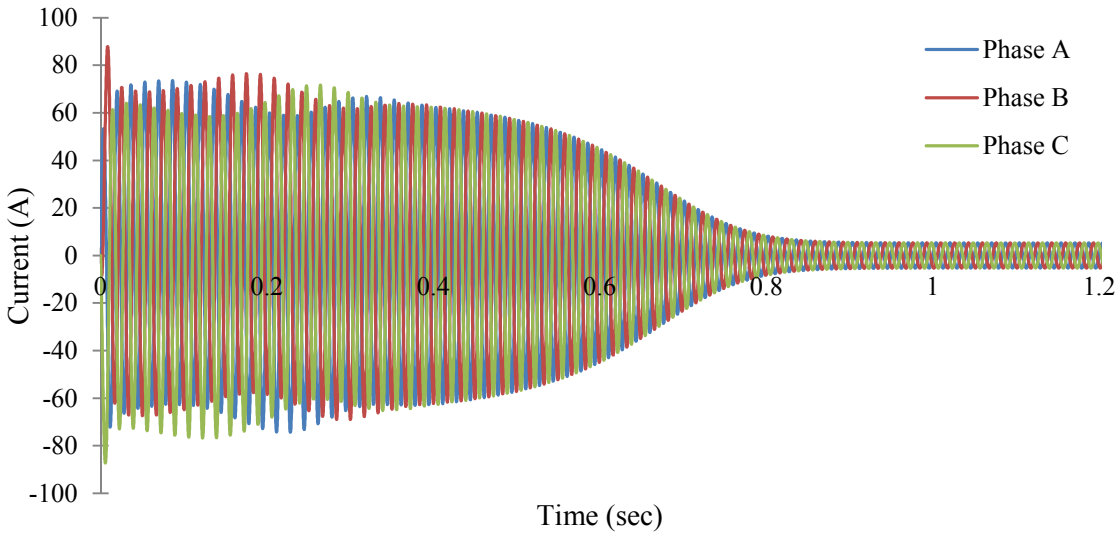

(a)

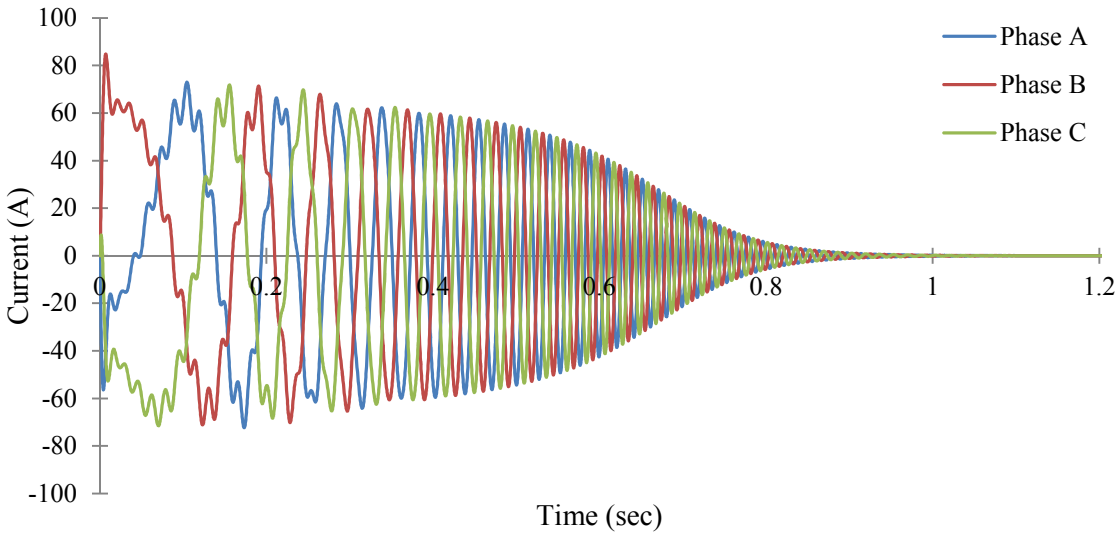

(b)

Fig. 6.3: Starting current in an induction motor. a) Stator current. b) Rotor current.

The total rotor resistance of an induction motor is known to be $R_r/s+j\omega L_{lr}$ from the steady state circuit of an induction motor. R_r and ωL_{lr} are constant (considering the frequency of the grid is constant). Thus, the only variable is the slip s. Just at the moment when the rotor begins to spin the value of slip is unity. As the rotor begins to speed up the value of the slip gradually decreases. Thus, at starting the total impedance of the rotor is less than when the rotor has gained speed. This is the reason why the current in the rotor of an induction is high at starting. As the stator is connected to the grid, and the power flows from the stator to the rotor, the stator current is also high in the beginning. As the motor attains its set speed, currents in both the stator and the rotor minimize. If the rotor is spinning very close to the synchronous speed, the slip is very low and the effective impedance of the rotor is very high. Because of this rotor hardly carries any current. At this stage the current drawn by the machine is necessary to sustain its speed. Figure 6.3 gives a graphical interpretation of this phenomenon.

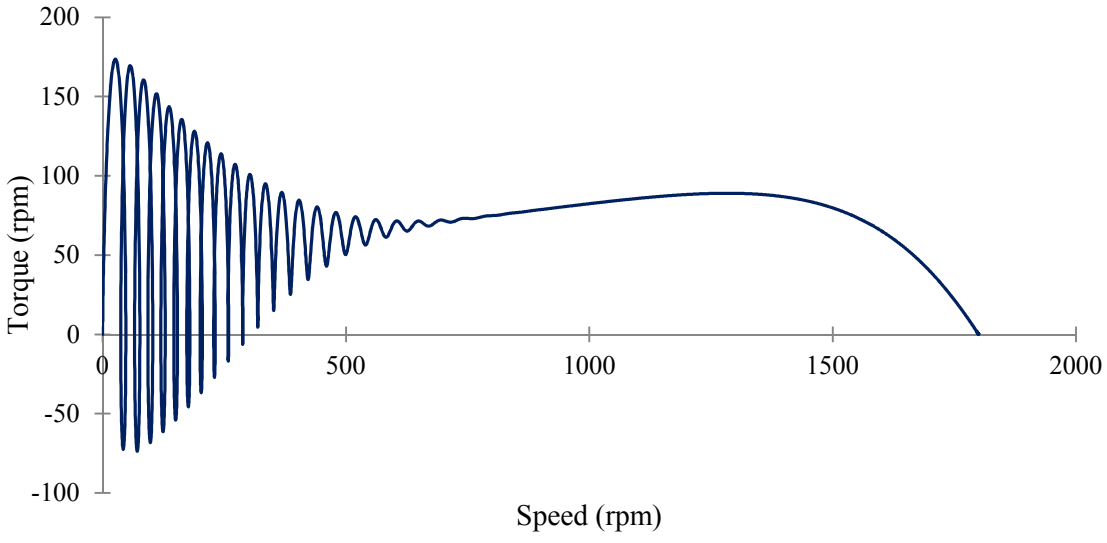

Fig. 6.4: Torque vs. speed characteristics of the 7.5 hp induction motor.

The next step is to look at the torque and speed profiles of the motor under review. By inspection of figure 6.4 it can be immediately concluded that the transient torque varies in nature than the steady state torque. The oscillations seen in figure 6.4 when the speed is close to zero varies at 60 Hz, the same as the supply frequency and varies about a mean value. It gradually decays as the motor attains steady state. Another interesting characteristic that can be inferred from the diagram is that the motor always tries to stay in the region defined by the linear region of the curve closer to the synchronous speed.

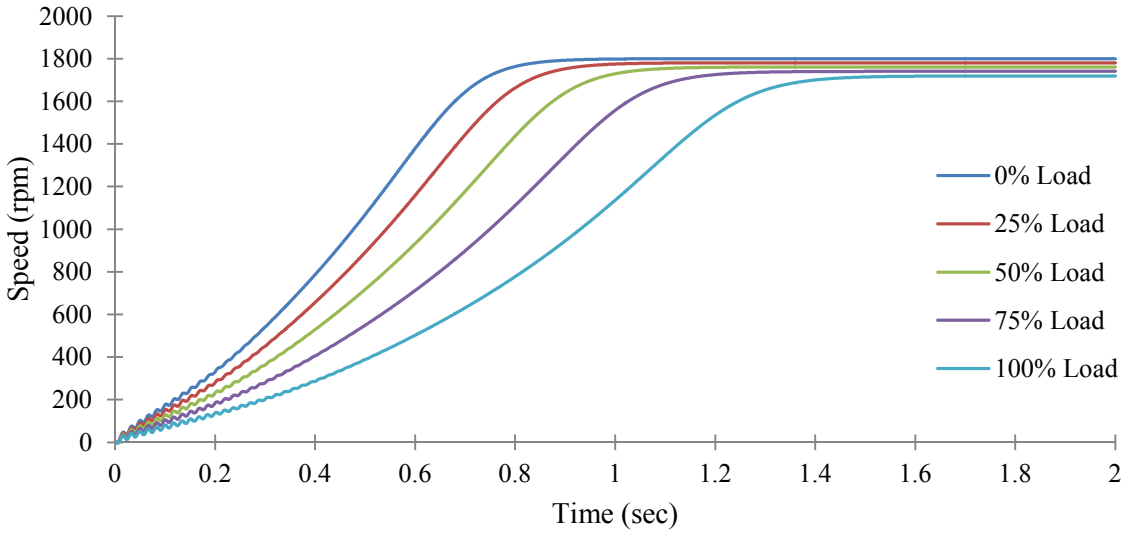

Fig. 6.5: Speed of the induction motor under different loading conditions.

The running of the motor is simulated under different loads varying from 0% to 100% in steps of 25%. Figure 6.5 describes the speed profile of the motor. As expected, the motor runs close to synchronous speed at 0% load and as the load increases the steady state speed of the motor settles at a lesser value. However, even at full load the speed of the motor is not drastically less than the synchronous speed (1800 rpm in this case). Figure 6.6 describes the speed profile when a step change in load occurs at 1.25 sec. It

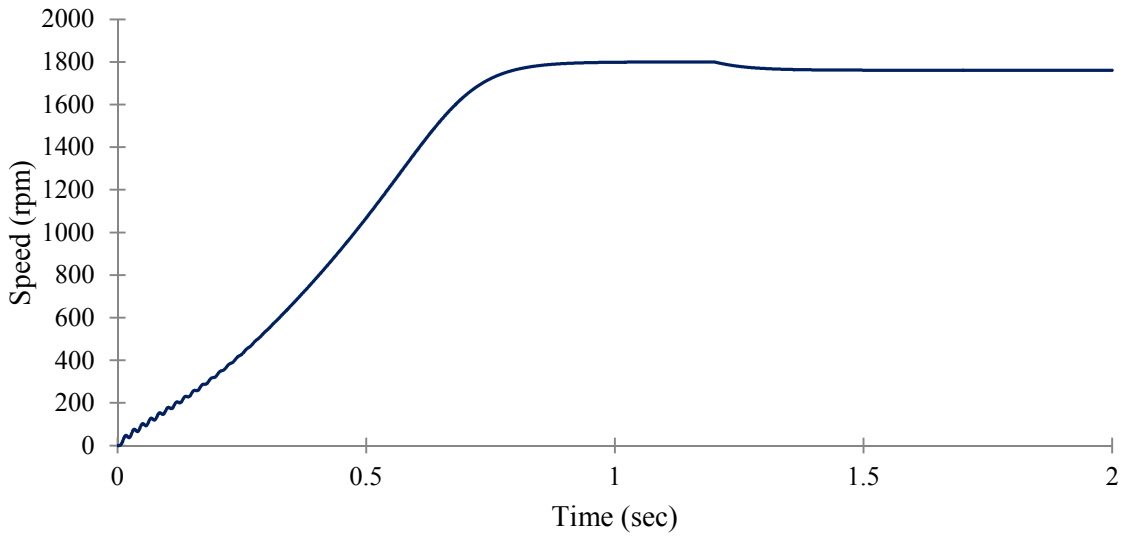

Fig. 6.6: Change in rotor speed due to loading variation from 0% to 50%.

can be concluded that the speed does not immediately drop but gradually decreases to a lower value and settles down.

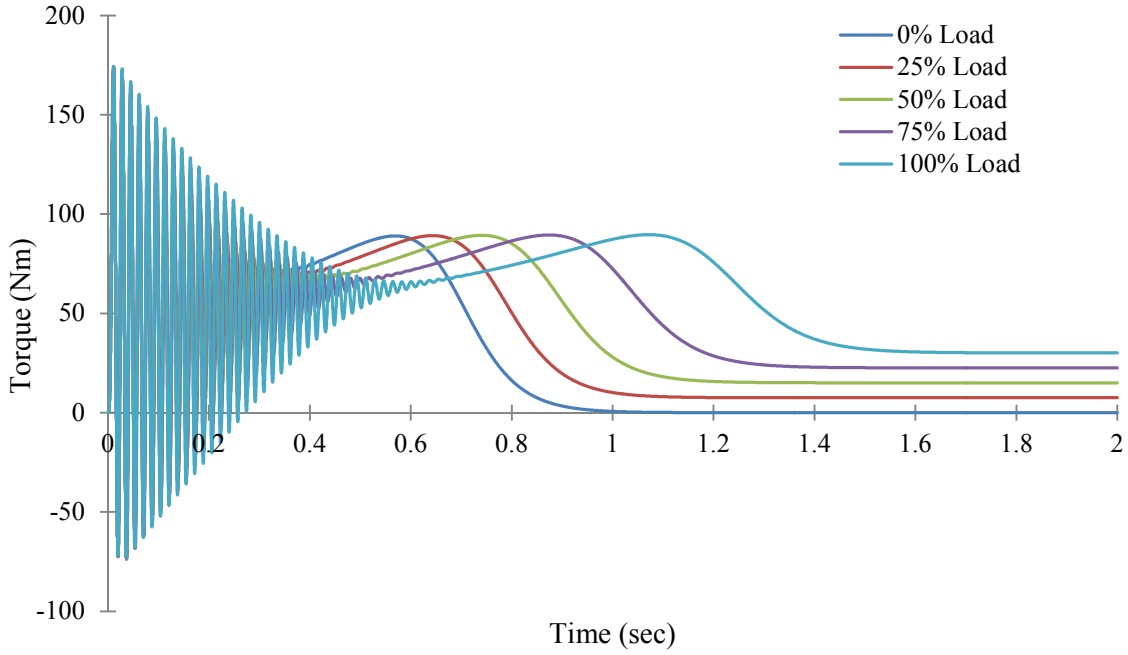

Fig. 6.7: Torque profile of the induction motor under different loading conditions.

Figure 6.7 showcase the torque profile of the motor under different loading conditions. This figure gives a clearer picture about the oscillations during the transient phase. There are 12 peaks in the torque profile till 0.2 secs. This proves that the frequency of these oscillations is equal to 60 Hz. Also the higher the percentage of load, the longer the machine takes to reach steady state. Figure 6.8 shows how the torque varies when a step change in load is introduced at 1.25 sec. Initially the motor started at no load. The increase in load to 50% makes the motor generate more torque to meet the load demand. As in the case of change in speed, the torque too takes some time to reach its ne steady state value.

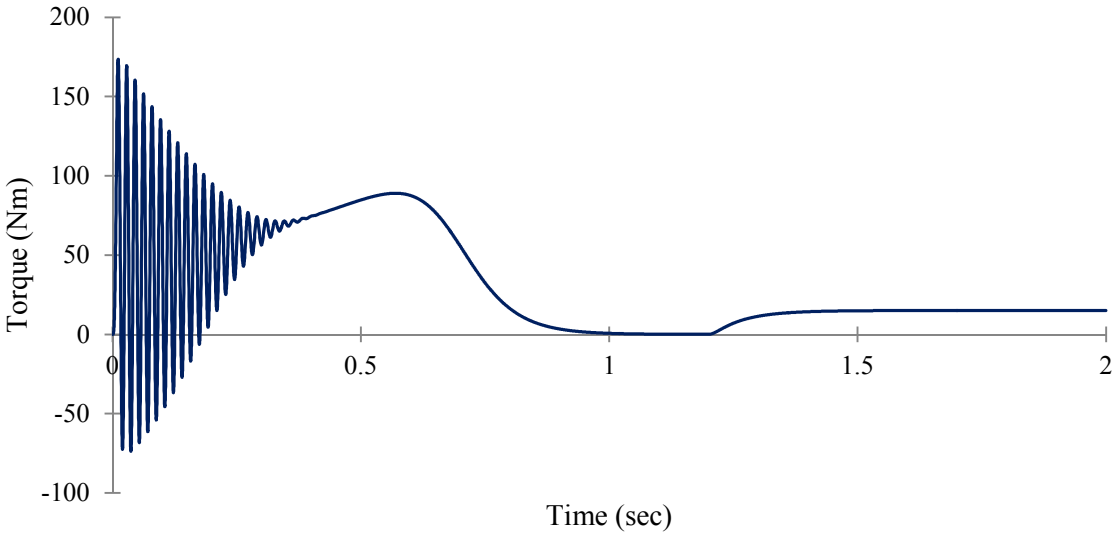

Fig. 6.8: Variation in torque when load changes from 0% to 50%.

Figures 6.9 to 6.12 shows how the currents vary during startup of the motor from no load to full load until it reaches steady state. The currents appear as DC because they are viewed from synchronously rotating reference frame. Due to the addition of the core loss figures 6.11 and 6.12 demonstrate how the currents vary in the core loss branch and

magnetizing branch respectively in addition to the stator and rotor currents, shown in figures 6.9 and 6.10. Figures 6.13 and 6.14 shows the changes in the amplitude of stator and rotor currents due to the step change in load from 0% to 50% at 1.25 sec. This figure shows the variation in currents as it would be seen in practice and not dq reference frame. Increase in rotor slip reduces the effective impedance of the rotor. Considering the supply is kept constant, the current drawn from the grid increases.

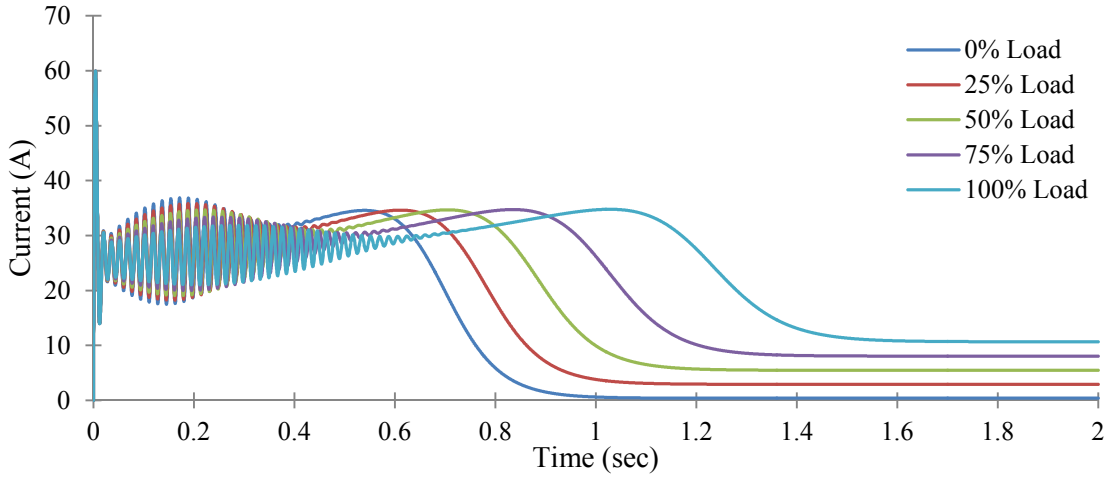

(a)

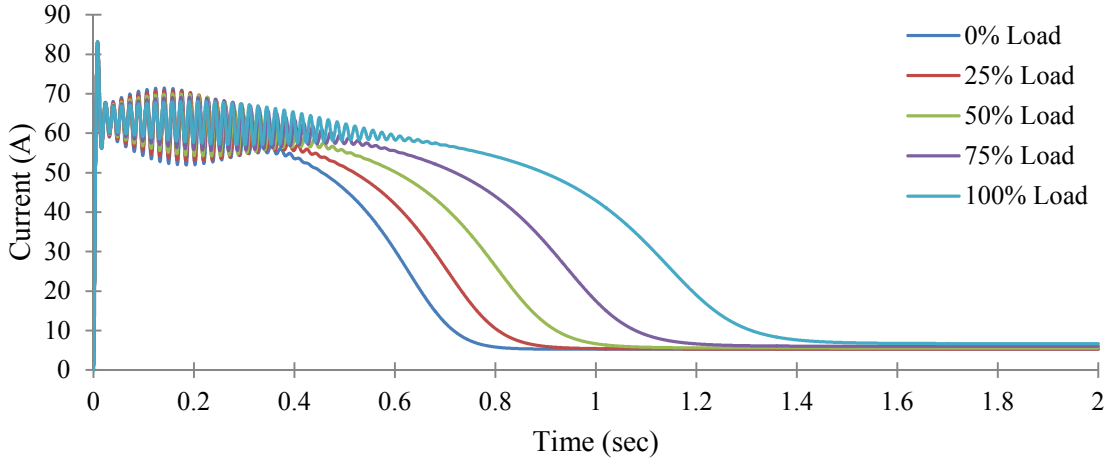

(b)

Fig. 6.9: Variation of stator current under different loading conditions. a) q-aixs. b) d-axis.

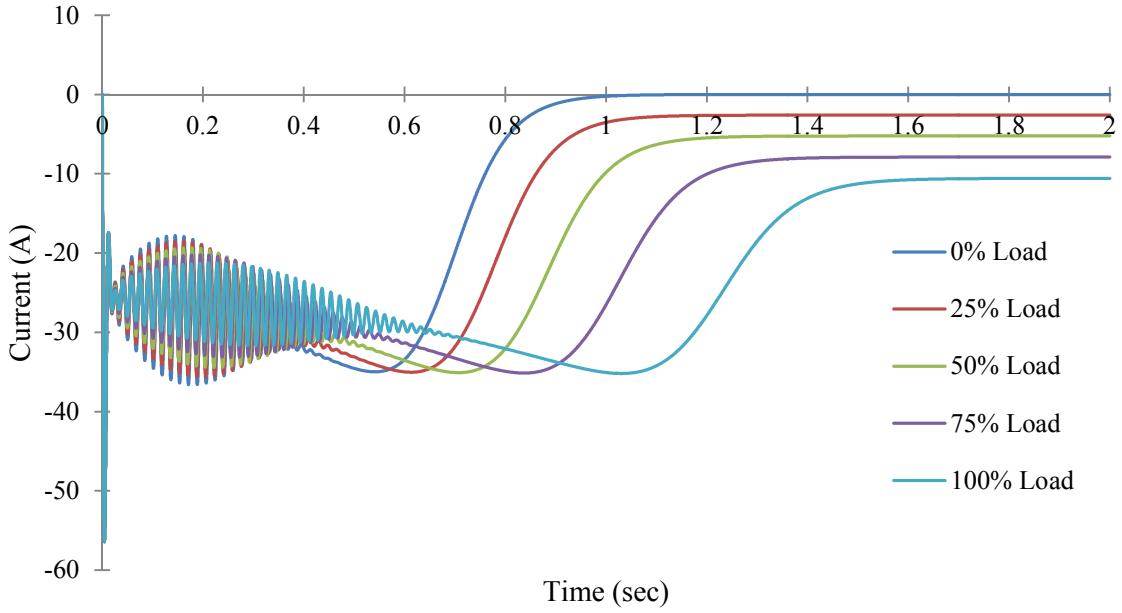

(a)

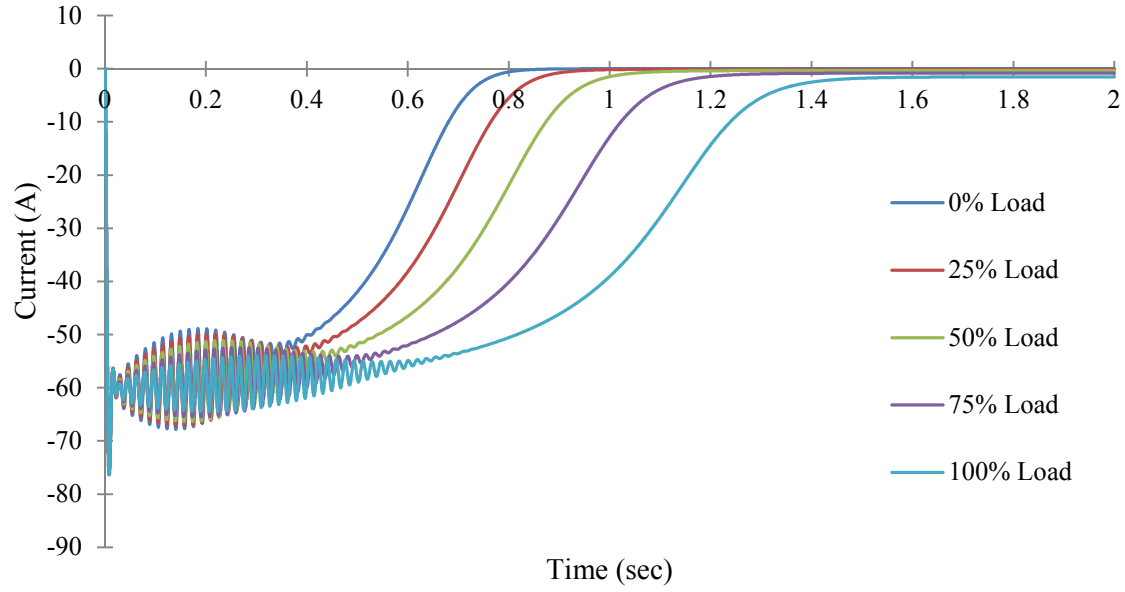

(b)

Fig. 6.10: Variation of rotor current under different loading conditions. a) q-aixs. b) d-axis.

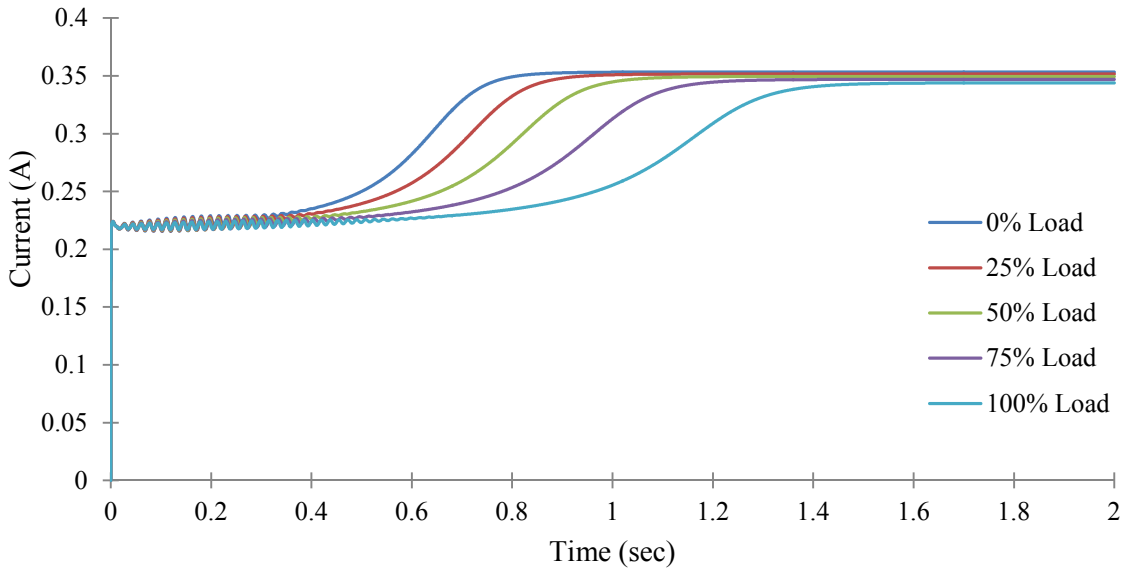

(a)

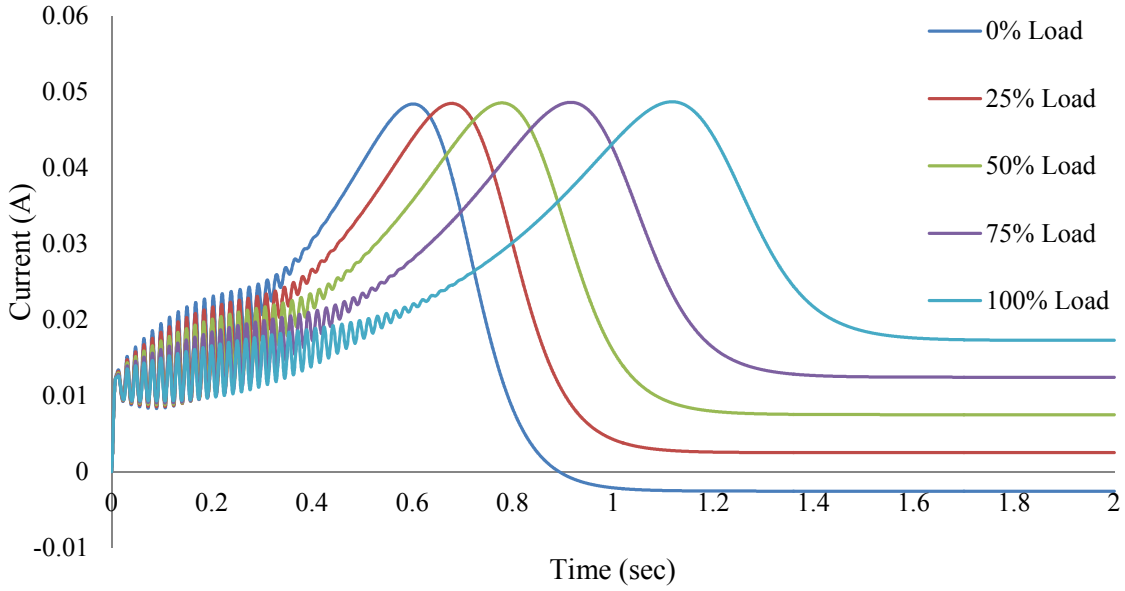

(b)

Fig. 6.11: Variation of core loss branch current under different loading conditions. a) q-axis. b) d-axis.

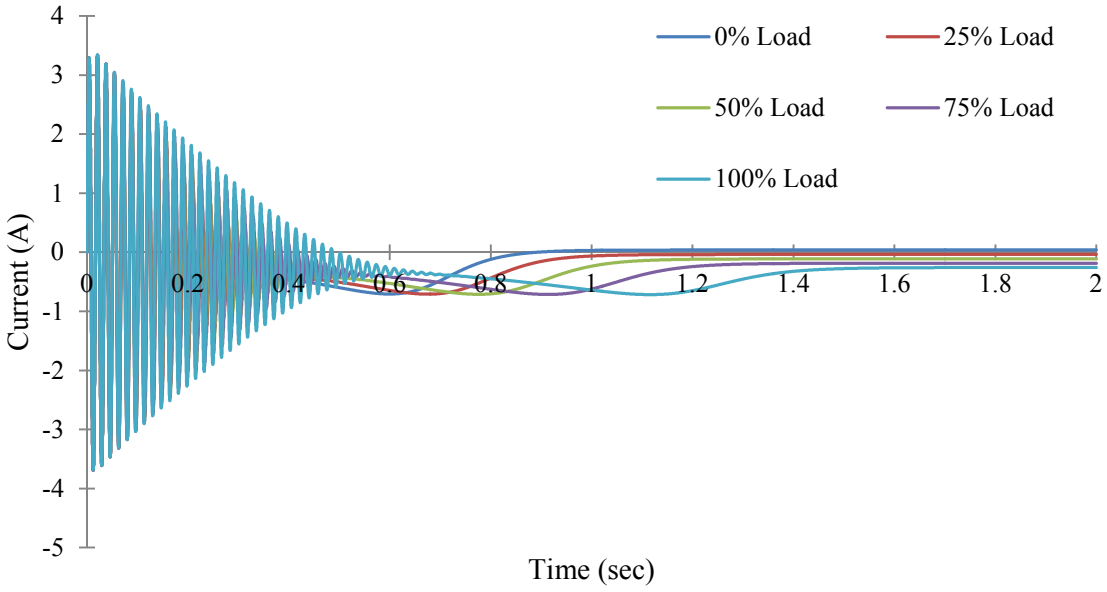

(a)

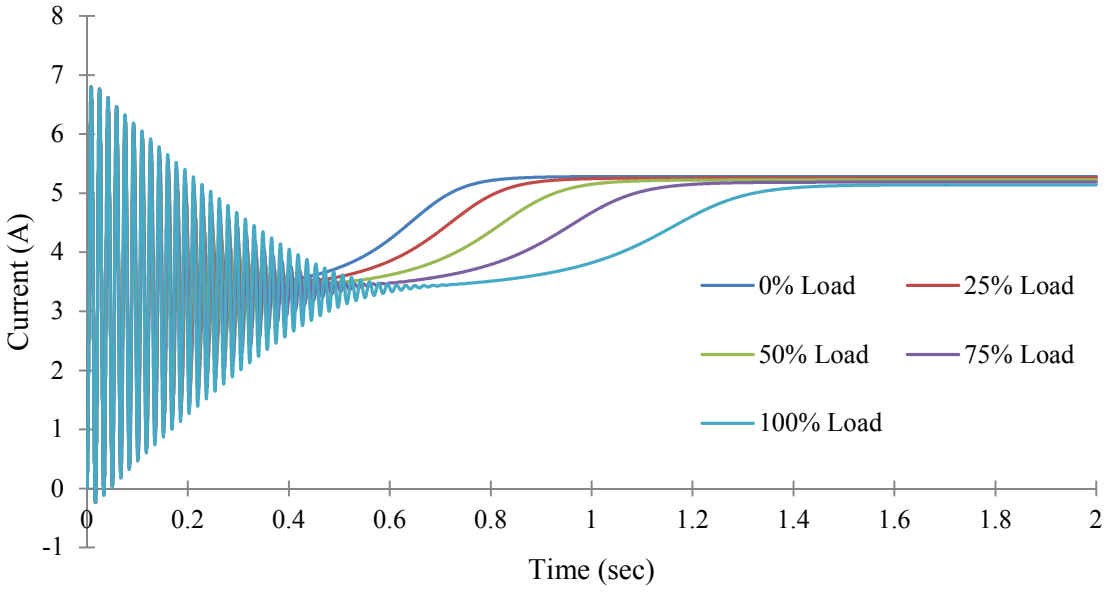

(b)

Fig. 6.12: Variation of magnetizing branch current under different loading conditions. a) q-axis. b) d-axis.

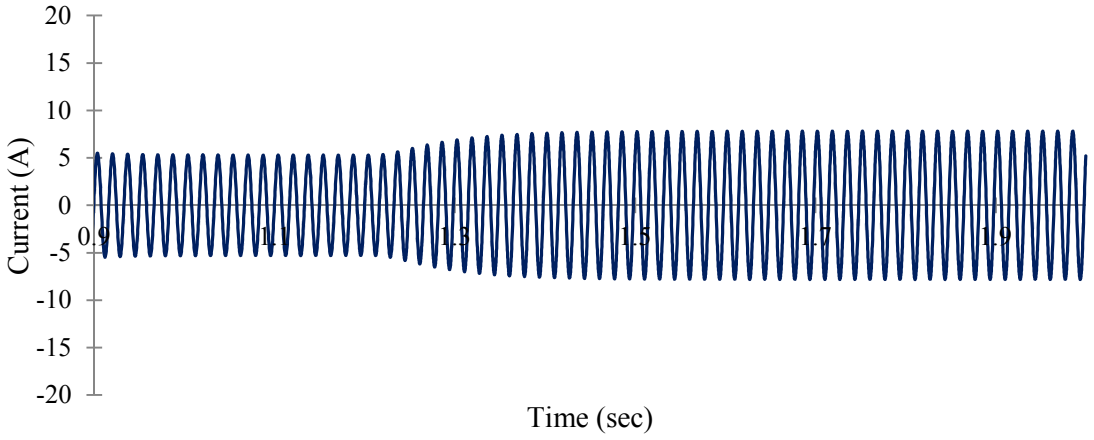

(a)

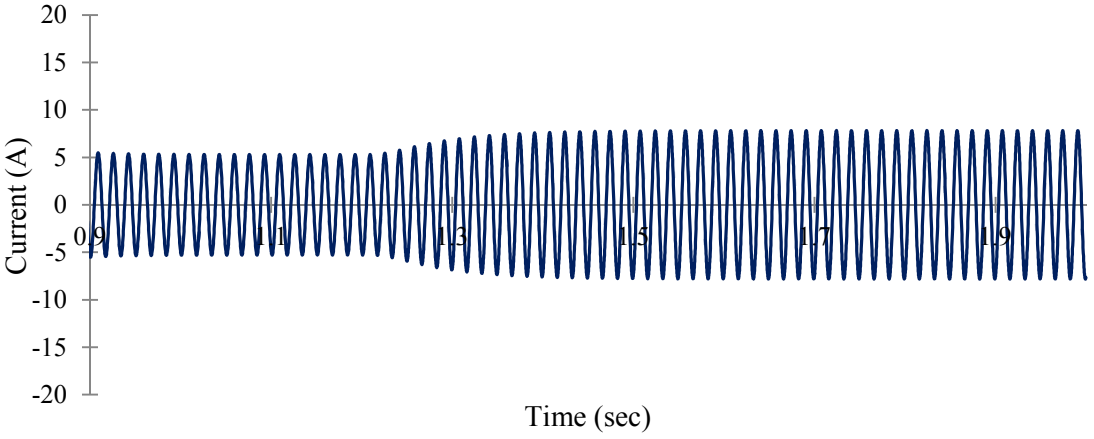

(b)

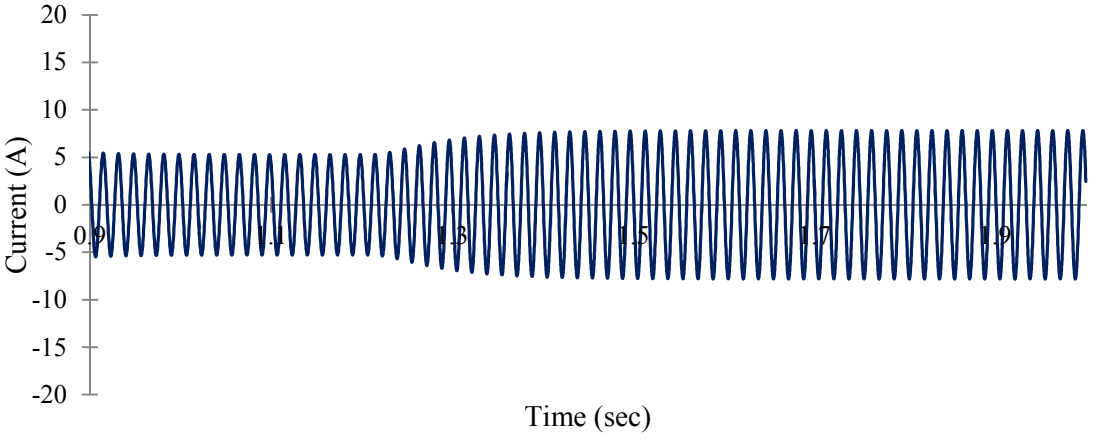

(c)

Fig. 6.13: Change in stator current amplitude due to increase in load from 0% to 50%. a) Phase A. b) Phase B. c) Phase C.

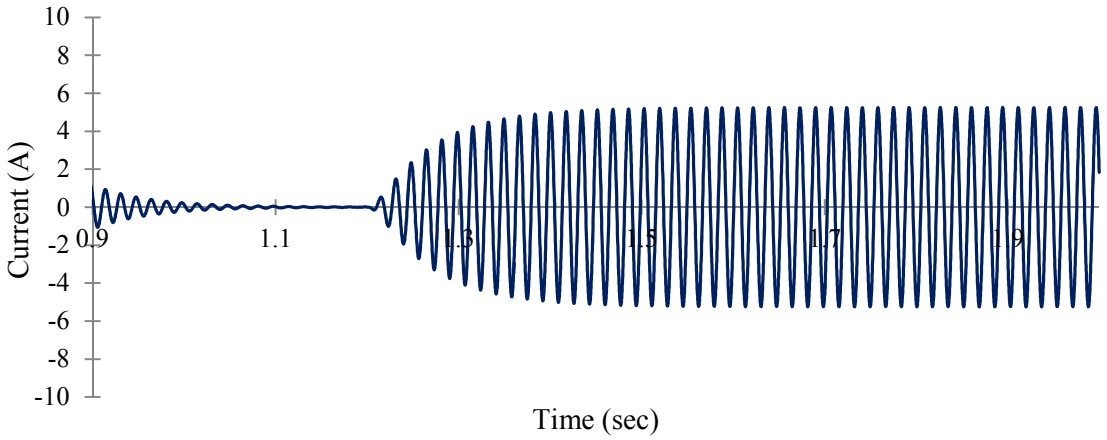

(a)

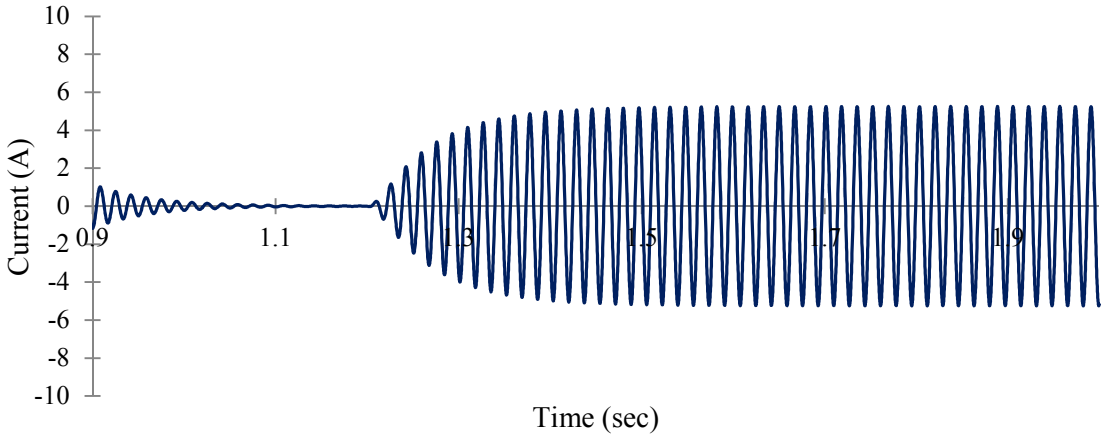

(b)

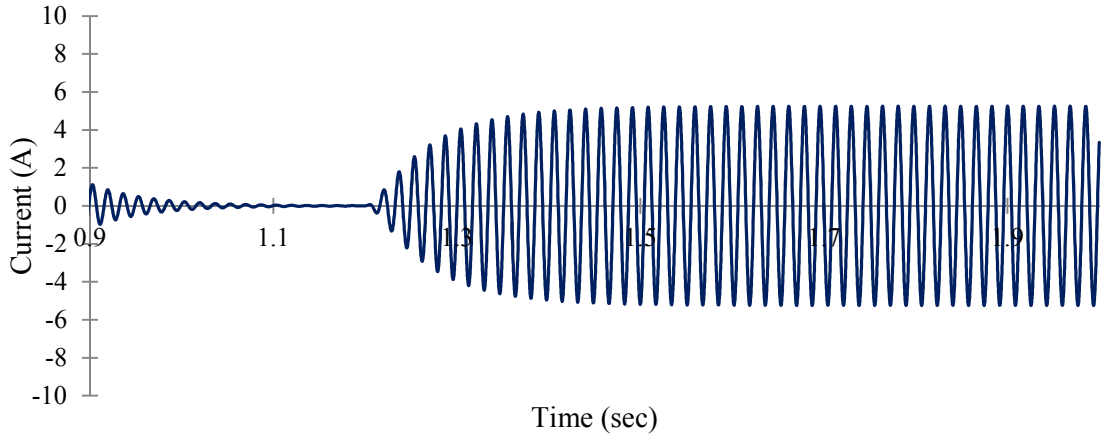

(c)

Fig. 6.14: Change in rotor current amplitude due to increase in load from 0% to 50%. a) Phase A. b) Phase B. c) Phase C.

6.2. MOTOR PERFORMANCE DURING VECTOR CONTROL

The details of vector control has already been mentioned in chapter 4. This section will present the performance characteristics of the induction motor under vector control. It is assumed that the machine is running at full load as shown in figure 6.15. The spikes observed at certain points of time are the point where a step change in speed has been introduced. The motor however reaches steady state in under 0.5secs from where the transient phase begins.

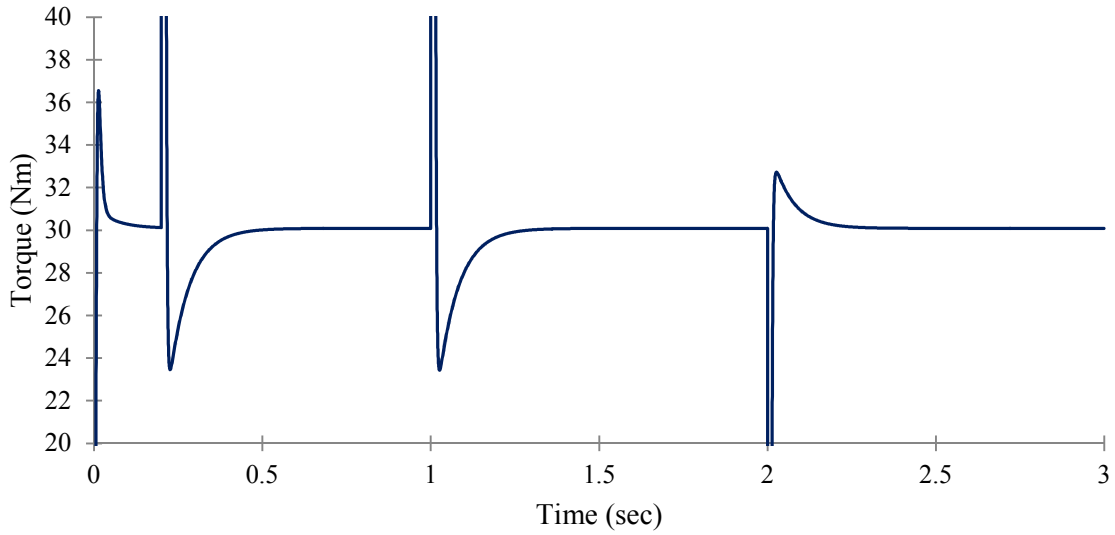

Fig. 6.15: Torque profile of the induction motor at full load under vector control.

Figure 6.16 shows the variation in speed as introduced by the user. There is a step change in speed at 0.2 secs, where the speed is changed from 0 rpm to 500 rpm. At 1 sec the speed is again increased to 1,000 rpm before dropping back to 800 rpm at 2 sec. All the changes in speed are step changes because this is the most abrupt change a system can encounter at any given point of time. If the system can cope with this change it will able to cope with other types of changes such as ramp changes in speed. Whenever there is a

change in speed, whether it is step up or step down, there is a slight overshoot in the actual rotor speed as the controller continuously strives to match the actual speed with the reference speed. This overshoot is about 15 rpm and the controller successfully matches the actual speed with the reference speed in about 0.3 secs as shown in figure 6.17.

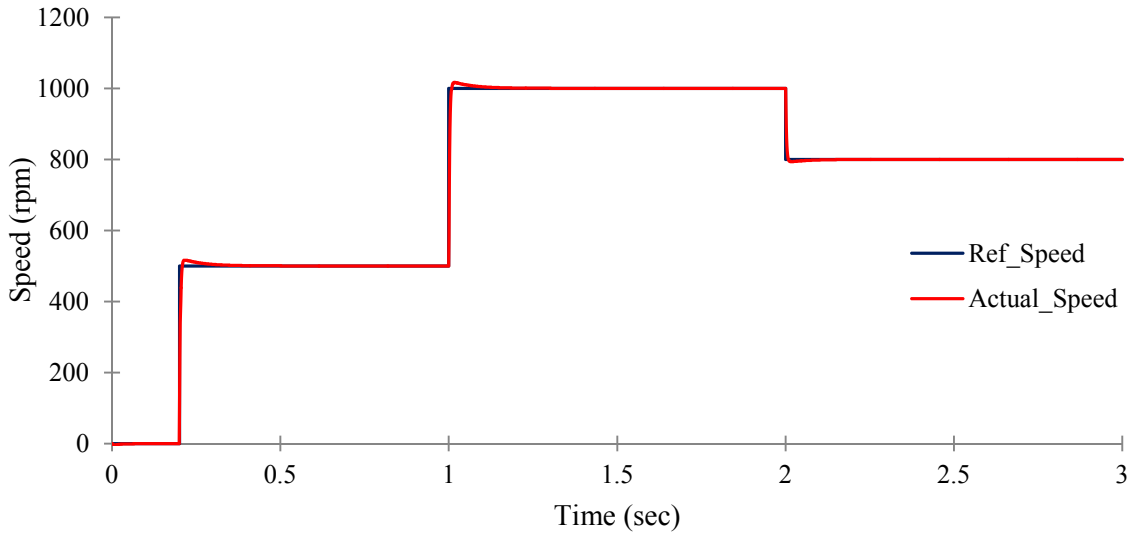

Fig. 6.16: Changes in reference speed as given by the user and dynamics of the actual rotor speed.

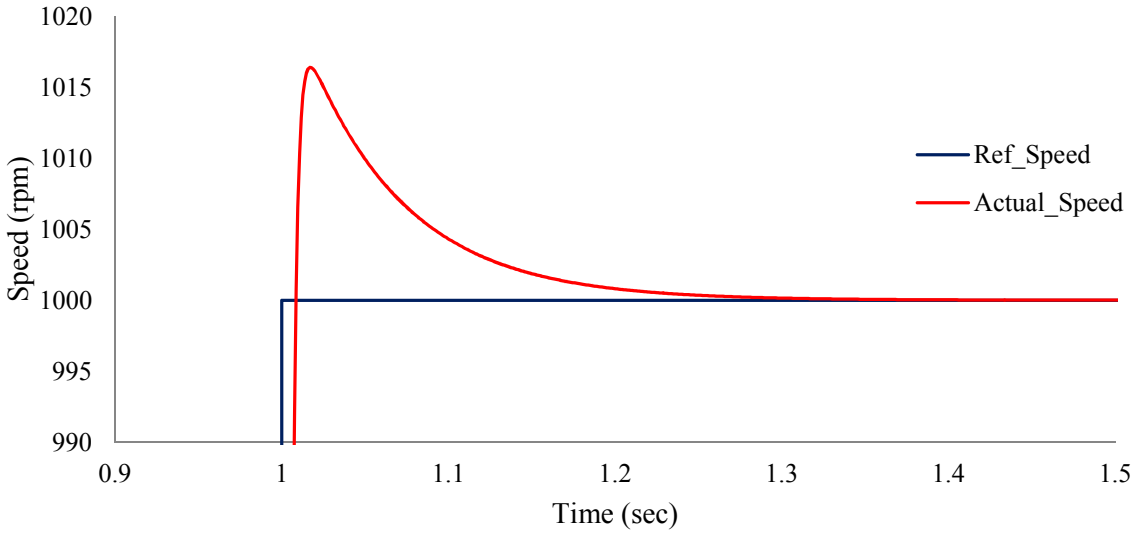

Fig. 6.17: Dynamics of the actual rotor speed during a step change in reference speed.

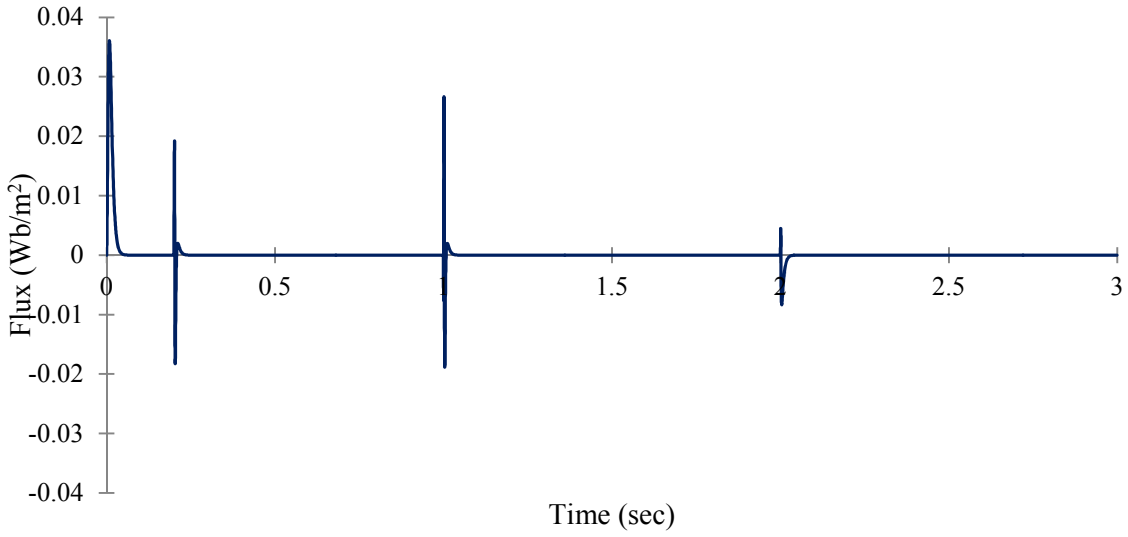

(a)

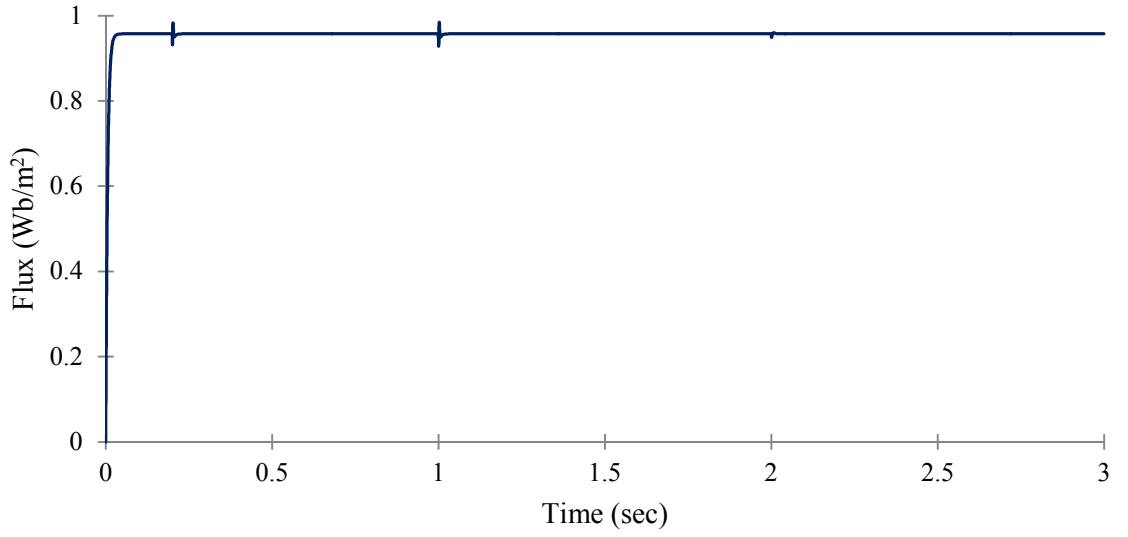

(b)

Fig. 6.18: Rotor flux profile as forced by the vector controller. a) q-axis flux. b) d-axis flux.

The conditions for vector control state that λ_{qr} should be zero and λ_{dr} should be equal to the rated flux. Figures 6.18 (a) and 6.18 (b) shows how these conditions are enforced if vector control is implemented successfully. The spikes seen in the figures are

due to changes in reference speed. Figure 6.19 shows the time taken to setup the rated rotor flux in the machine. For this machine it is about 0.04 secs. Maintaining rated rotor flux is the main reason for fast changes in torque. However, this value of flux needs to be changed to facilitate loss minimization as will be shown in the next section.

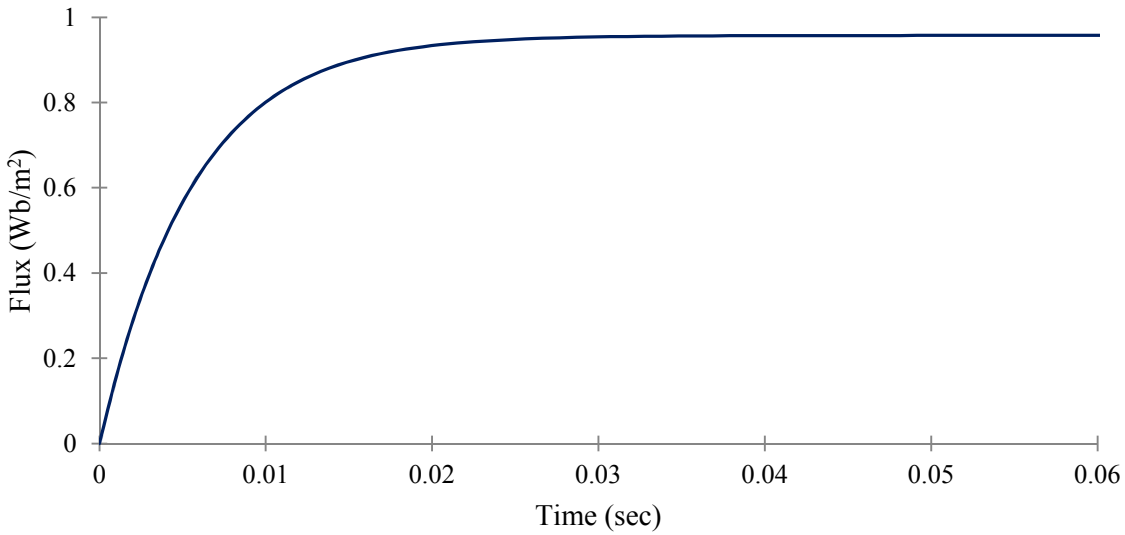

Fig. 6.19: Time taken to set up rated flux.

Figure 6.20 shows variation of the magnetizing currents as the speed changes throughout the control process. The reference current is generated and the controller tries to generate a signal to match the actual current with the generated reference. Also, any variation in the q-axis current does not affect the d-axis current. This proves that the currents have been completely decoupled. Figures 6.22 and 6.23 show the variations in stator currents. The frequency of the current waveform varies due to the fact that the action of controller eventually affects the synchronous speed which is again directly proportional to the frequency. Thus, any change in supply frequency is reflected in the current waveforms.

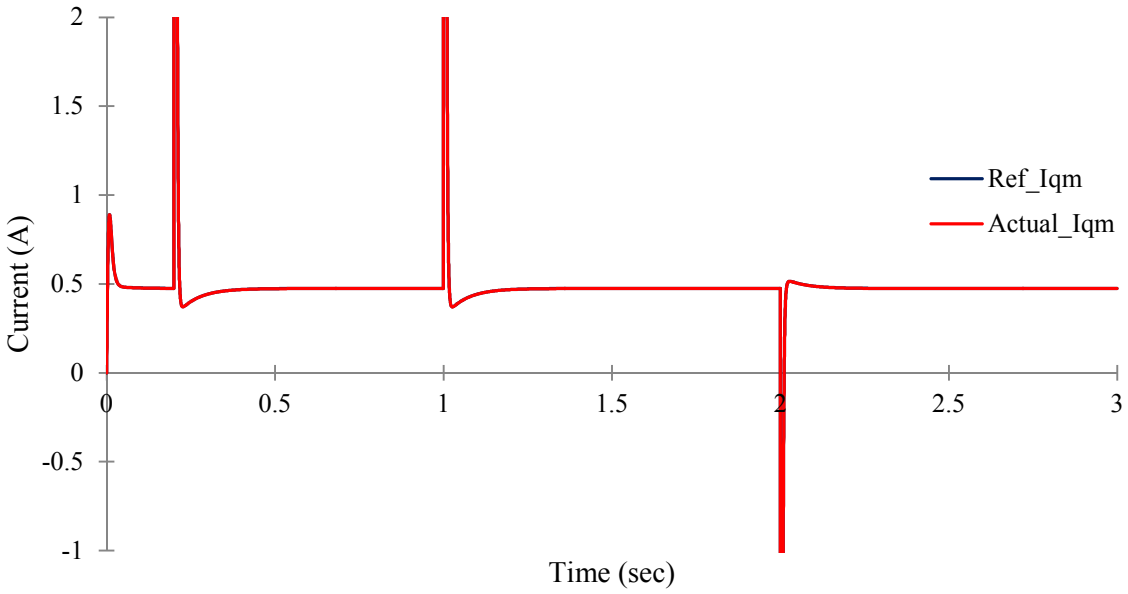

(a)

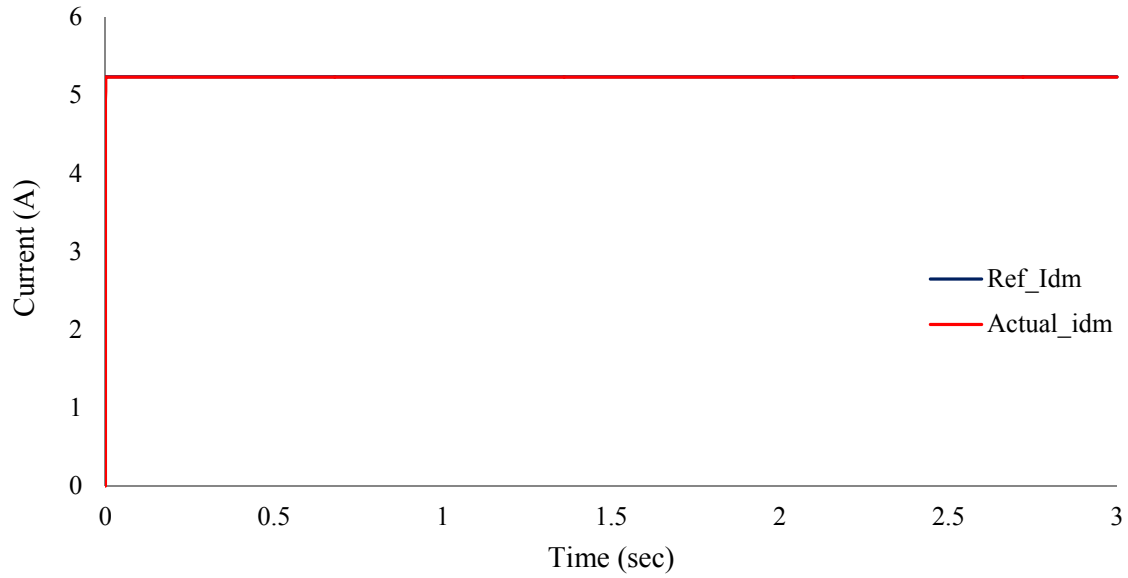

(b)

Fig. 6.20: Reference and actual magnetizing currents. a) q-axis. b) d-axis.

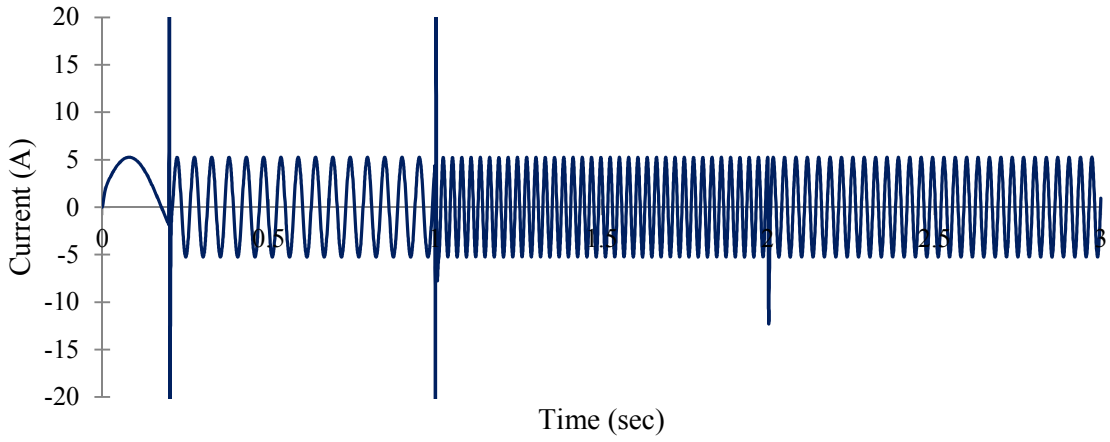

(a)

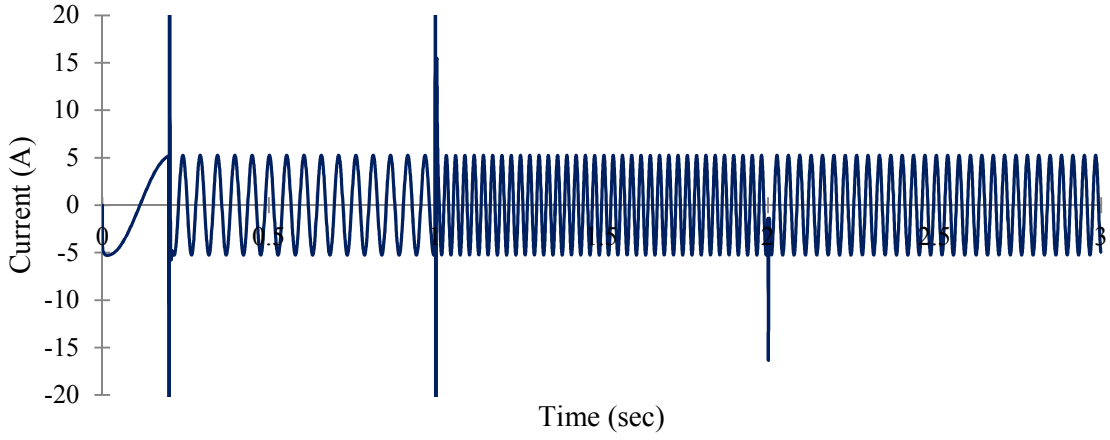

(b)

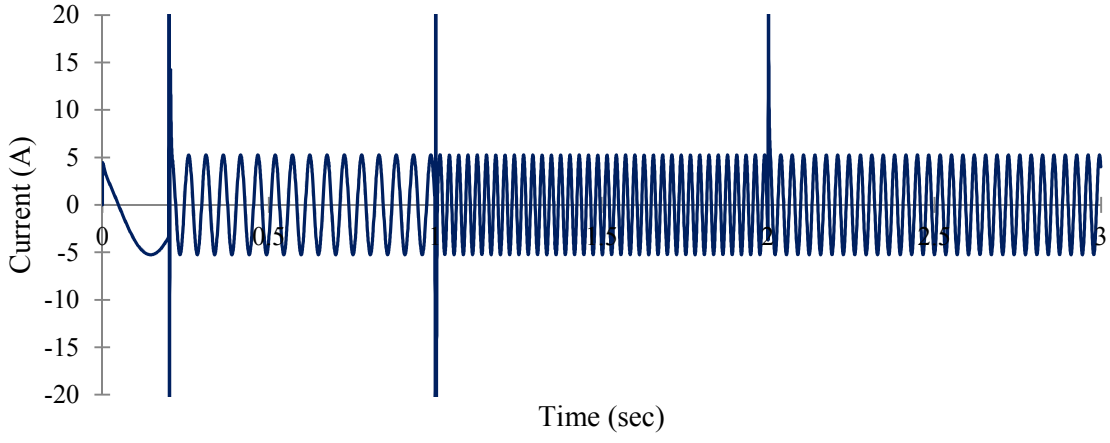

(c)

Fig. 6.21: Magnetizing currents in three phase. a) Phase A. b) Phase B. c) Phase C.

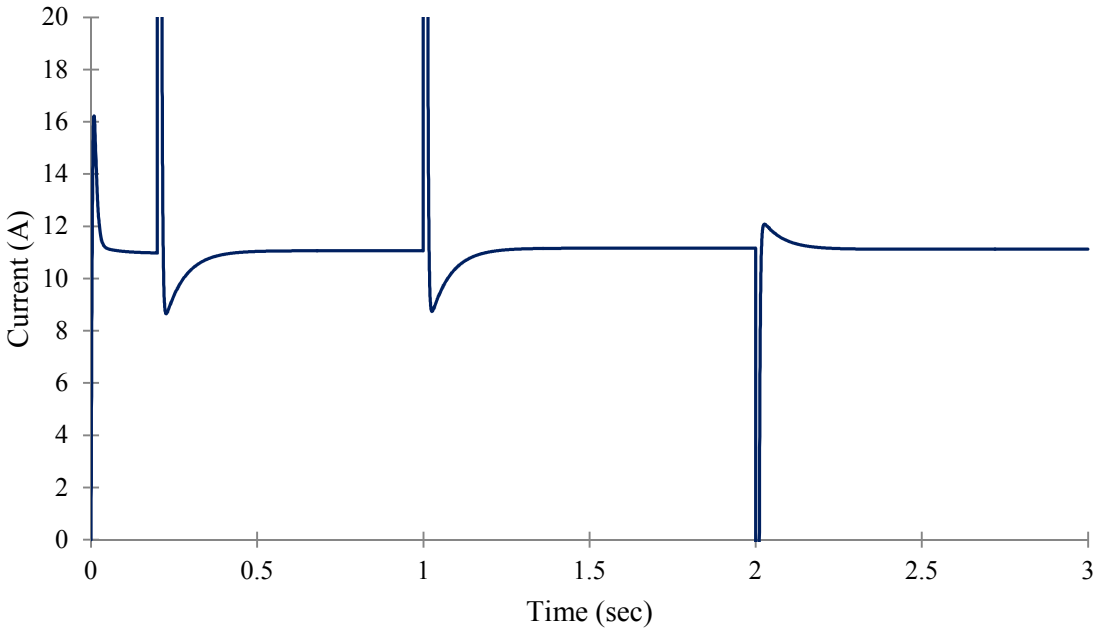

(a)

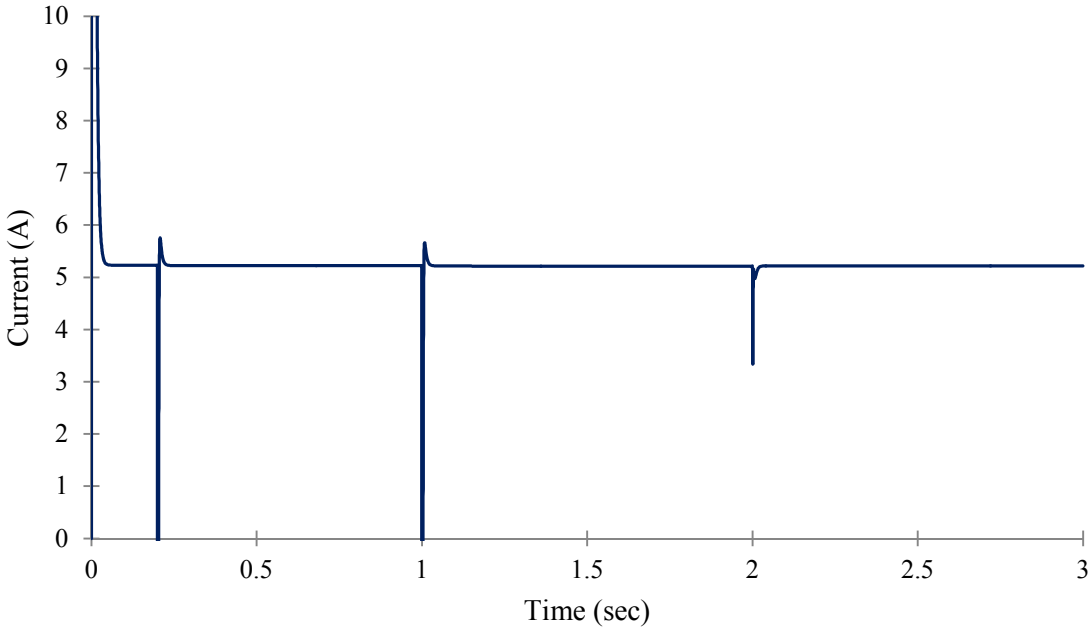

(b)

Fig. 6.22: Stator currents. a) q-axis. b) d-axis.

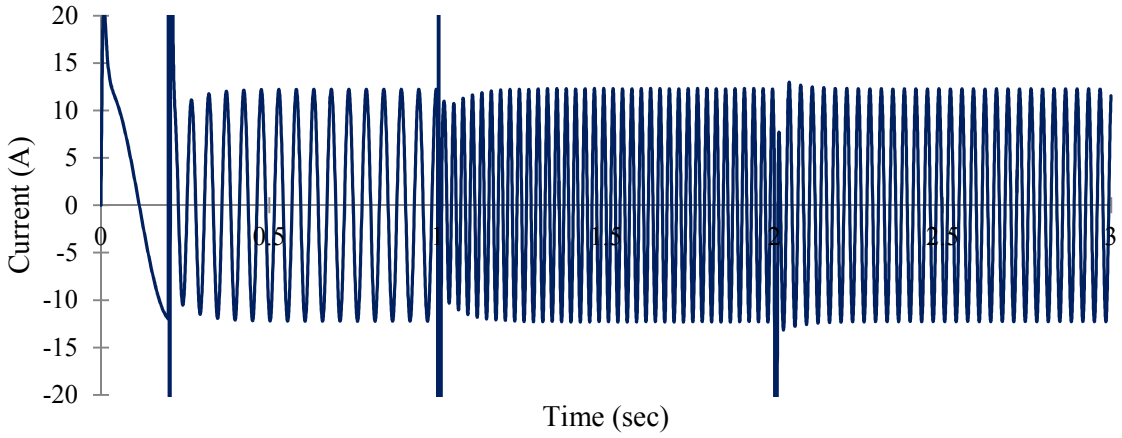

(a)

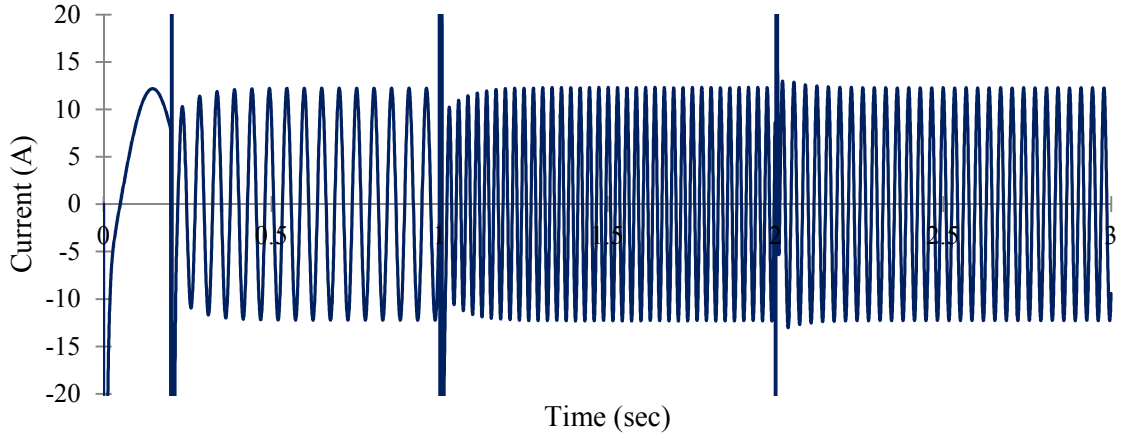

(b)

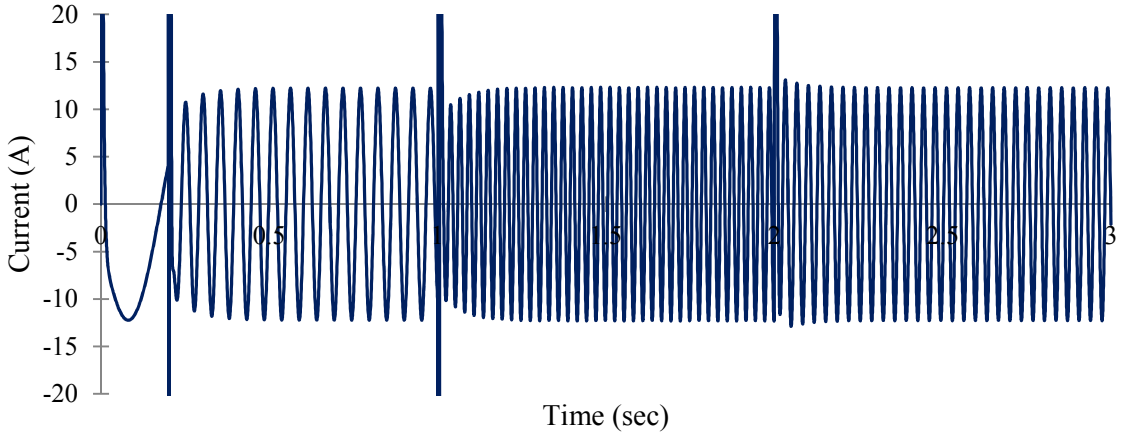

(c)

Fig. 6.23: Stator currents in three phase. a) Phase A. b) Phase B. c) Phase C.

6.3. LOSS MINIMIZATION CONTROLLER

The performance of the loss minimization controller will be broken into two parts. The first part will analyze the performance at full load and the second part analyzes the same at quarter load. The performance analysis at no load is neglected because when the machine is used as a part of a drive it is rarely run at 0% load. For both full and quarter loads the performance of the controller is simulated a speed of 1,700 rpm (high speed) and 500 rpm (low speed). The controller is switched on at 0.1 sec. Thus, any part of the curve which falls below this time will be neglected. This is true for all the curves in this section.

Case I: Full load

Figure 6.24 shows the torque profile of the induction motor. The vector control is switched on at 0.1 sec. The torque comes to a steady state. At 0.2 secs the speed reference is increased (either to 500 rpm or 1,700 rpm) as shown in figure 6.25. The controller the tracks the actual speed and forces the motor to maintain the set speed. At 1 sec the loss minimization controller is activated. The speed controller forces the motor to maintain the set speed. However, there is a slight transient that can be seen in the torque profile but dies down very quickly. The magnetizing current references thus change as per the loss minimization algorithm as evident from figures 6.26 and 6.32. The q-axis reference current reduces and the d-axis reference current increases. The current controller readjusts the actual magnetizing currents to follow the reference. The net effect of this is that the stator and rotor currents decrease as shown in figures 6.27, 6.28, 6.33 and 6.34. This reduces copper losses but the core loss increases. However, the increase in core loss

is less than the decrease in copper losses and hence the total loss is minimized as shown in figure 6.30 and 6.36.

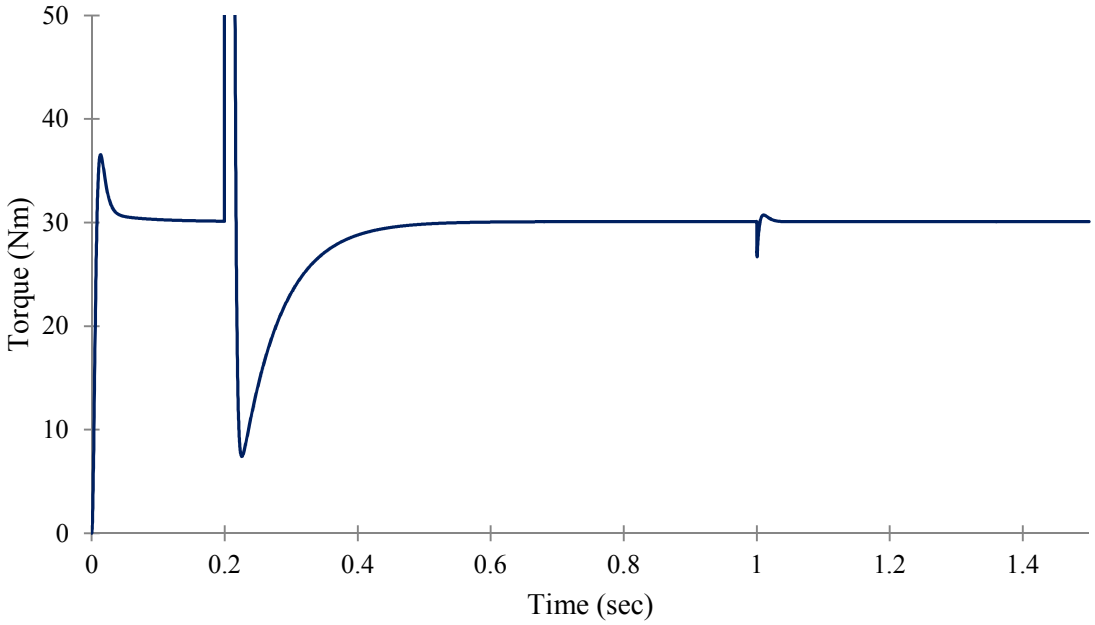

(a)

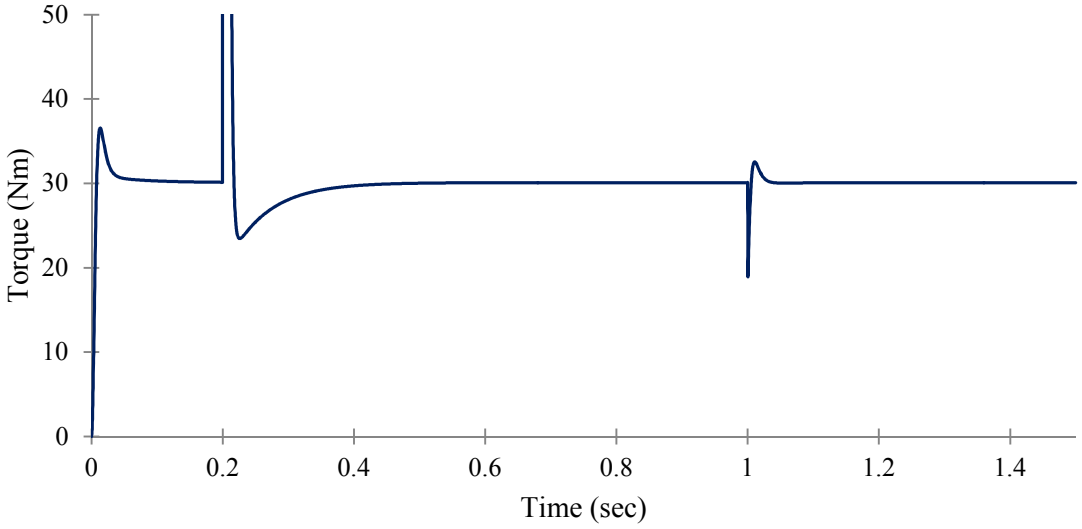

(b)

Fig. 6.24: Torque profile under the influence of loss minimization controller. a) Speed at 1,700 rpm. b) Speed at 500 rpm.

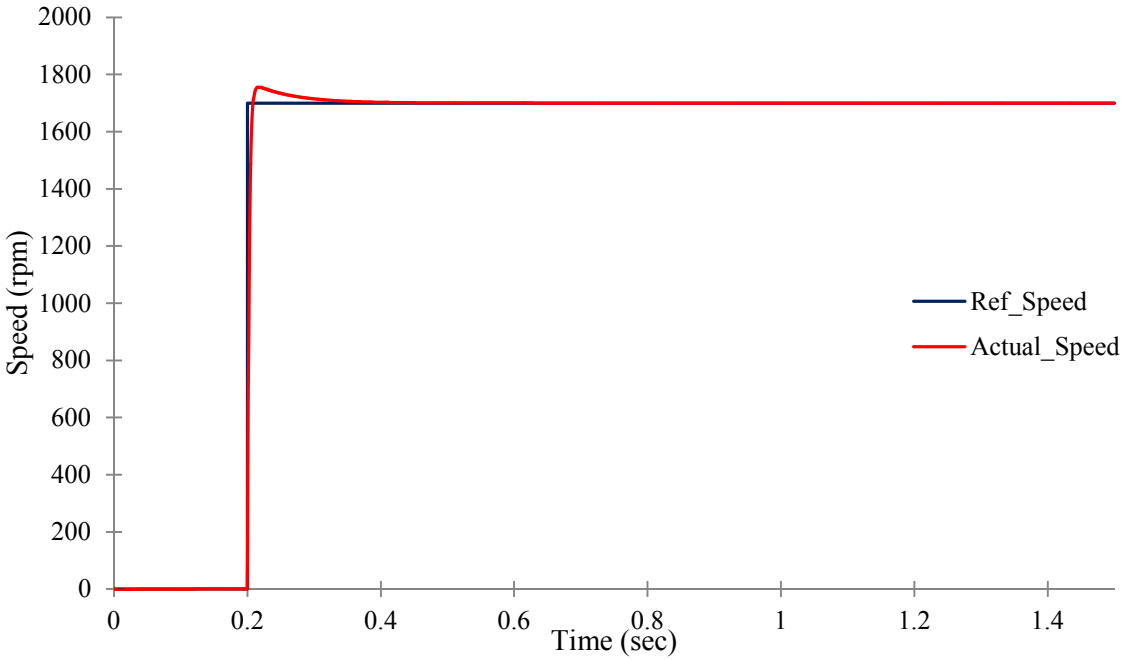

(a)

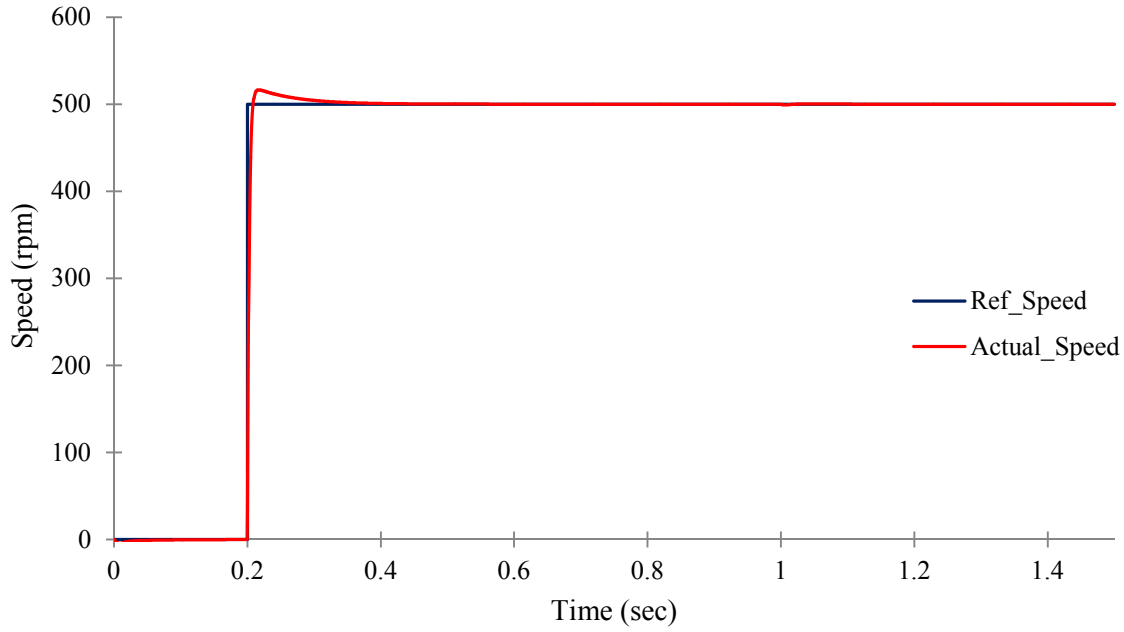

(b)

Fig. 6.25: Reference Speed and dynamics of actual rotor speed. a) Speed at 1,700 rpm. b) Speed at 500 rpm.

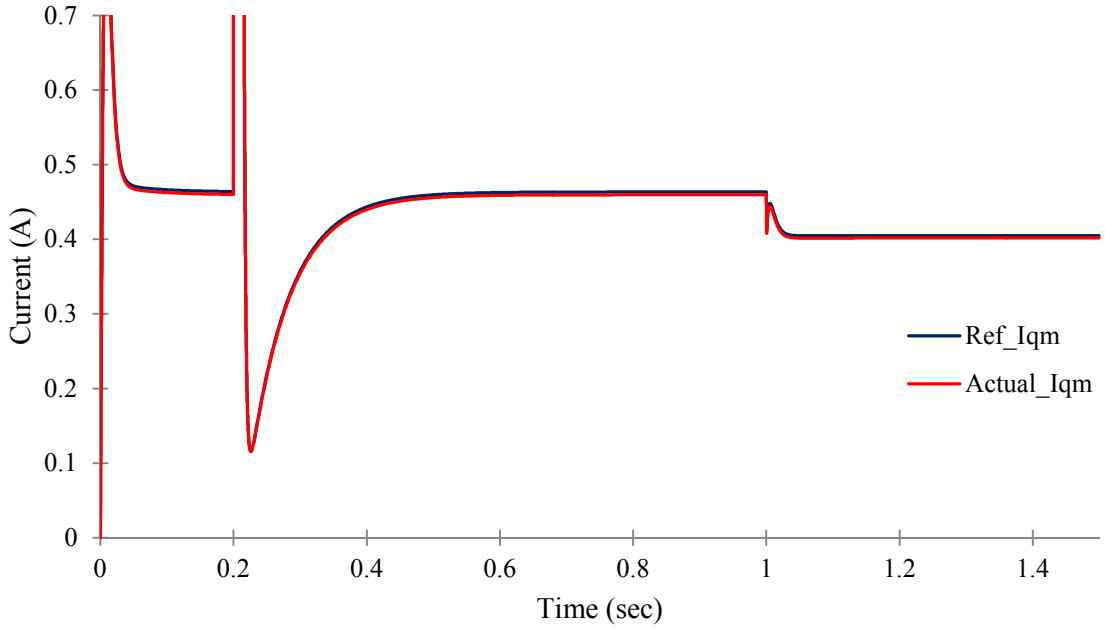

(a)

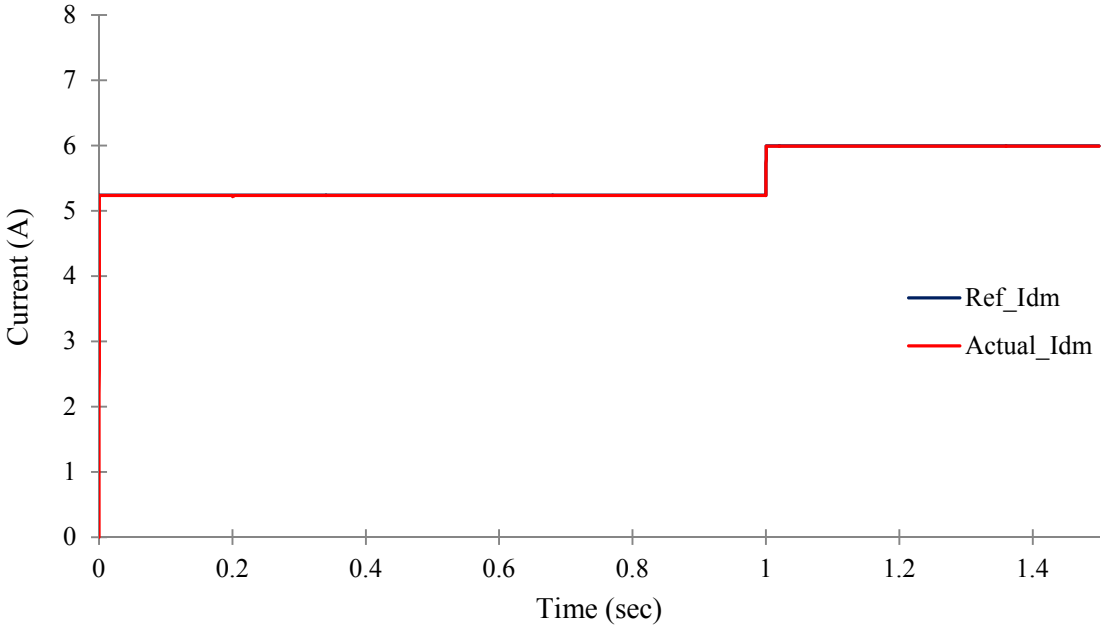

(b)

Fig. 6.26: Reference and actual magnetizing currents at 1,700 rpm. a) q-axis. b) d-axis.

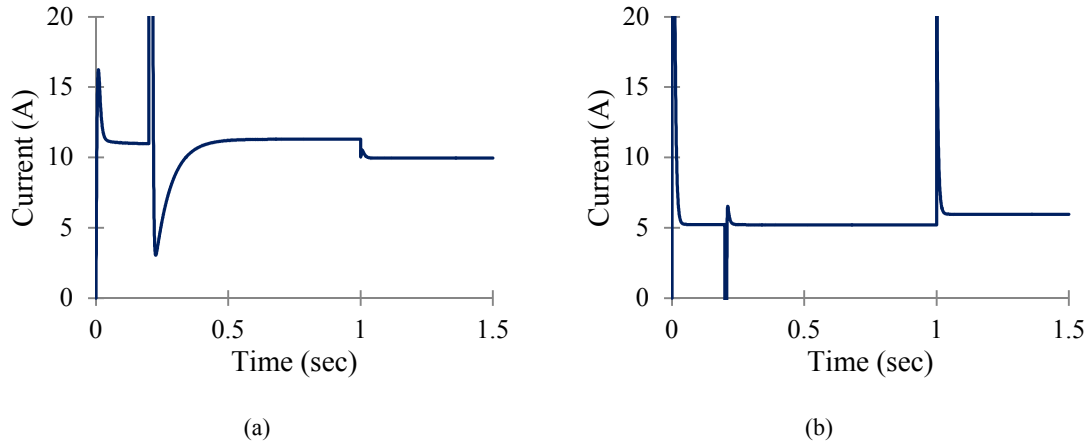

Fig. 6.27: Dynamics of stator current at 1,700 rpm. a) q-axis. b) d-axis.

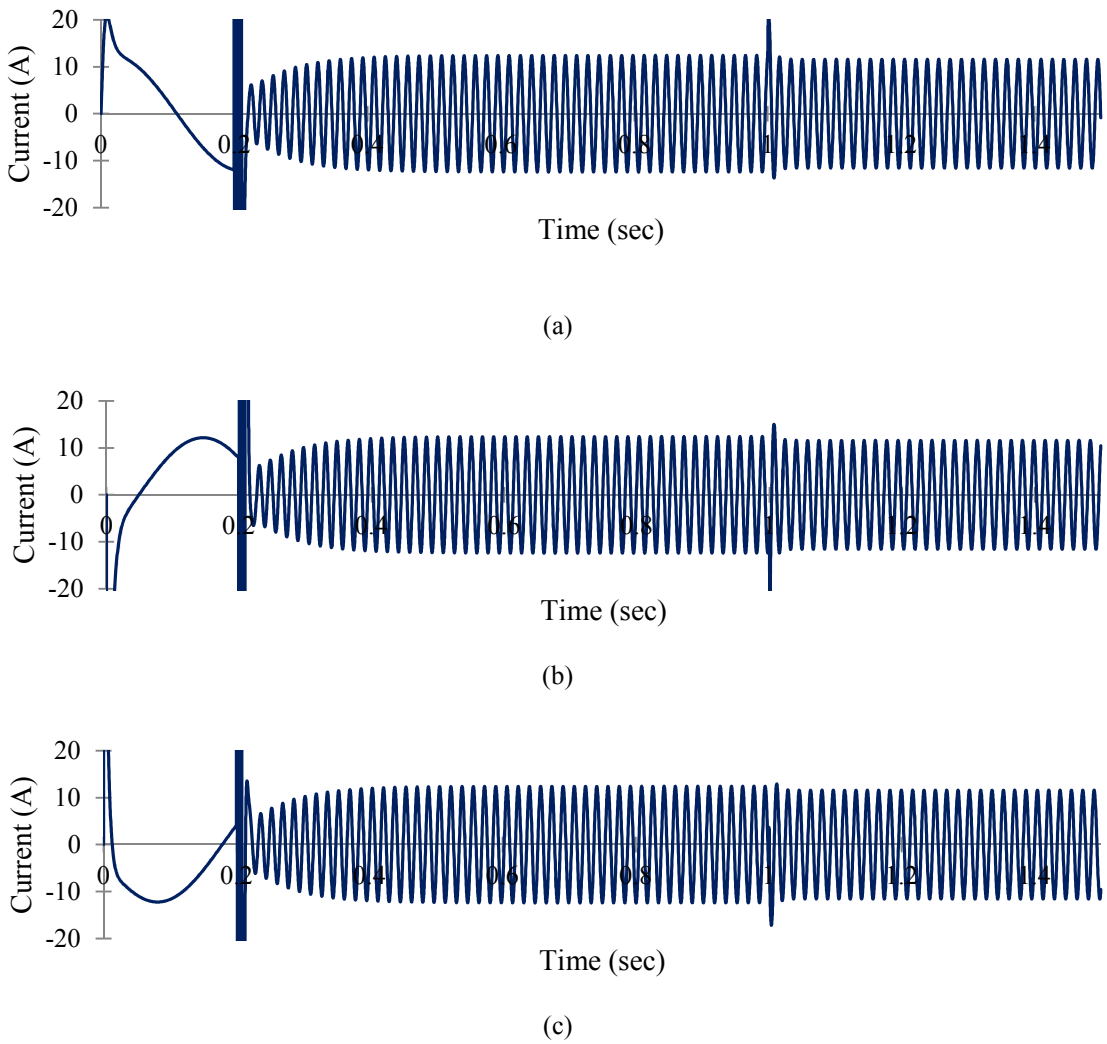

Fig. 6.28: Stator currents in three phase at 1,700 rpm. a) Phase A. b) Phase B. c) Phase C.

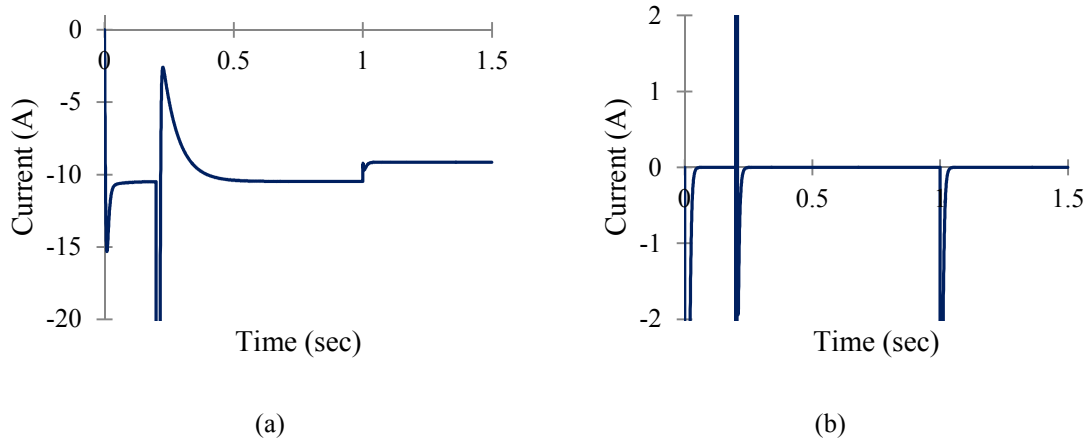

(a) (b)

Fig. 6.29: Dynamics of rotor current at 1,700 rpm. a) q-axis. b) d-axis.

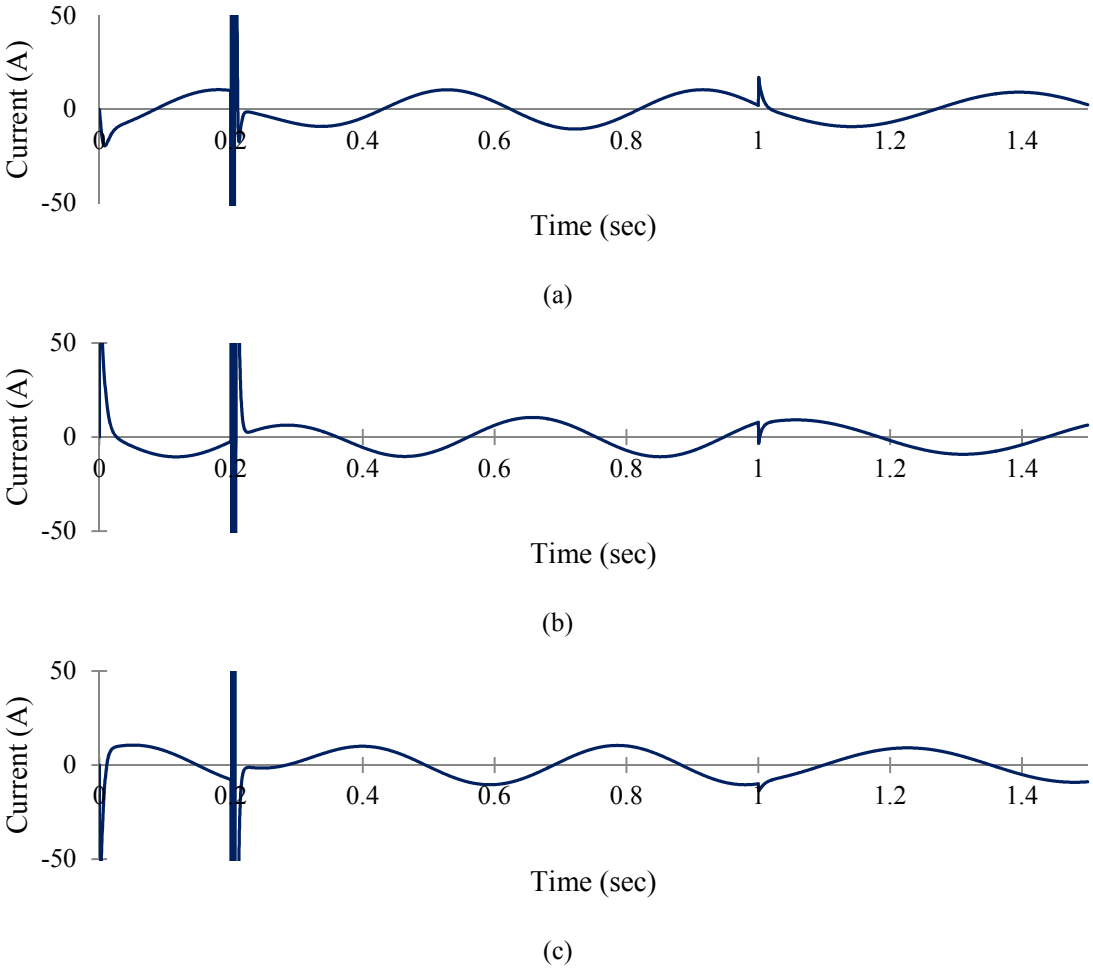

(a)

(b)

(c)

Fig. 6.30: Rotor currents in three phase at 1,700 rpm. a) Phase A. b) Phase B. c) Phase C.

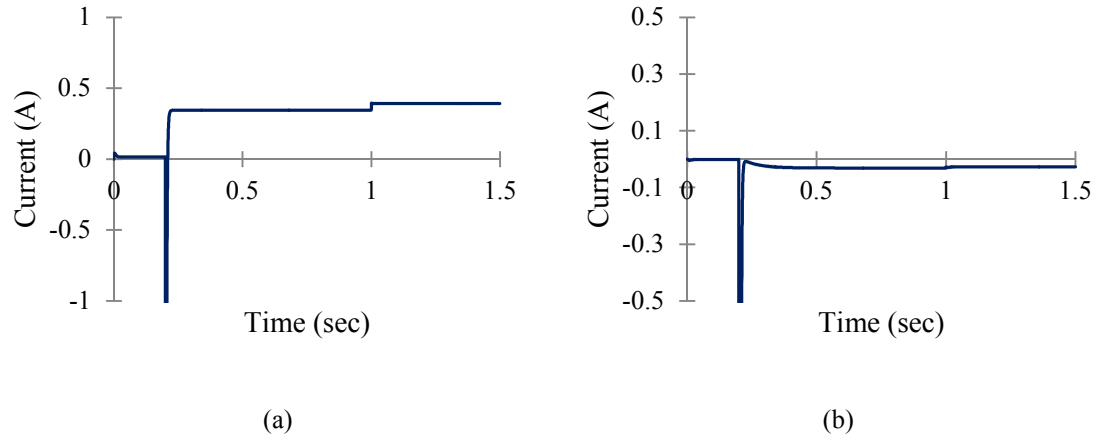

(a) (b)

Fig. 6.31: Dynamics of core loss branch current at 1,700 rpm. a) q-axis. b) d-axis.

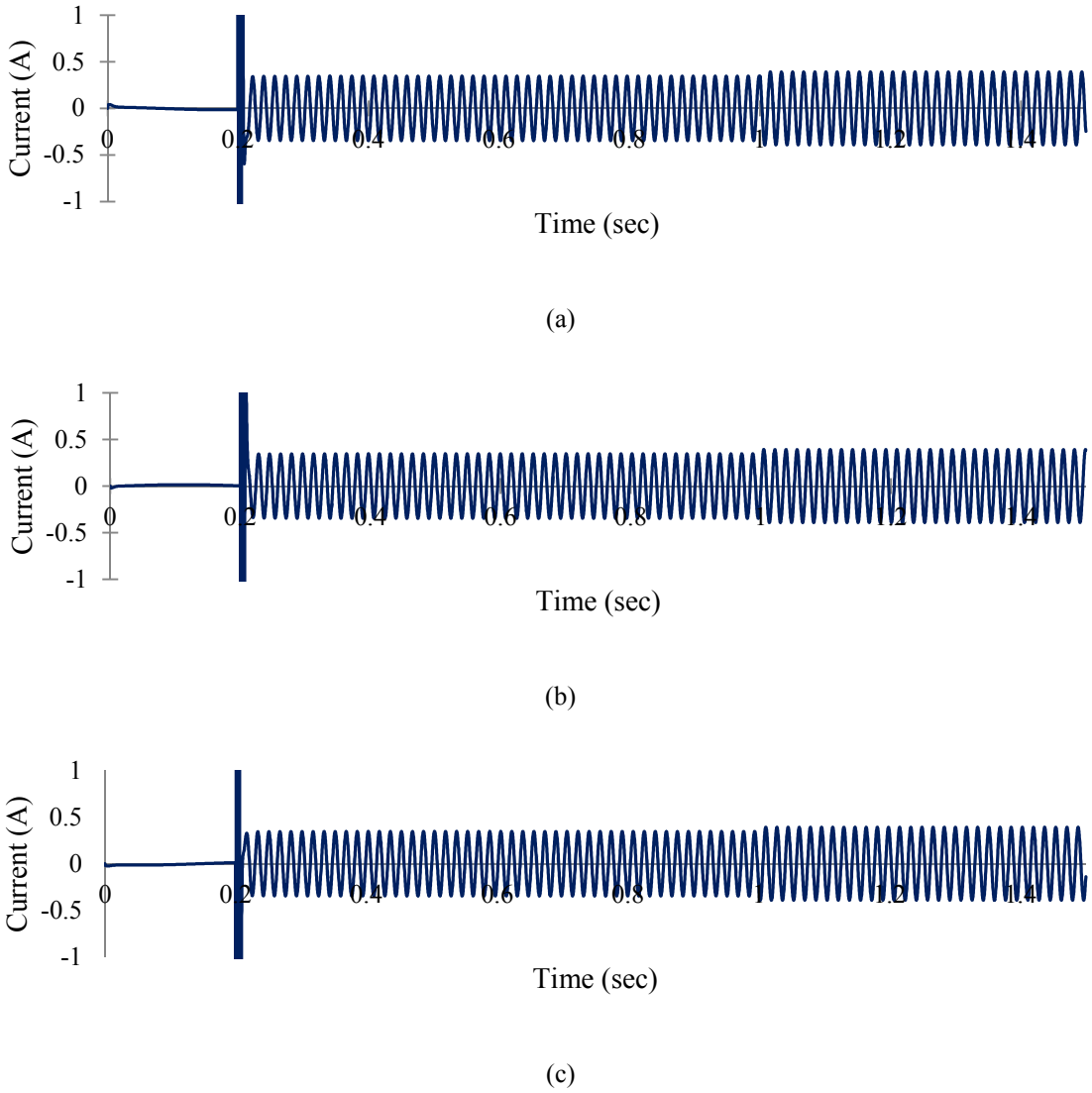

(a)

(b)

(c)

Fig. 6.32: Core loss branch currents in three phase at 1,700 rpm. a) Phase A. b) Phase B. c) Phase C.

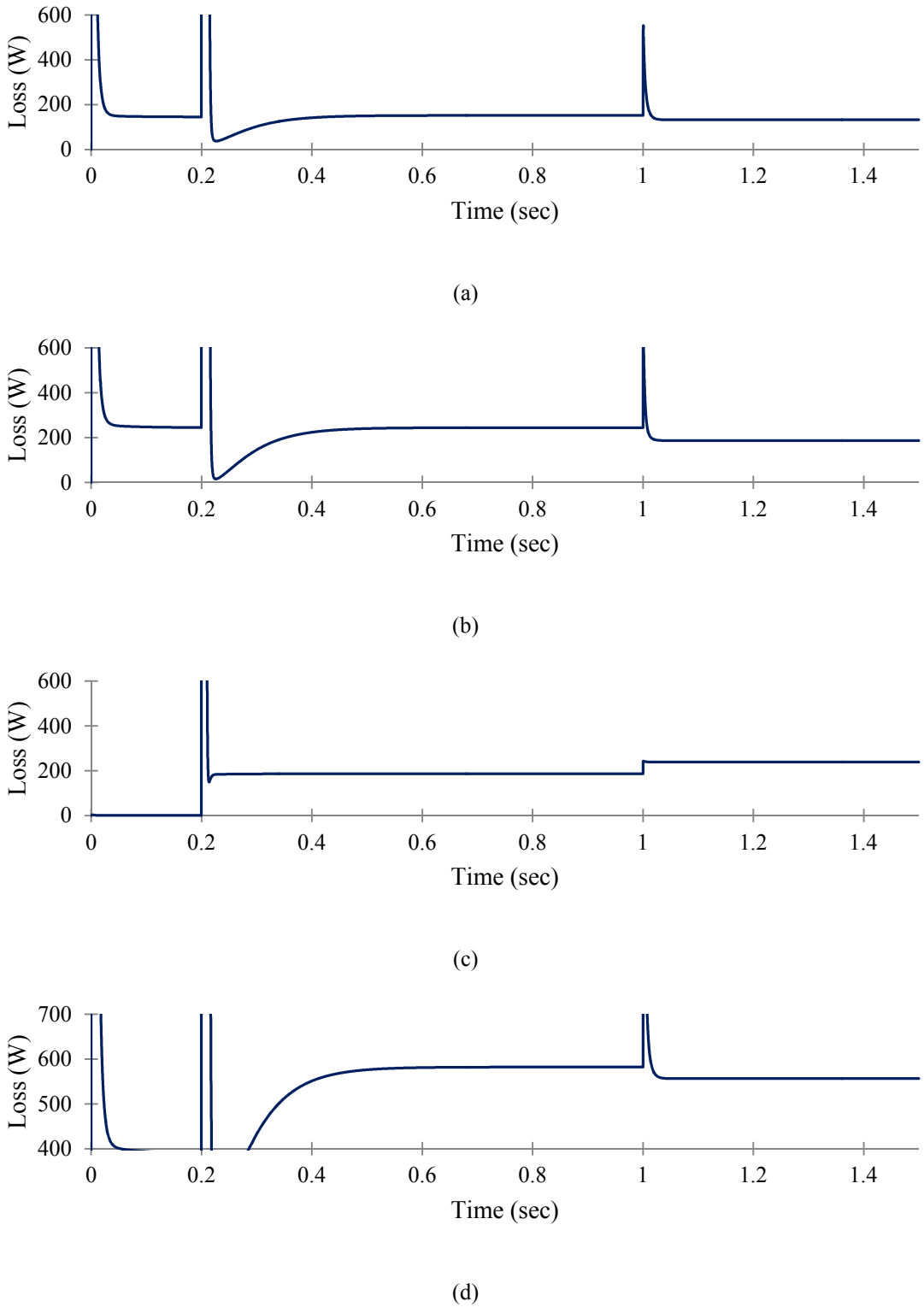

Fig. 6.33: Losses in the motor at 1,700 rpm. a) Stator copper loss. b) Rotor copper loss. c) Core loss. d) Total loss.

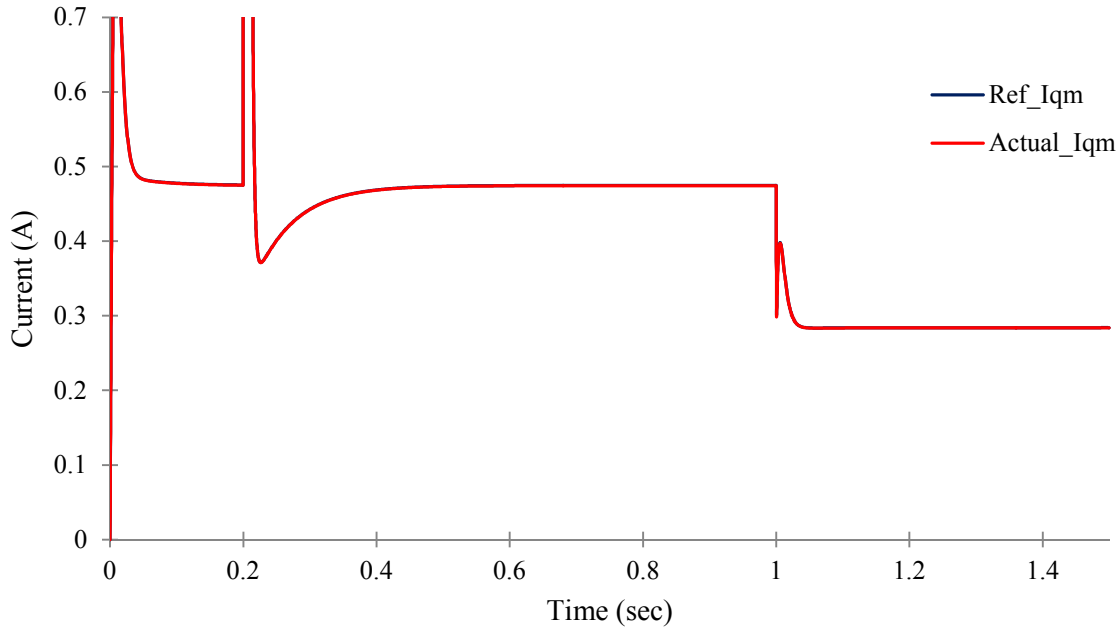

(a)

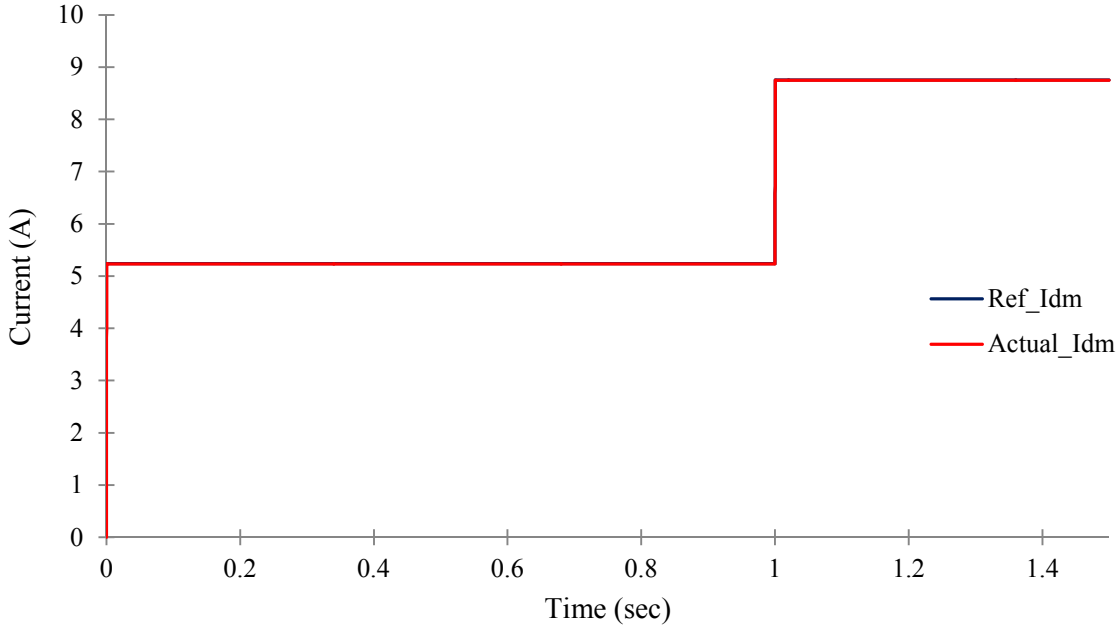

(b)

Fig. 6.34: Reference and actual magnetizing currents at 500 rpm. a) q-axis. b) d-axis.

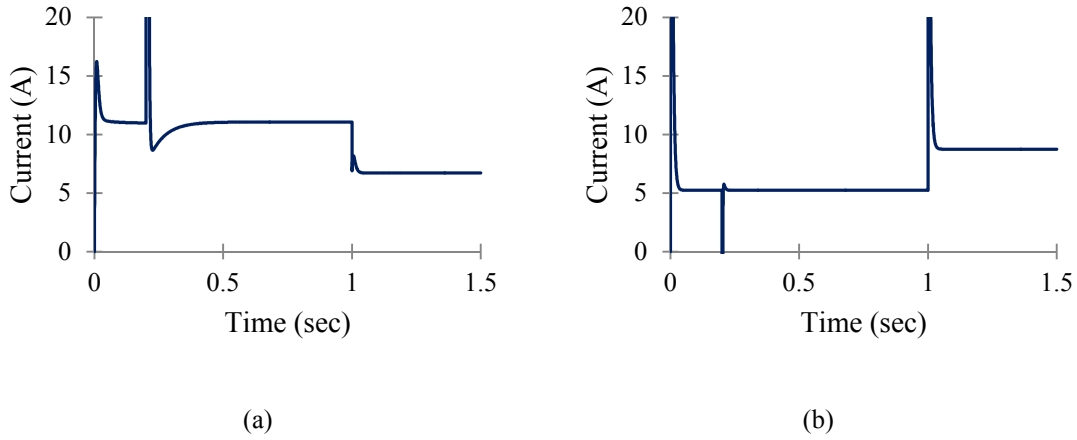

(a) (b)

Fig. 6.35: Dynamics of stator current at 500 rpm. a) q-axis. b) d-axis.

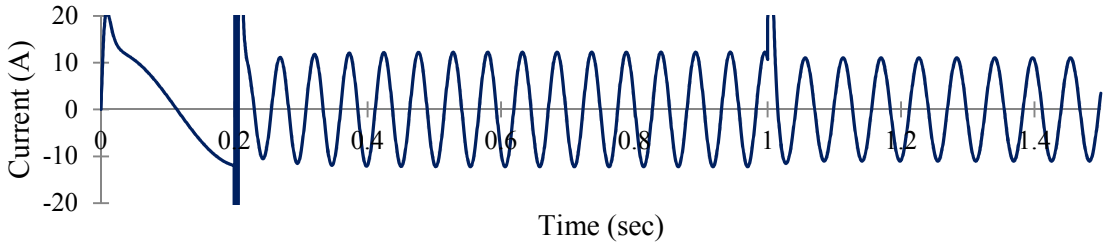

(a)

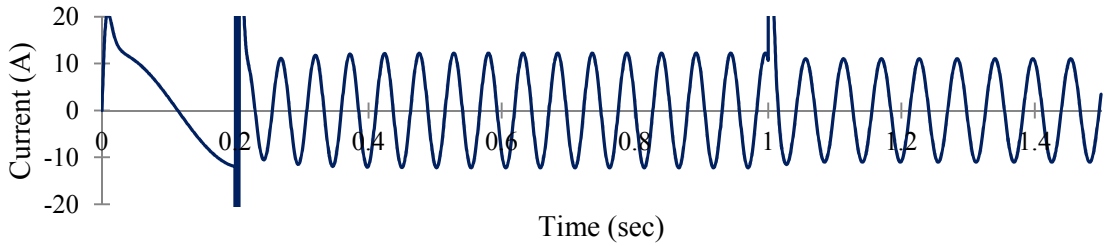

(b)

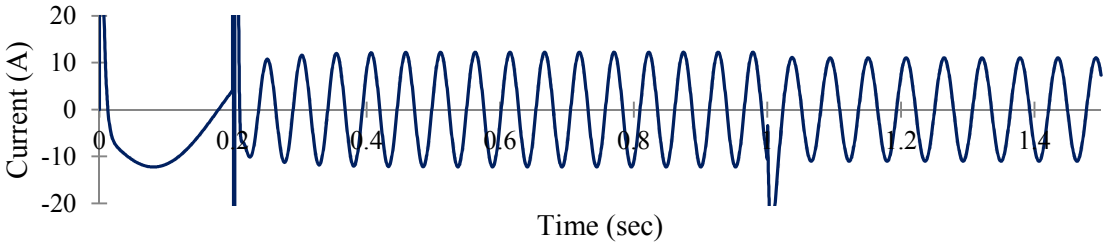

(c)

Fig. 6.36: Stator currents in three phase at 500 rpm. a) Phase A. b) Phase B. c) Phase C.

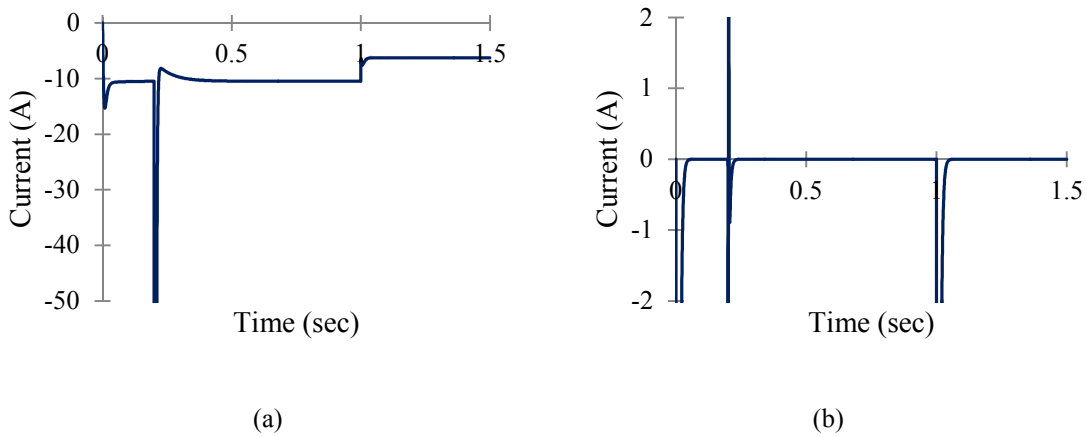

(a) (b)

Fig. 6.37: Dynamics of rotor current at 500 rpm. a) q-axis. b) d-axis.

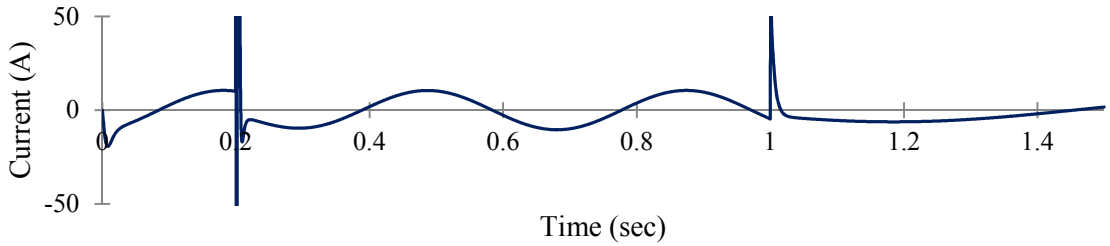

(a)

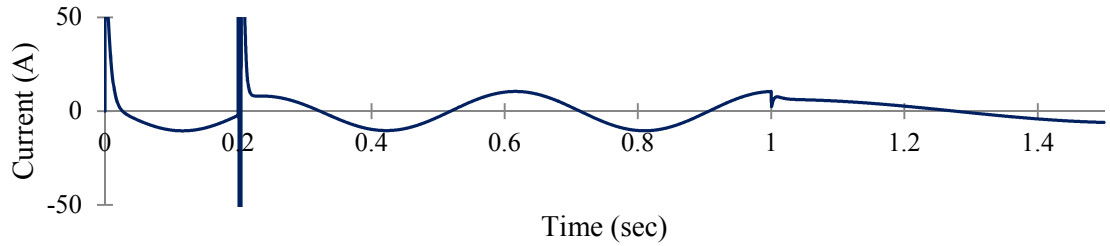

(b)

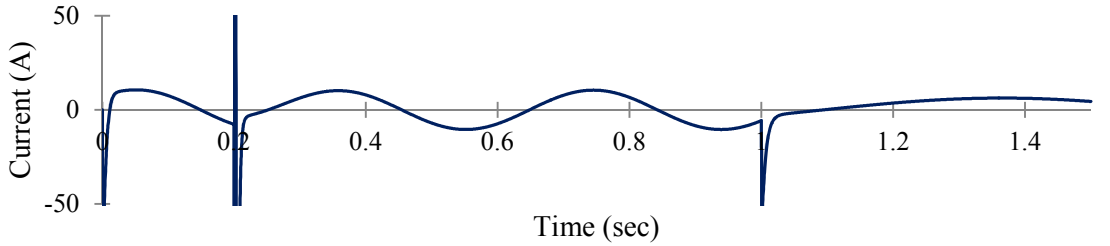

(c)

Fig. 6.38: Rotor currents in three phase at 500 rpm. a) Phase A. b) Phase B. c) Phase C.

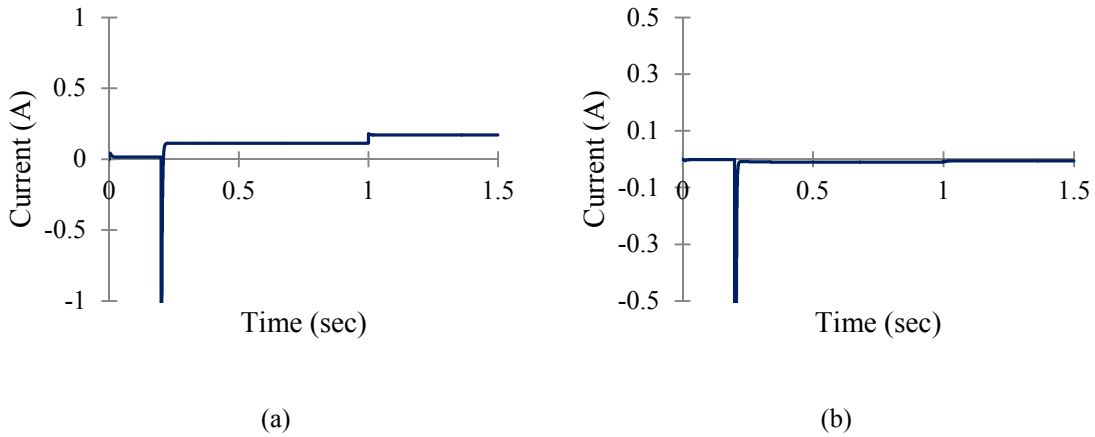

Fig. 6.39: Dynamics of core loss branch current at 500 rpm. a) q-axis. b) d-axis.

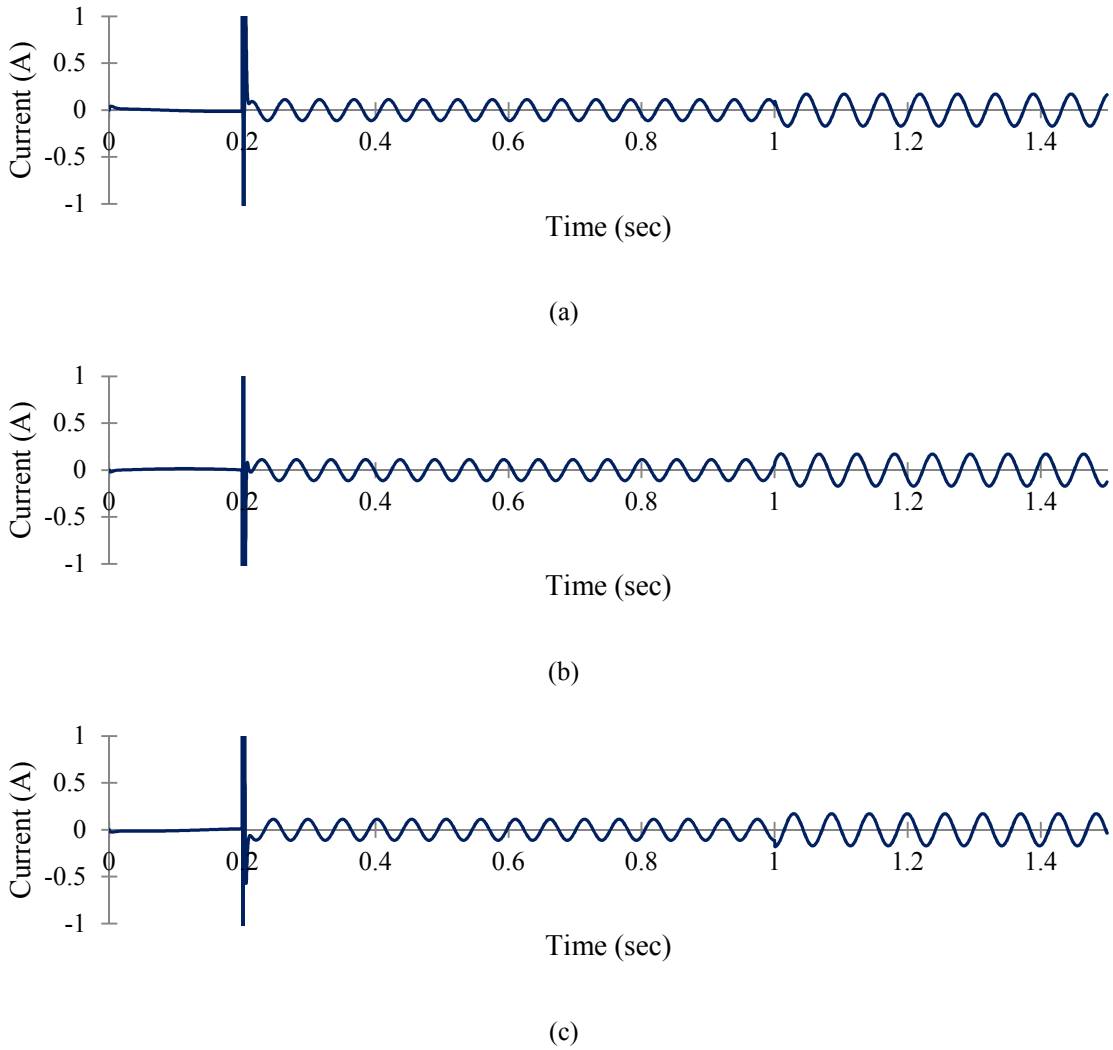

Fig. 6.40: Core loss branch currents in three phase at 500 rpm. a) Phase A. b) Phase B. c) Phase C.

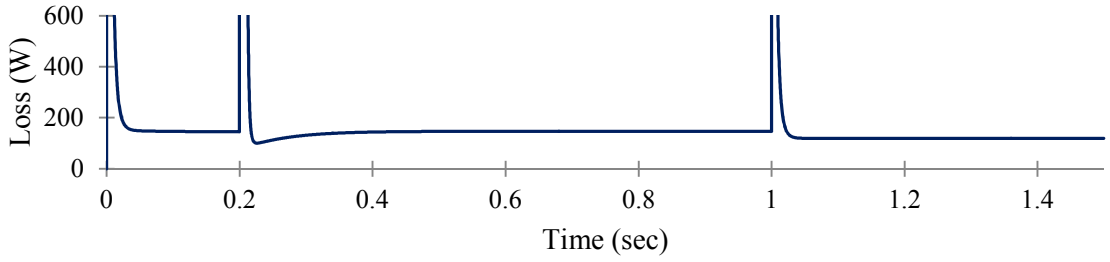

(a)

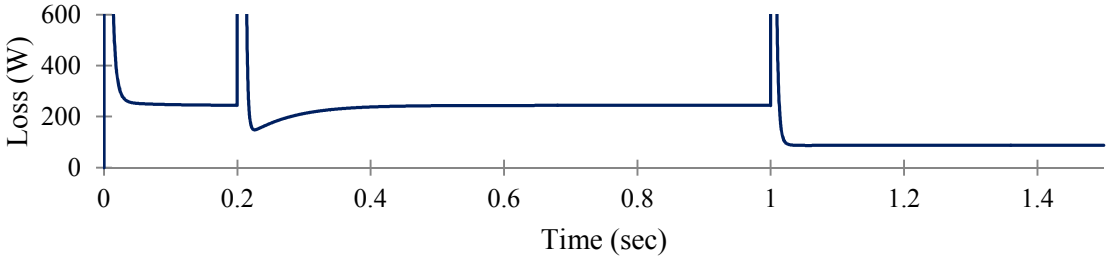

(b)

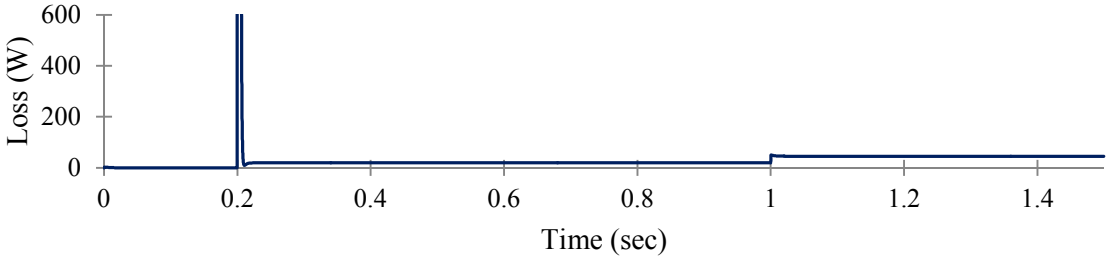

(c)

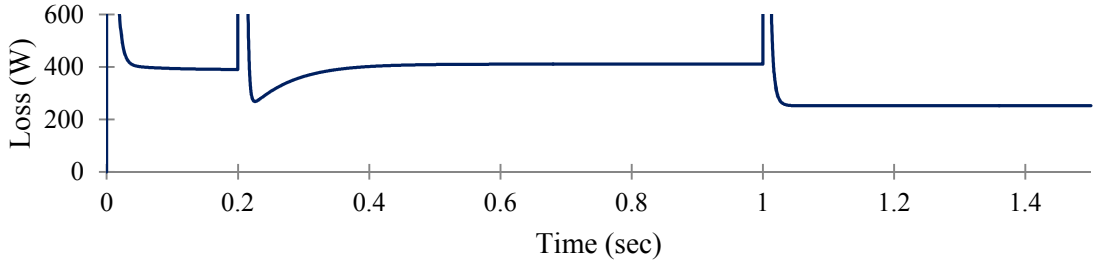

(d)

Fig. 6.41: Losses in the motor at 500 rpm. a) Stator copper loss. b) Rotor copper loss. c) Core loss. d) Total loss.

Case II: Quarter Load

The operation of the controller at quarter load is the same as explained in case I above. Vector control is switched on at 0.1 sec. The reference speed from the user is set to change to 1,700 rpm or 500 rpm, as the case may be. The motor is allowed to reach the reference speed. The loss minimization algorithm is then switched on at 1 sec. The controller ensures the rotor speed is successfully maintained at 500 rpm or 1,700 rpm, as per the reference set point. Figure 6.43 shows the speed profile of the induction motor. Unlike case I, here the motor needs to drive a load at 25% of its capacity. The motor develops this required torque with the exception of a minute transient when the loss minimization controller is switched on as shown in figure 6.42. It should be noted here that contrary to case I, when the loss minimization controller is activated, the reference q-axis magnetizing currents increases and reference d-axis magnetizing current decreases. The two axis current profiles are shown in figures 6.41 and 6.52. The net effect this has on the entire system is quite different from case I. The stator current reduces as shown in figures 6.46 and 6.54. The rotor current, on the other hand, increases as shown in figures 6.48 and 6.56. Another difference from case I, is that the core loss branch current reduces as evident from figures 6.50 and 6.58. Due to the reduction in the value of the stator and core loss branch currents, both stator copper loss and core loss thus decrease. Because the rotor current rises, the rotor copper loss increases. However, this increment of the rotor copper loss is overwhelmed by the decrement of the stator loss and core loss. Thus, the total loss is eventually minimized.

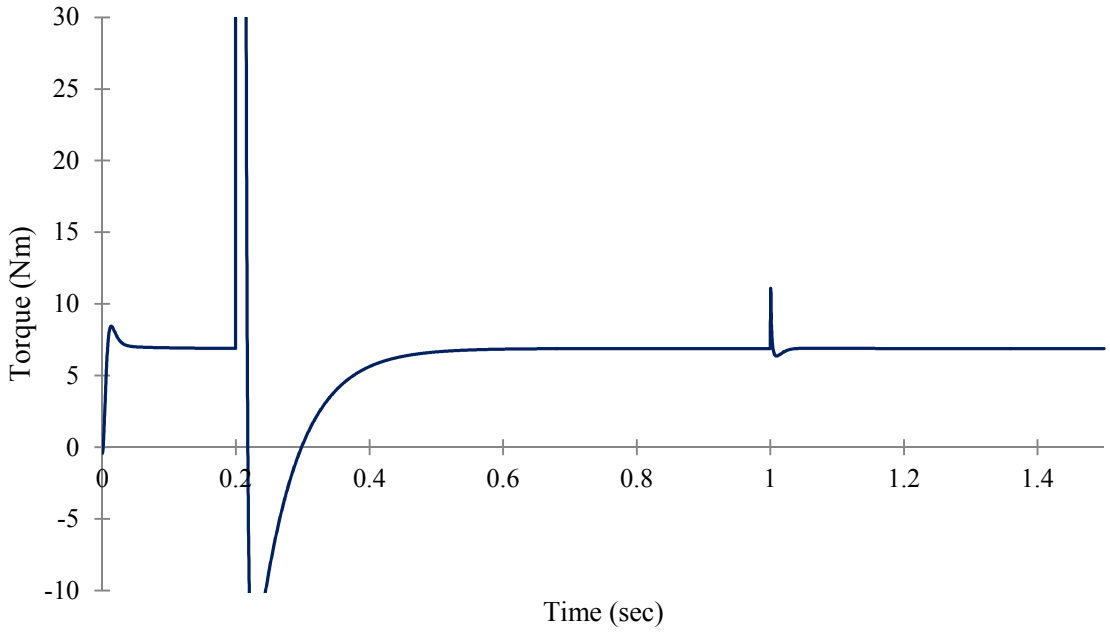

(a)

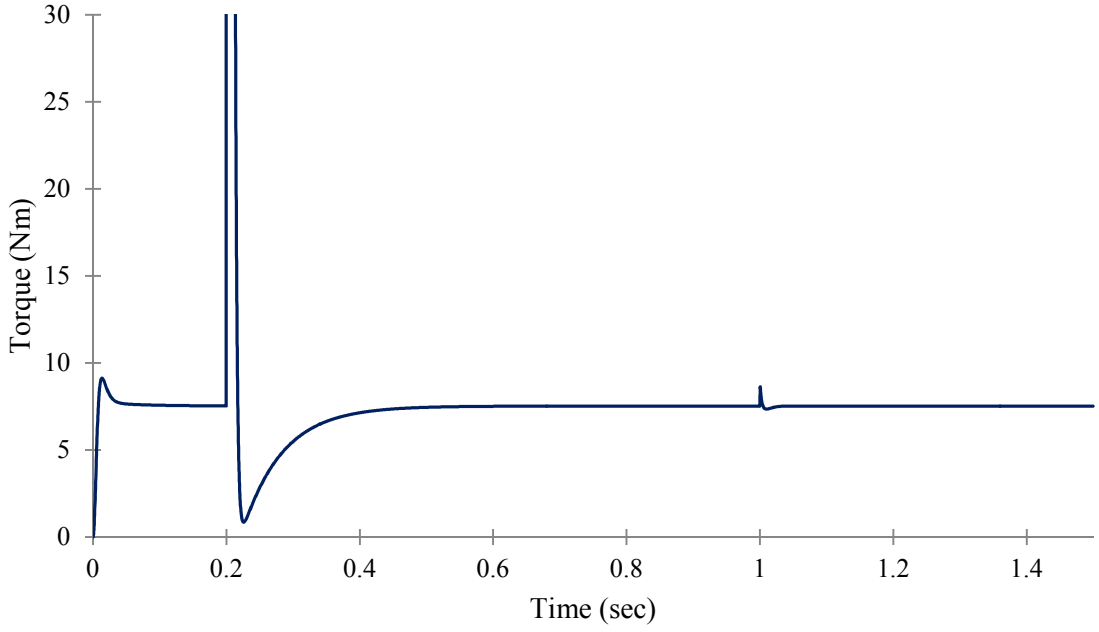

(b)

Fig. 6.42: Torque profile under the influence of loss minimization controller. a) Speed at 1,700 rpm. b) Speed at 500 rpm.

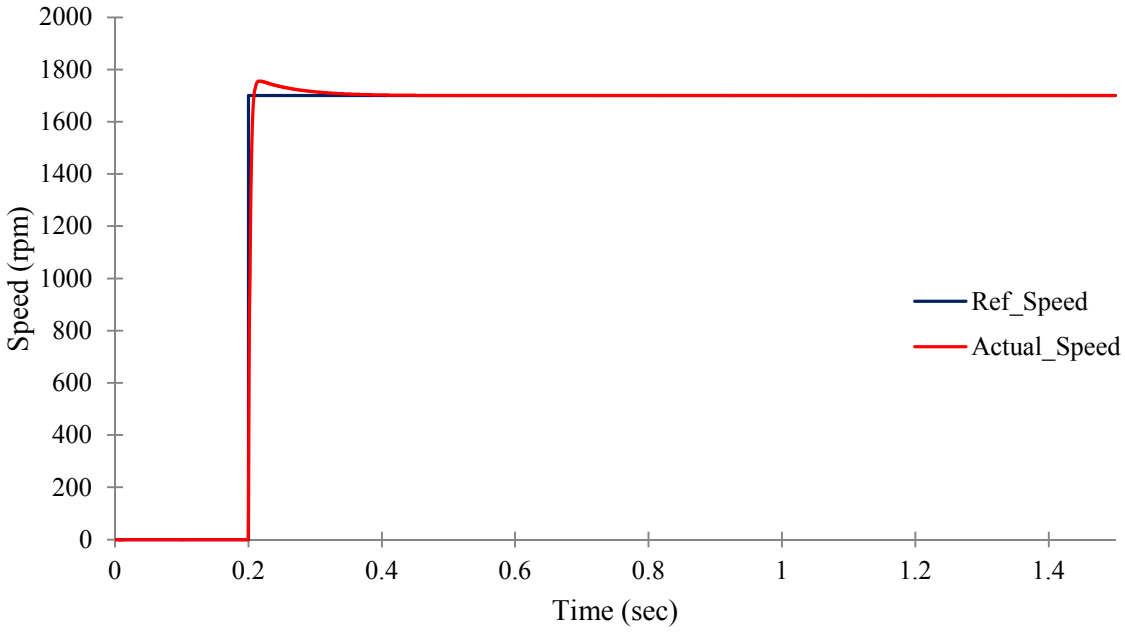

(a)

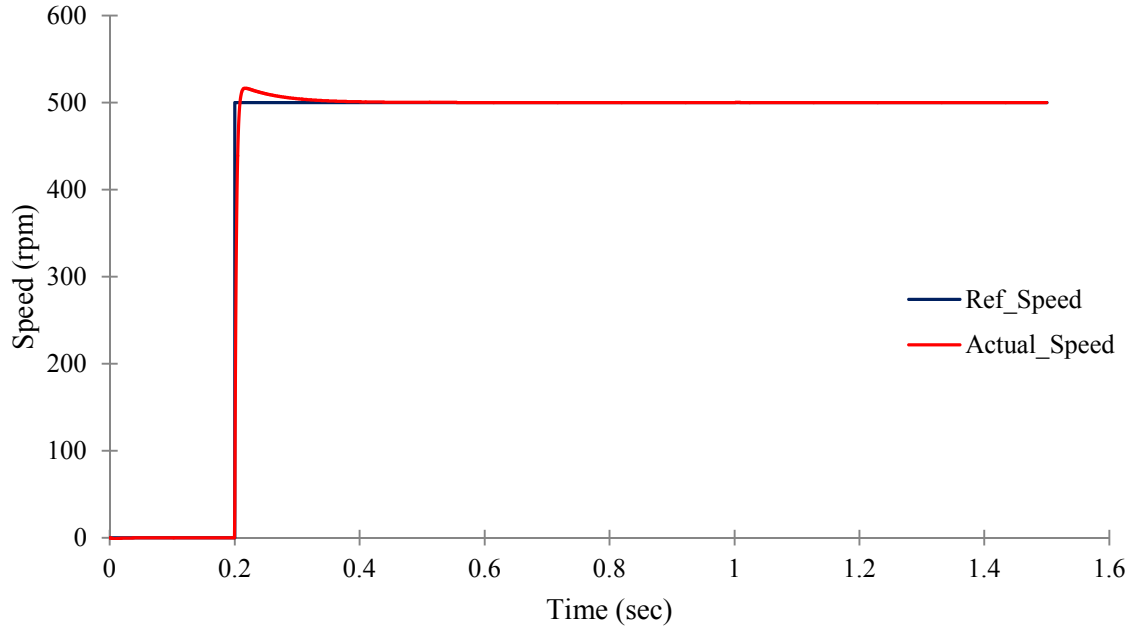

(b)

Fig. 6.43: Reference Speed and dynamics of actual rotor speed. a) Speed at 1,700 rpm. b) Speed at 500 rpm.

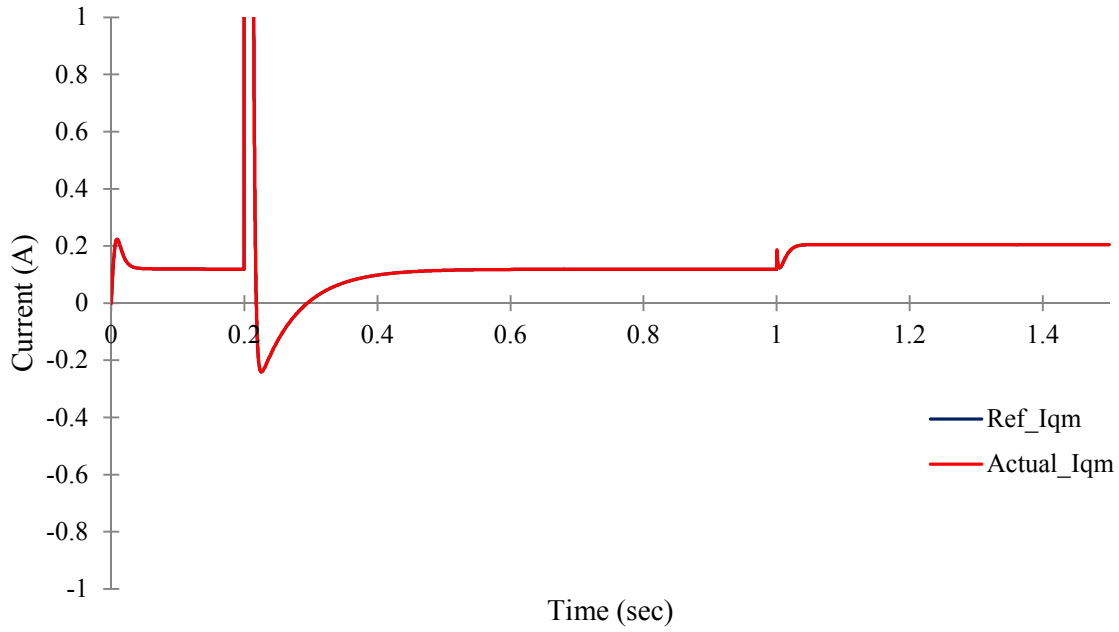

(a)

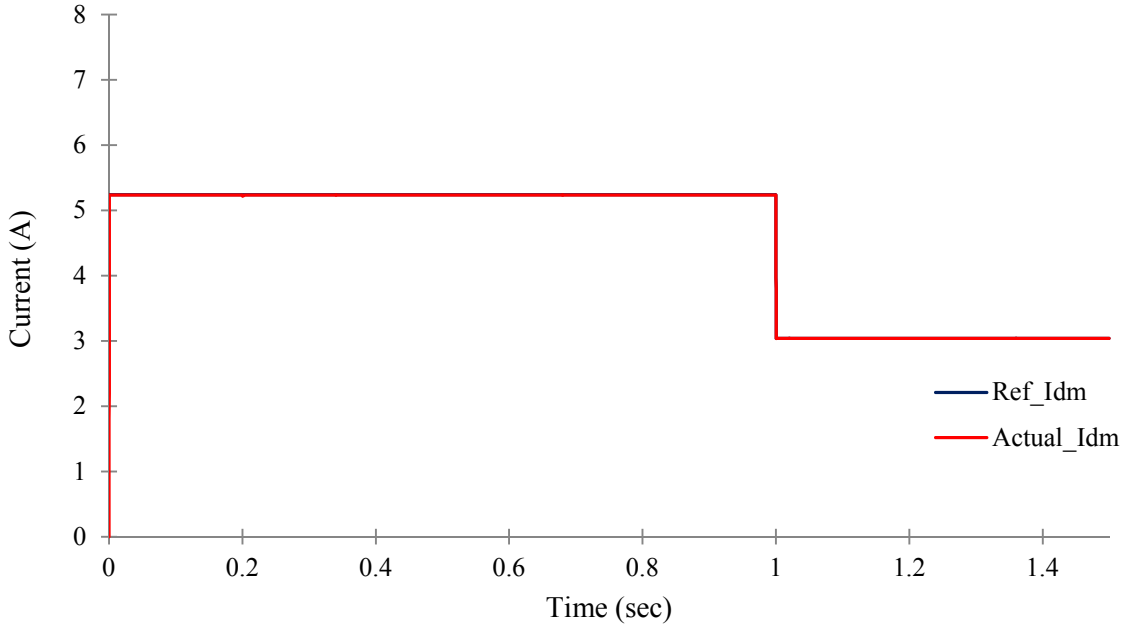

(b)

Fig. 6.44: Reference and actual magnetizing currents at 1,700 rpm. a) q-axis. b) d-axis.

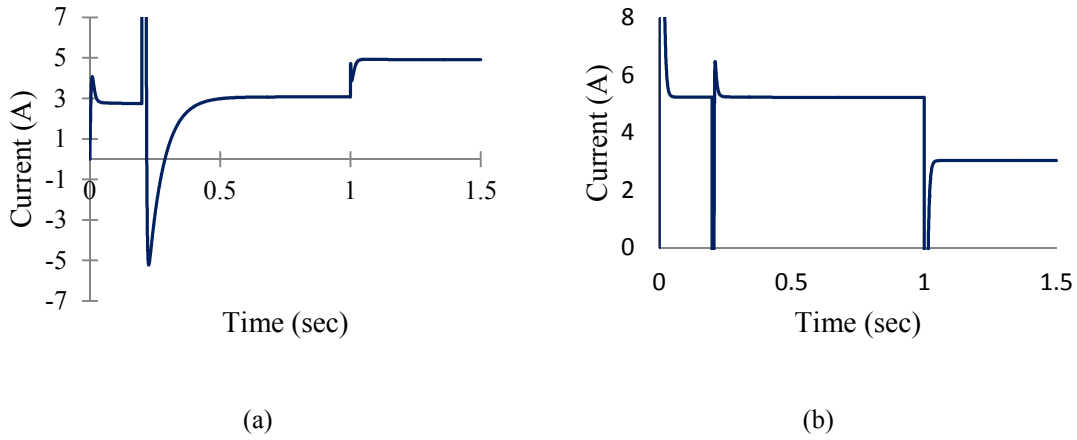

(a) (b)

Fig. 6.45: Dynamics of stator current at 1,700 rpm. a) q-axis. b) d-axis.

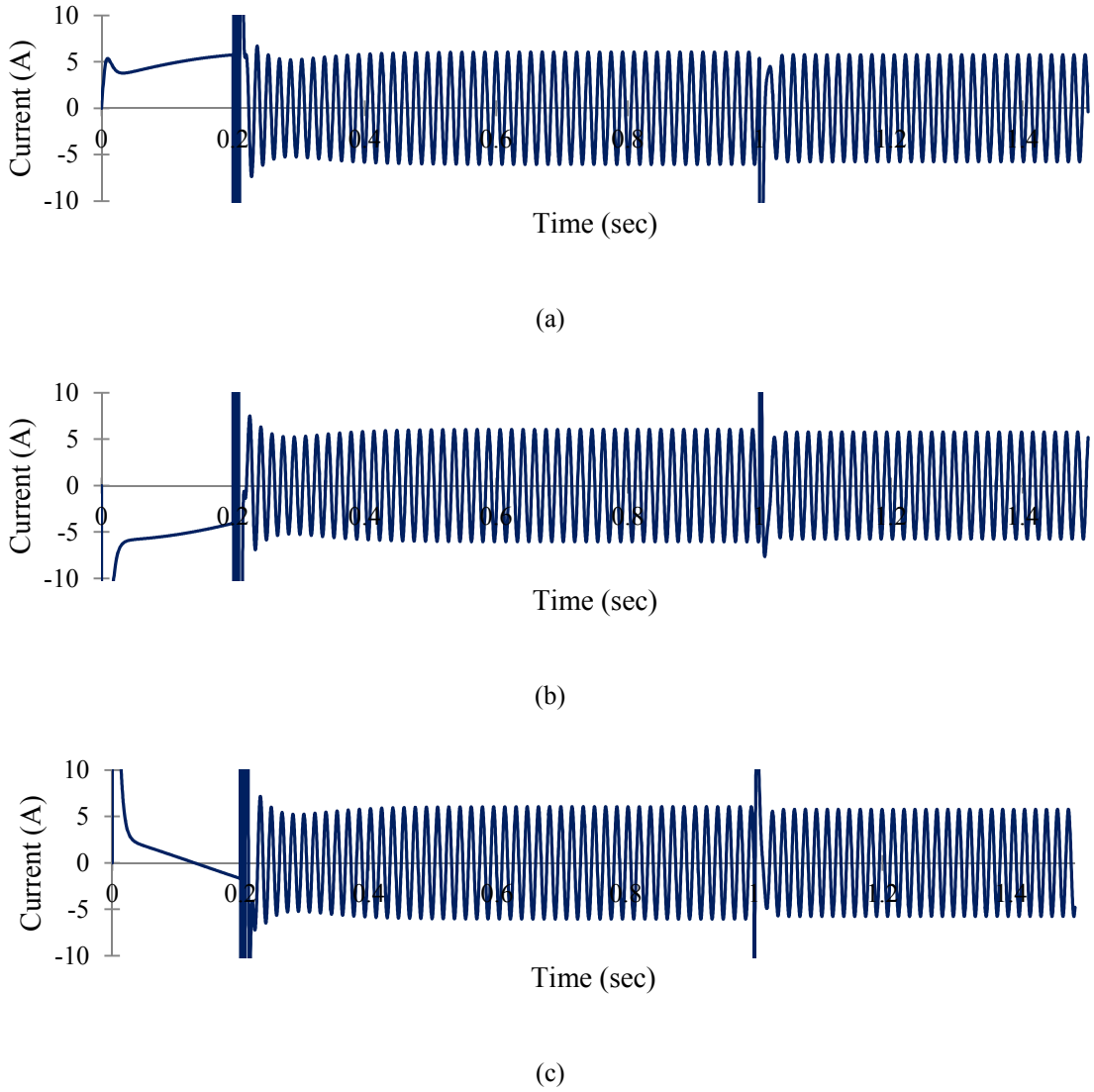

(a)

(b)

(c)

Fig. 6.46: Stator currents in three phase at 1,700 rpm. a) Phase A. b) Phase B. c) Phase C.

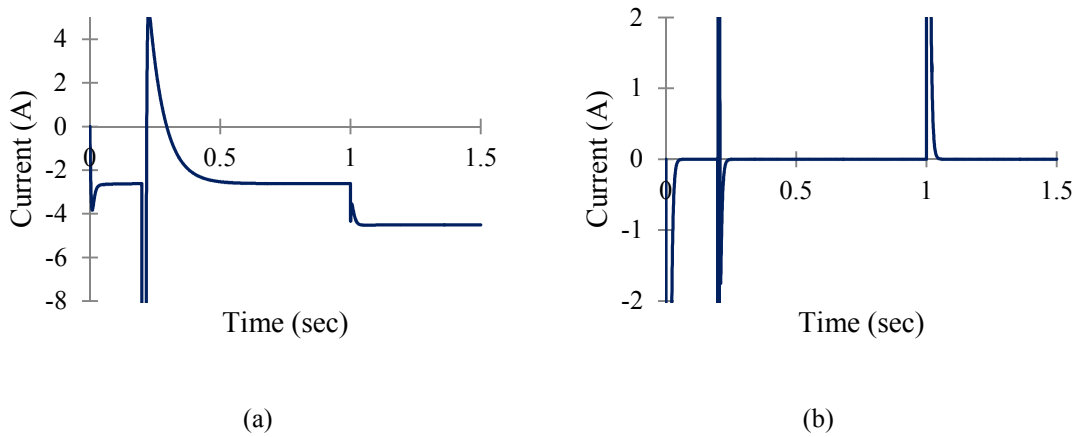

Fig. 6.47: Dynamics of rotor current at 1,700 rpm. a) q-axis. b) d-axis.

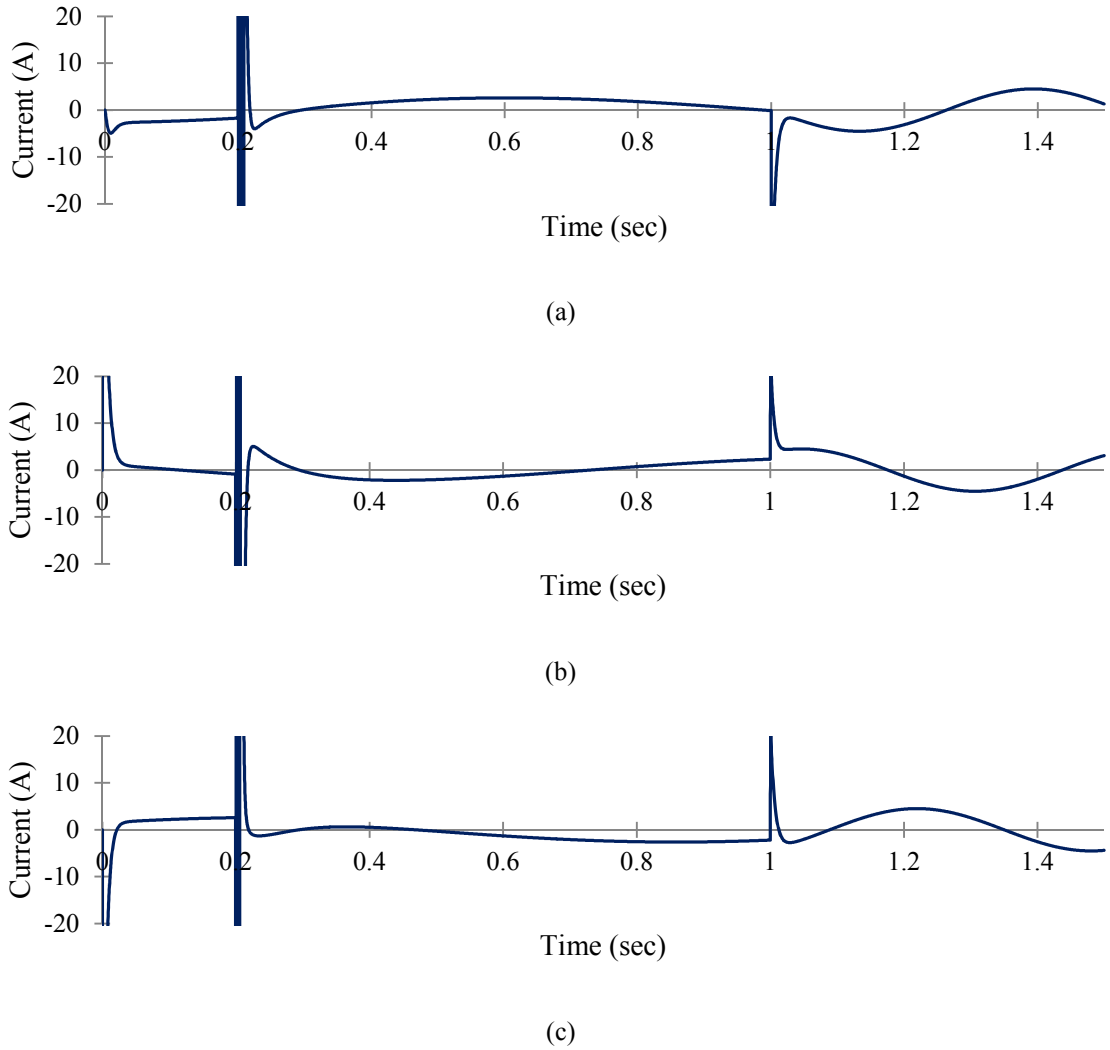

Fig. 6.48: Rotor currents in three phase at 1,700 rpm. a) Phase A. b) Phase B. c) Phase C.

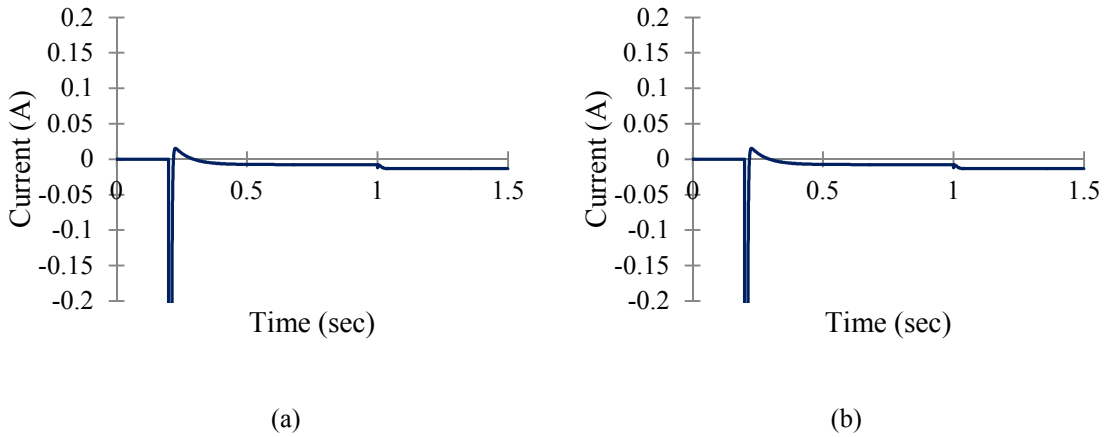

Fig. 6.49: Dynamics of core loss branch current at 1,700 rpm. a) q-axis. b) d-axis.

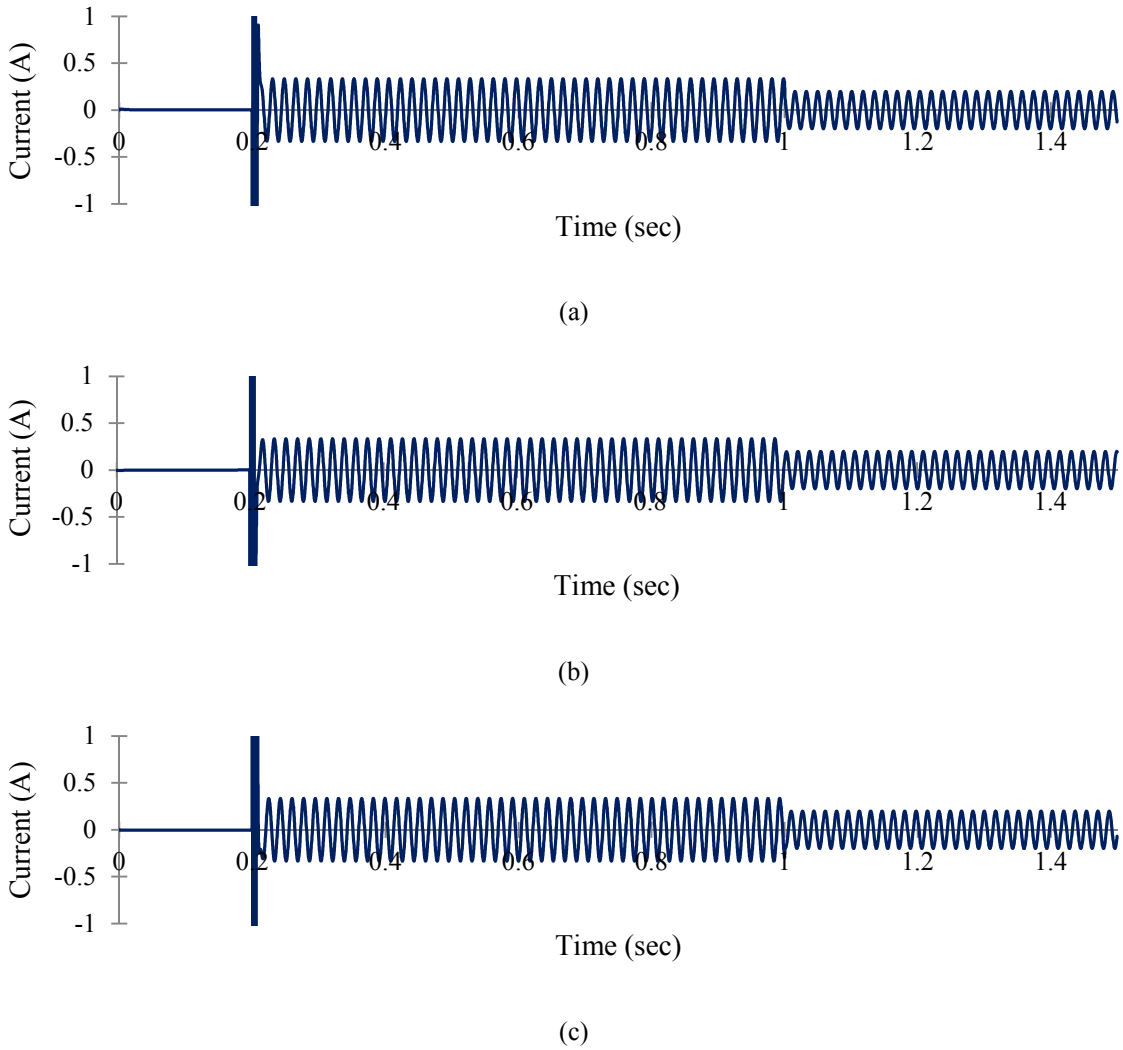

Fig. 6.50: Core loss branch currents in three phase at 1,700 rpm. a) Phase A. b) Phase B. c) Phase C.

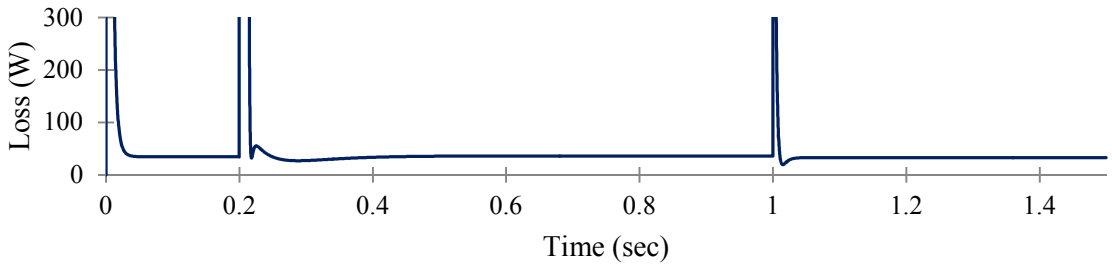

(a)

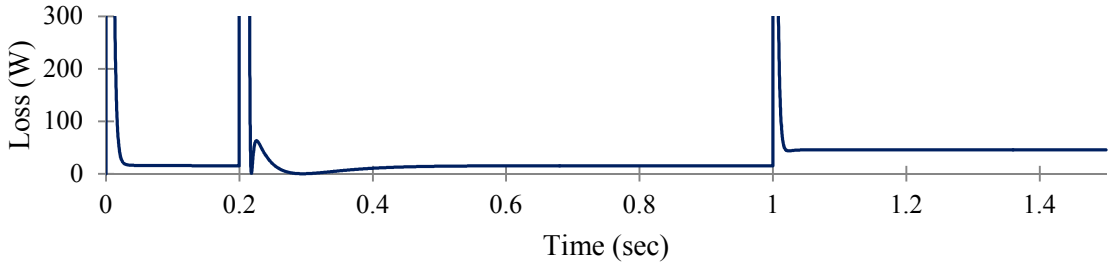

(b)

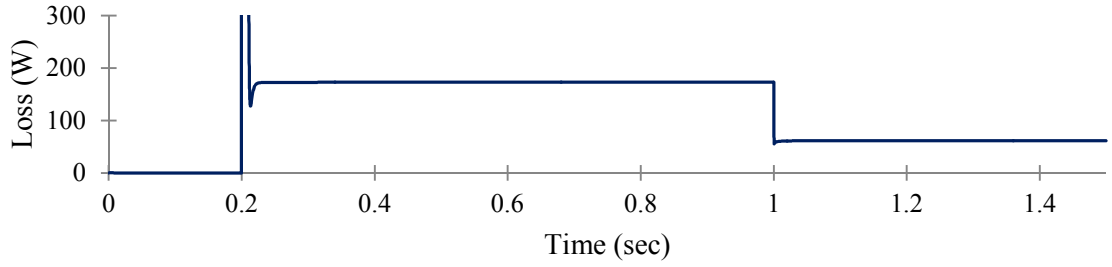

(c)

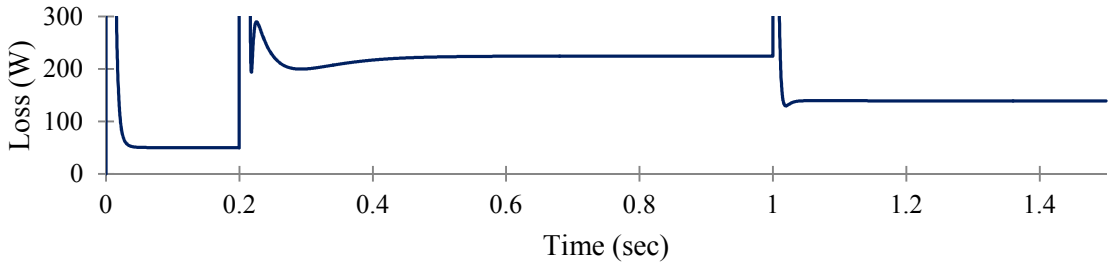

(d)

Fig. 6.51: Losses in the motor at 1,700 rpm. a) Stator copper loss. b) Rotor copper loss. c) Core loss. d) Total loss.

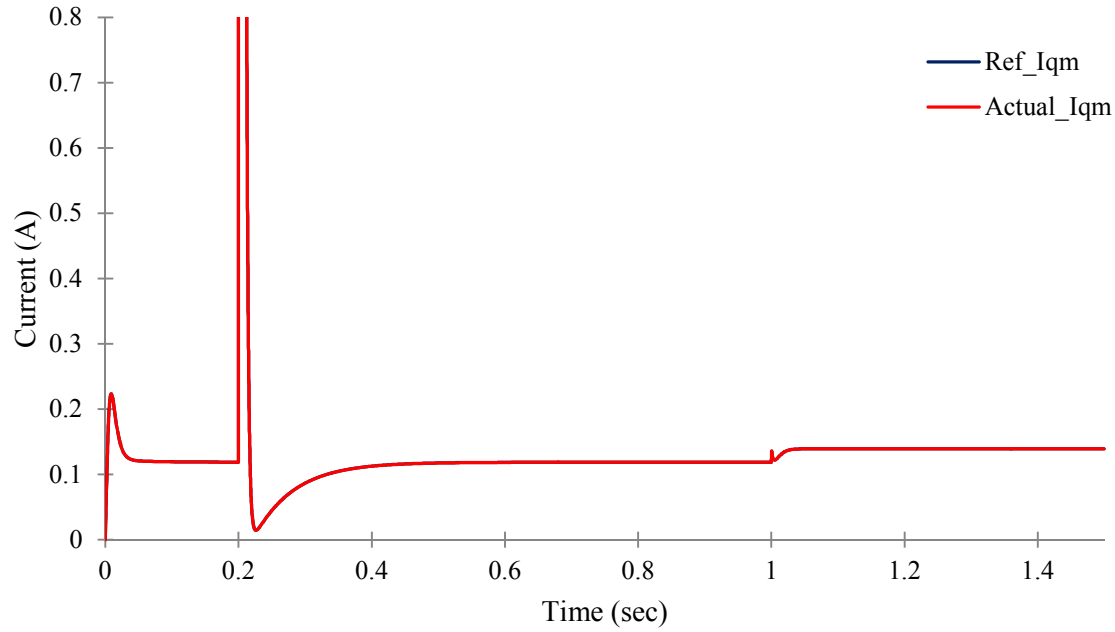

(a)

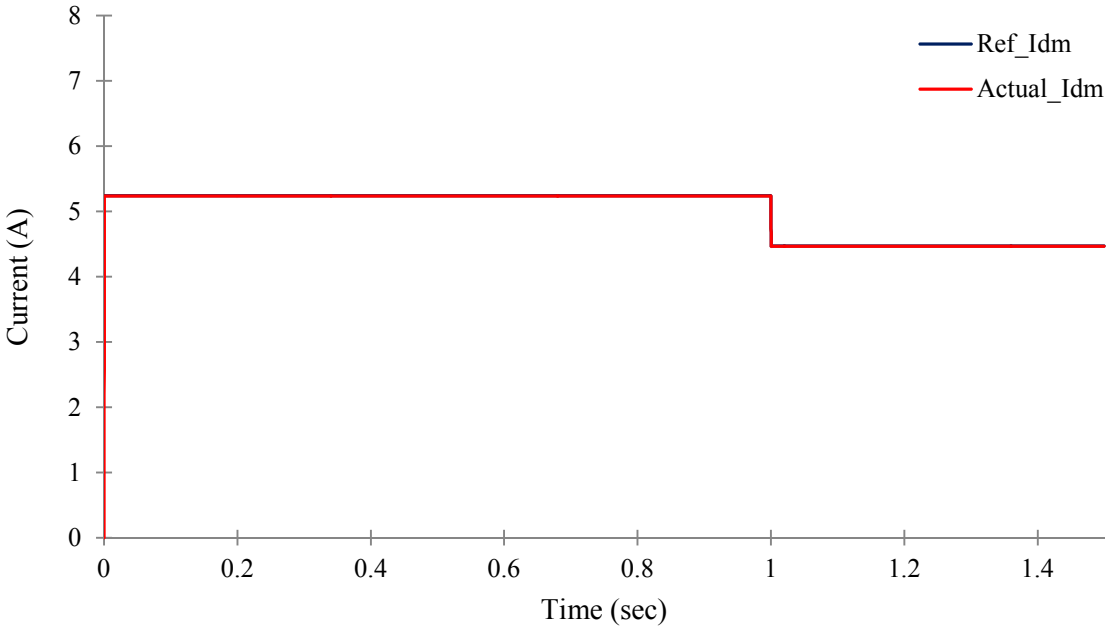

(b)

Fig. 6.52: Reference and actual magnetizing currents at 500 rpm. a) q-axis. b) d-axis.

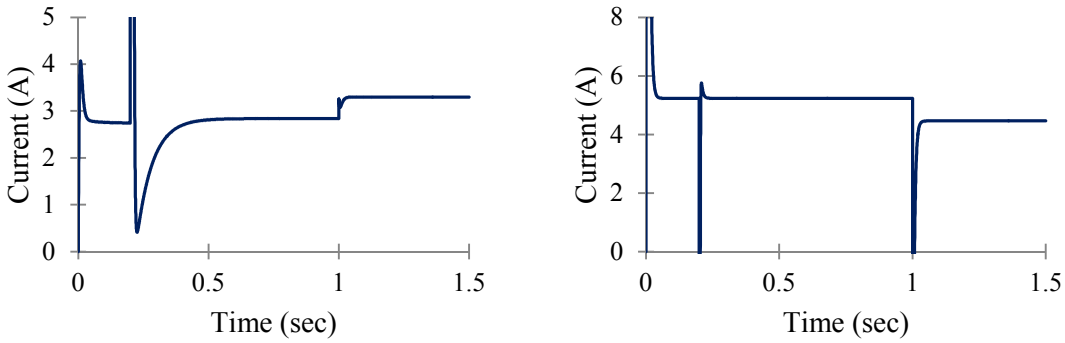

(a) (b)

Fig. 6.53: Dynamics of stator current at 500 rpm. a) q-axis. b) d-axis.

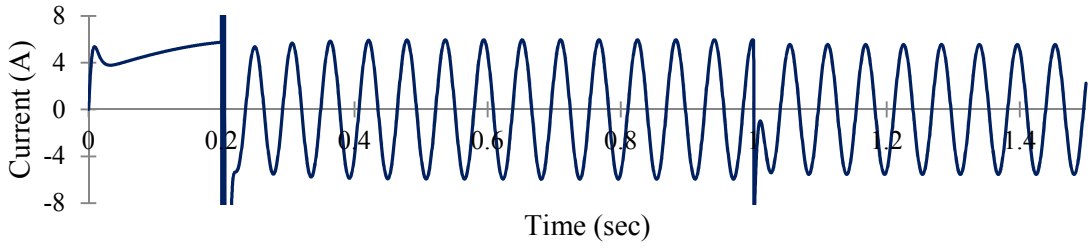

(a)

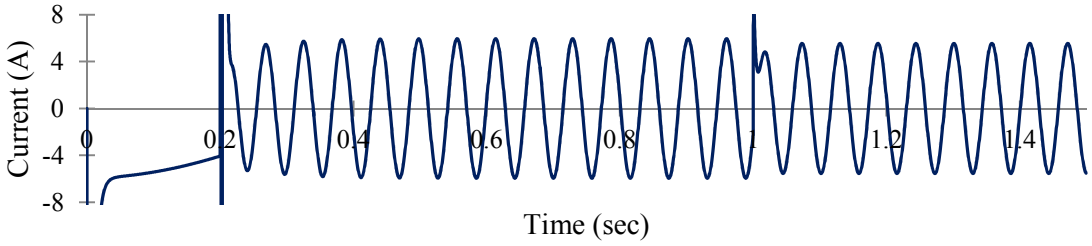

(b)

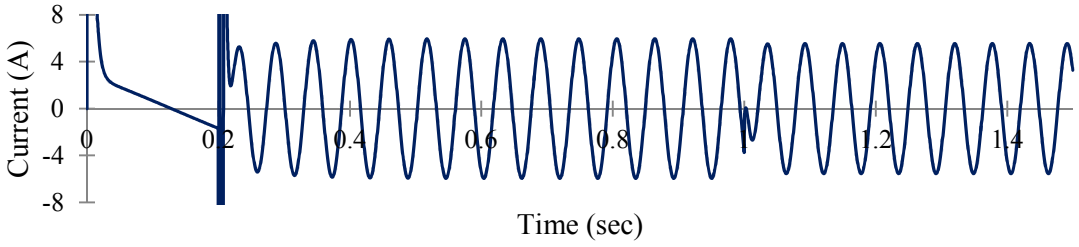

(c)

Fig. 6.54: Stator currents in three phase at 500 rpm. a) Phase A. b) Phase B. c) Phase C.

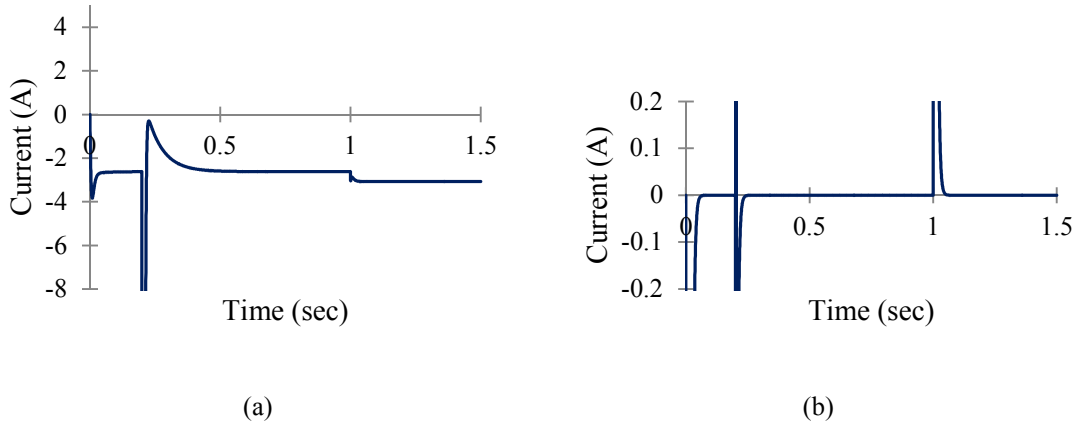

(a) (b)

Fig. 6.55: Dynamics of rotor current at 500 rpm. a) q-axis. b) d-axis.

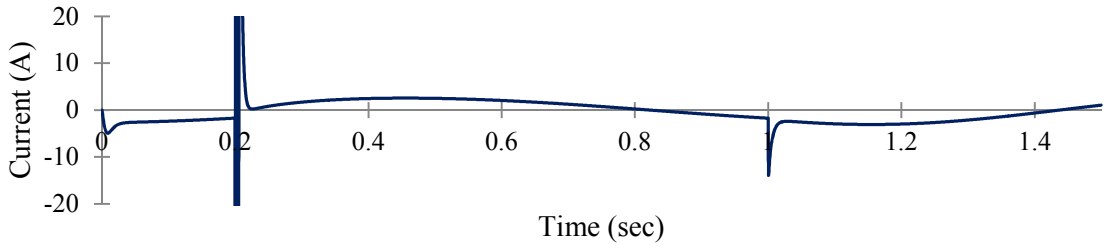

(a)

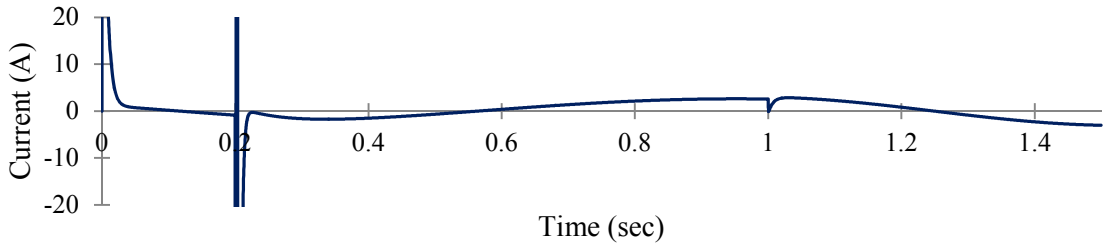

(b)

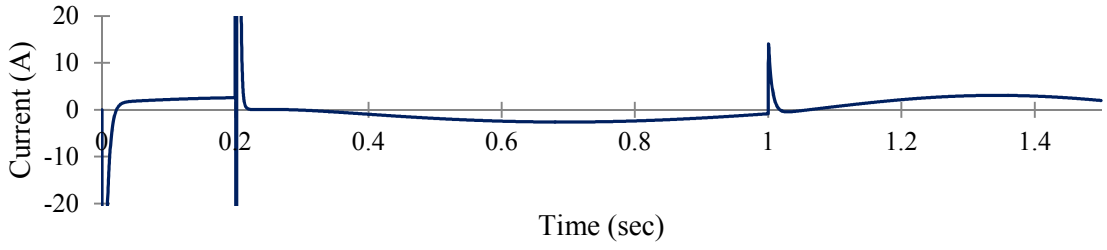

(c)

Fig. 6.56: Rotor currents in three phase at 500 rpm. a) Phase A. b) Phase B. c) Phase C.

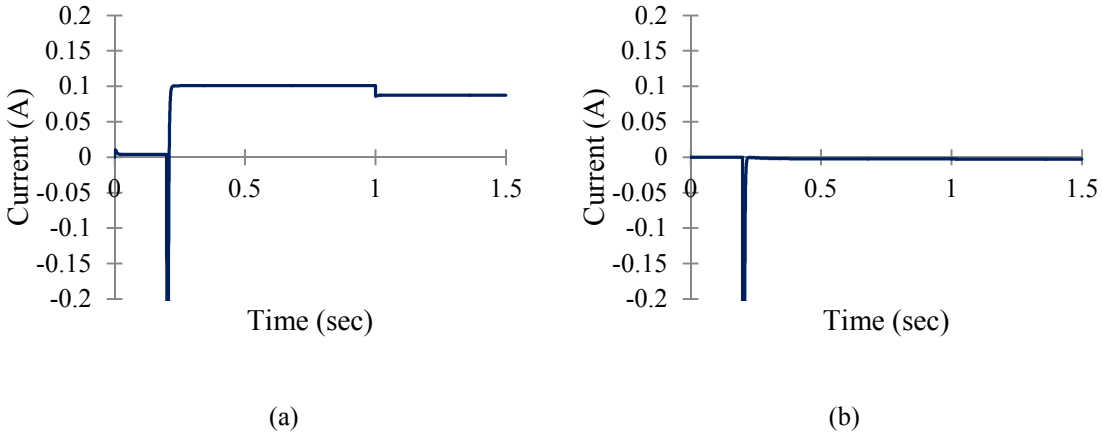

Fig. 6.57: Dynamics of core loss branch current at 500 rpm. a) q-axis. b) d-axis.

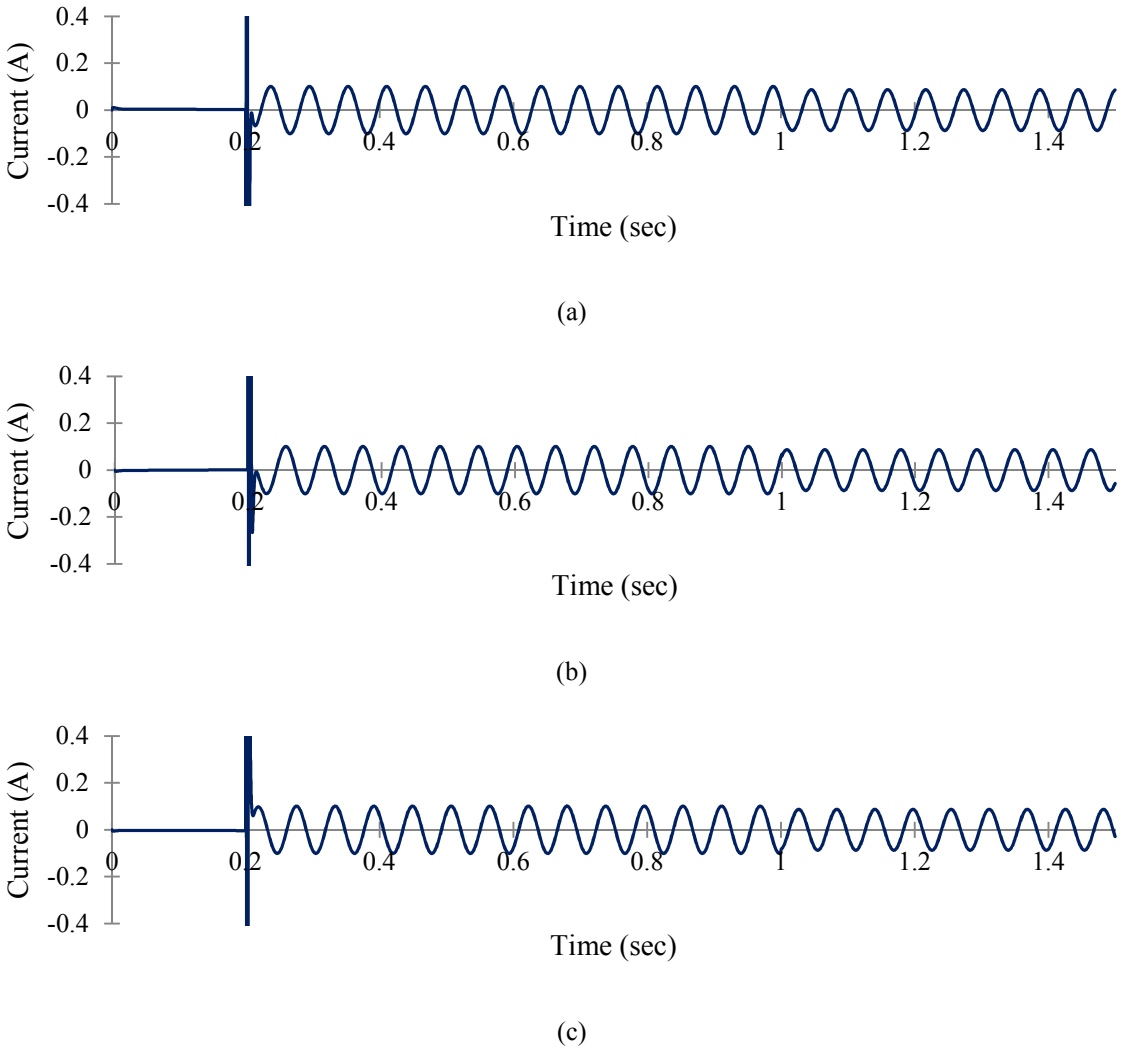

Fig. 6.58: Core loss branch currents in three phase at 500 rpm. a) Phase A. b) Phase B. c) Phase C.

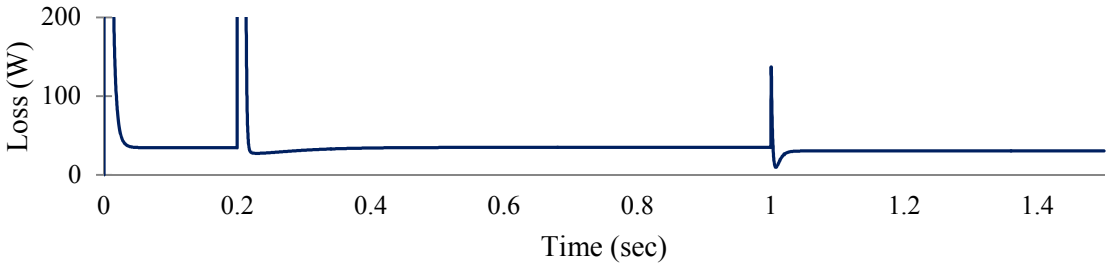

(a)

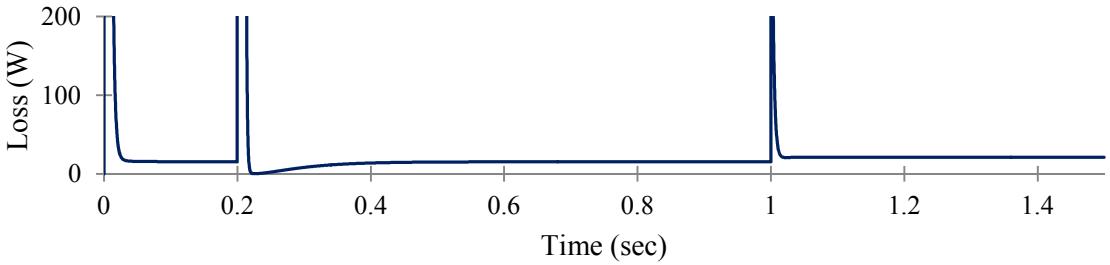

(b)

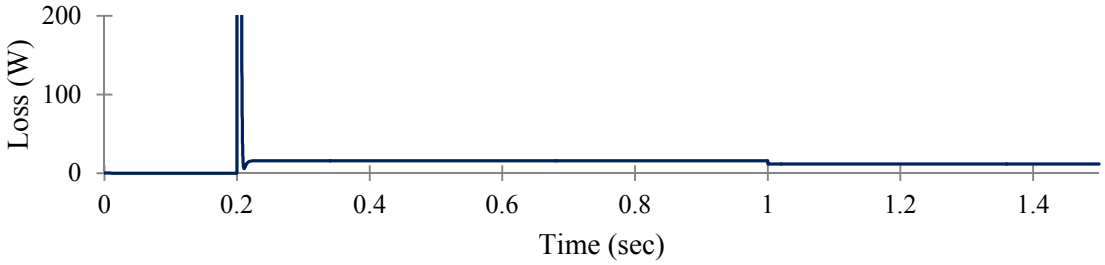

(c)

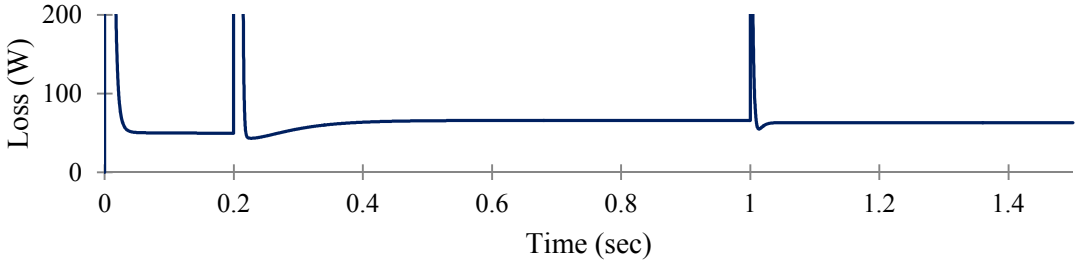

(d)

Fig. 6.59: Losses in the motor at 500 rpm. a) Stator copper loss. b) Rotor copper loss. c) Core loss. d) Total loss.

7. CONCLUSION

This research is an effort to analyze the performance of a vector controlled loss minimization controller. In order to achieve this it was necessary to modify the already established dynamic model of the induction motor. Because it does not contain the core loss element, it was necessary to add this element as core loss has substantial impact on the induction motor especially at low speeds. It was found that adding the core loss increased the order of the mathematical model of the induction motor by two. While deriving the conditions for vector control it was found that the control variable could no longer be chosen as the stator current. Instead, for proper decoupling the control variable had to be the magnetizing branch currents.

In order to fully verify the effectiveness of the induction motor model with core loss, simulations were carried out. The mathematical model was programmed in MATLAB/Simulink and tested by using actual parameters from a 7.5 hp motor. The simulations included loading the machine from 0% to 100%. The results obtained were in unison with the characteristics of an induction motor.

In order to implement vector control all the necessary equations had to be derived because the control variable was different from classical vector control. The design phase of the PI controller however added new challenges due to the complexity brought about by including the core loss branch. The derivation of the equations to compute the controller gains were visibly cumbersome and assumptions had to be made to avoid the system from getting more complex. However, simulations were successfully carried to implement vector control. All the conditions for vector control were satisfied and the

magnetizing currents were decoupled completely as per the objective of vector control. An outer speed loop was added to complete the entire system. The results thus obtained are concrete proof that the control strategy was successfully implemented.

The main objective of this research was to design a system which will implement a loss minimization controller. To achieve this, a loss model was developed which consisted of the copper losses and core loss. The optimal current to minimize was then derived with the help of this loss model. Simulations were then carried out to prove the potency of this theory. The end result was the design of a vector controlled induction motor drive which could also increase the efficiency of the motor itself.

7.1 CONTRIBUTIONS OF THIS RESEARCH

The contributions of this research are as follows:

- Using the already established dynamic model of the induction motor to implement vector controlled loss minimization controller.
- Calculating the gains of a PI controller mathematically instead of using the trial and error method.

7.2 FUTURE SCOPE

The model of the induction motor used in this research only incorporates the core loss. However, a more accurate model of the induction motor can be used to implement loss minimization. Accuracy of the motor model can be increased by incorporating effects such as saturation. Also, loss minimization controller is affected by parameter variation. If effects due to parameter variation can be incorporated to design this

controller then it would truly add value to this research. As an immediate scope for future work the development of an experimental setup to implement this controller would help in validating the simulations further.

REFERENCES

[1] M. N. Uddin, and S. W. Nam, "New Online Loss-Minimization-Based Control of an Induction Motor Drive," *IEEE Trans. on Power Electronics,* Vol. 23, No. 2, March 2008.

[2] B. L. Theraja and A. K. Theraja, *A Textbook of Electrical Technology*. S. Chand & Company Ltd., 1999.

[3] F. Blaschke,"The principle of Field Orientation as Applied to the New Transvector Closed Loop Control System for Rotating-Field Machines," SiemensReview,vol.34, pp.217-220, May 1972.

[4] A. Kusko and D. Galler,"Control Means for Minimization of Losses in AC and DC Motor Drives,"*IEEE Trans, on Industry Applications*, vol.19,pp.561-570, July/Aug.1983.

[5] D. S. Kirschen, D. W. Novotny, and W. Suwanwisoot,"Minimizing Induction Motor Losses by Excitation Control in Variable Frequency Drives,"*IEEE Trans, on Industry Applications*,vol.20, pp.1244-1250, Sept./Oct.1984.

[6] H. G. Kim, etal.,"Optimal Efficiency Drive of a Current Source Inverter Fed Induction Motor by Flux Control," *IEEE Trans, on Industry Applications*,pp. 1453- 1459,1984.

[7] I. Kioskeridis and N. Margaris,"Loss Minimization in Induction Motor Adjustable-Speed Drives," *IEEE Trans, on Industrial Electronics*,vol.43, pp.226- 231, Feb.1996.

[8] P. Famouri and J. J. Cathey,"Loss Minimization Control of an Induction Motor Drive," *IEEE Trans, on Industry Applications*,vol.27, pp.32-37, Jan./Feb.1991.

[9] R. D. Lorenz and S. M. Yang,"Efficiency-Optimized Flux Trajectories for Closed-cycle Operation of Field-Orientation Induction Machine Drives,"IEEE Trans, on Industry Applications,vol.28, pp.574-580, May/June1992.

[10] G. O. Garica, J. C. M. Luis, R. M. Stephan, and E. H. Watanabe,"An Efficient Controller for an Adjustable Speed Induction Motor Drive*," IEEE Trans, on Industrial Electronics*, vol. 41, pp.533-539, Oct. 1994.

[11] C. Chakraborty and Y. Hori,"Fast Efficiency Optimization Techniques for the Indirect Vector-Controlled Induction Motor Drive," *IEEE Trans, on Industry Applications*, vol.39, pp.1070-1076, no.4, July/Aug. 2003.

[12] F. Femandez-Bemal, A. Garcia-Cerrada, and R. Faure,"Model-based Loss Minimization for DC and AC Vector-Controlled Motors Including Core

Saturation,"*IEEE Trans, on Industry Applications*, vol.36,no.3,pp.755-763, May/June 2000.

[13] S. Lim and K. Nam,"Loss-Minimising Control Scheme for Induction Motors," *IEEE Proc-Electr. Power Appl*., vol.151, no.4, pp.385-397, July 2004.

[14] J. C. Moreira, T. A. Lipo, and V. Blasko,"Simple Efficiency Maximizer for an Adjustable Frequency Induction Motor Drive,"*IEEE Trans, on Industry Applications*, vol.27, pp.940-946,Sept./Oct.1991.

[15] S. K. Sul and M. H. Park, "A Novel Technique for Optimal Efficiency Control of a Current-Source Inverter-Fed Induction Motor," IEEE *Trans, on Power Electronics*,vol.3, pp. 192-199, Apr.1988.

[16] D. S. Kirschen, D. W. Novotny, and W. Suwanwisoot, "On-line Efficiency Optimization of a Variable Frequency Induction Motor Drive," *IEEE Trans, on Industry Applications*, vol.21, pp.610-615, May/June 1985.

[17] G. C. D. Sousa, B. K. Bose, and J. G. Cleland,"A fuzzy Logic Based On-Line Efficiency Optimization Control of an Indirect Vector-Controlled Induction Motor Drive,"*IEEE Trans, on Industrial Electronics*, vol.42,pp. 192-198,Apr. 1995.

[18] G. K. Kim, I. J. Ha, and M. S. Ko,"Control of Induction Motors for Both High Dynamic Performance and High Power Efficiency,"*IEEE Trans, on Industrial Electronics*, vol.39, pp.323-333, Aug.1992.

[19] C. M. Ta and Y. Hori,"Convergence Improvement of Efficiency-Optimized Control of Induction Motor Drives,"*IEEE Trans, on Industry Applications*,vol.37, pp.1746-1753, Nov./Dec. 2001.

[20] P. C. Krause, O. Wasynczuk, and S . D. Sudhoff, *Analysis of Electric Machinery*. New York IEEE Press, 1995.

[21] B. K. Bose, *Modern Power Electronics and AC Drives*. Prentice Hall PTR., 2002.

[22] M. Khan, "Study of Challenges in Technology Development and Market Penetration of Hybrid Electric Vehicles in Canada," M. A. Sc. Thesis, Elec. Eng Dep., University of Windsor, 2009.

[23] E. Levi, "Impact of Loss on Behaviour of Vector Controlled Induction Machines," *IEEE Trans. on Industry Applications*, Vol. 31, No. 6, Nov/Dec 1995.

[24] U. A. Bakshi and V. U. Bakshi, *Control Engineering*. Technical Publications Pune, 2001.

[25] K. J. Aström and R. M. Murray, *Feedback Systems*. Princeton University Press. 2009.

[26] Copper.org, CDA Press Releases, "Building a better electrical motor," January 2005.

[27] A. H. Bonnett, "Understanding the Changing Requirements and Opportunities for Improvement of Operating Efficiency of AC Motors", *IEEE Trans, on Industry Application*, vol.29, pp.600-610, May/Jun.1993.

[28] F. Abrahamsen, F. Blaabjerg, J. K. Pedersen, P. Grabowski, P. Thogersen, E. J. Petersen, "On the Energy Optimized Control of Standard and High-Efficiency Induction Motors in CT and ITVAC Applications," in *Conf. Rec. IEEE-IAS Annual Meeting*, vol.l, pp.621-628,1997.

[29] I. Takahashi, H. Mochikawa, "A New Control of PWM Inverter Waveform for Minimum Loss Operation of an Induction Motor Drive", *IEEE Trans, on Industry Applications*,vol.21, pp.580-587, May/June.1985.

[30] F. C. Zach, H. Ertl, "Efficiency Optimal Control for AC Drives with PWM Inverters," *IEEE Trans, on Industry Applications*, vol.21, pp.60-66, July/Aug.1985.

[31] S. W. Nam, "Adaptive Backstepping Based Online Loss Minimization Control of an Induction Motor Drive," M. A. Sc. Thesis, Elec. Eng Dep., Lakehead University, 2006.

[32] S. M. Yang and F. C. Lin, "Loss-Minimization Control of Vector Controlled Induction Motor Drives," *Journal of the Chinese Institute of Engineers*, vol. 26, No. 1, pp. 37-45, 2003.

APPENDIX

TABLE I: INDUCTION MOTOR PARAMETERS

R_s	0.65417 Ω
R_r	1.48166 Ω
R_c	1031.24032 Ω
L_{ls}	0.00552H
L_{lr}	0.00828H
L_m	0.18293 H
Poles	4
J	0.27 kgm^2
Rated voltage	460 V
Rated current	9.5 A
Output power	7.5 hp
Frequency	60 Hz

Table I tabulates the parameters of the induction motor to obtain the simulation results in this thesis. The value of J was extrapolated from induction motor parameters listed in [20]. This reference was used because the voltage and frequency ratings of the machines used in [20] matches with the one used in this thesis.

VITA AUCTORIS

Name: Debarshi Biswas

Place of birth: India

Year of birth: 1986

Education: 2008: Bachelor of Technology
Electronics and Communication Engineering,
Sikkim Manipal Institute of Technology,
Sikkim, India.